

# **Immobilisation of non-selective catalysts in permselective microcapsules**

Zur Erlangung des akademischen Grades eines

**Dr.-Ing.**

von der Fakultät Bio- und Chemieingenieurwesen  
der Technischen Universität Dortmund

genehmigte Dissertation

vorgelegt von

**M.Sc. Pavadee Pachariyanon**

aus

**Bangkok, Thailand**

Tag der mündlichen Prüfung: 24 May 2012

1. Gutachter: Prof. Dr. David W. Agar

2. Gutachter: Prof. Dr. Wichmann Rolf

**Dortmund 2012**

## **Acknowledgements**

This thesis has been written during my studying as a research associate at the Institute of Reaction Engineering B (TCB), Biochemical and Chemical engineering Faculty, TU Dortmund, Germany.

First of all, I would like to express my deep appreciation to Prof. Dr. David W. Agar for giving me an opportunity to pursue my doctoral degree under his supervision and guidance. His continuous support, precious advices and fruitful discussions have significantly contributed to the success of this thesis.

My gratitude is addressed to Prof. Dr.-Ing. Rolf Wichmann for kindly being the co-supervisor and for his interest in this work.

Furthermore, my thanks also go to all former and current colleagues at the Institute of Reaction Engineering B for the good collaboration as well as their wonderful friendship and support. They have made my four-year studying full of nice memories and happiness. These thanks are also extended to Guru Praveen Phaneendra and Dian Wardani Soerjawinata who have assisted me in completing this work within the scope of their master theses. Special thanks are sent to Ms. Monika Meuris from Institute of Biomaterial and Polymer and Mr. Stolle from fine mechanic workshop for their technical support.

Moreover, my gratefulness is sent to my 'friends'. Their wonderful friendship and support have made my life completed and passed the difficult time. Without them, my thesis would be less well completed.

Last but not least, I would like to express my sincere gratitude to my family for their love, encouragement and invaluable support, especially during my stay in Germany. I wish to thank my husband for his love, leadership, precious advice and his understanding during the time as I have been compiling this thesis. To them, I would like to dedicate this work and all of my achievements.

Dortmund, July 2012

Pavadee Pachariyanon

## Abstract

Microencapsulation, a technique for immobilising particles or liquids within a small spherical and usually polymeric shell is employed in a wide range of industrial, engineering, pharmaceutical, biotechnological and research applications. In addition to simply using the membrane shell to enclose or isolate an active component, its permselective properties may also be exploited as an additional functionality to mediate the mass transfer between the active core and its environment. Tailoring the permselective characteristics of microcapsule matrices and shells thus offers great potential for manipulating both the release of and access to the active material.

This dissertation focuses on the use of permselective polyacrylamide-alginate (pAAm-Alg) microcapsules to both immobilise an enzyme and deliberately regulate its accessibility for different substrates, in analogy to zeolitic catalysis. The microcapsules were prepared using a concentric double nozzle air-jet technique, for which the influence of the intrinsic and extrinsic operating parameters, such as polymerisation compositions and conditions, jet air flow and nozzle geometry, was studied. The equivalent diameter and circularity of the microcapsules were determined using conventional microscopy and image analysis software, while the membrane thickness of the microcapsules was ascertained with the help of a stereomicroscope. The average size and number of microcapsules produced decreased with increasing cross-linker and monomer concentrations, while the equivalent diameter rose with increasing initiator concentration. The effect of changes in cross-linker, monomer and initiator concentrations on the circularity of the microcapsules was insignificant. The use of compressed air cut the equivalent diameter of the microcapsules noticeably, while significantly increasing the rate of microcapsules production. The membrane thickness generally increased proportionally to the equivalent diameter of the microcapsules.

Diffusion experiments were carried out to assess the mass transport properties, i.e. permeability and molecular weight cut-off (MWCO) characteristics, of microcapsules, providing indications of membrane porosity and structure. The effect of monomer acrylamide (AAm), cross-linker N,N-methylene-bis-acrylamide (Bis-AAm), initiator and silica additive concentrations on the diffusion coefficient of dextran T1 and glucose was determined. Diffusion coefficients were determined by using the unsteady-state Crank model to describe the dynamic diffusion into the microcapsule liquid core from the surrounding solution. It was observed that the diffusion coefficients decreased with an increase in AAm, Bis-AAm and

silica additive concentrations, while varying the initiator concentrations had only a moderate effect. Correspondingly, the pore size of the pAAm-Alg microcapsule membrane could be manipulated by adjusting the aforementioned parameters. A broad spectrum of solutes: glucose, maltose, dextran T1, insulin,  $\alpha$ -lactalbumin, and trypsin were used to establish the MWCO of the pAAm-Alg microcapsules, which was found to be in the range of 1-5.7 kDa, suggesting that pAAm-Alg microcapsules can be applied for size-selective substrate discrimination in this molecular weight range.

Multi-competitive enzymatic reactions were performed to determine the specificity, i.e. selectivity, properties of encapsulated enzymes in pAAm-Alg microcapsules. The transesterification of fatty acid ethyl esters with different chain lengths ( $C_2$ - $C_{14}$ ) with various alcohols catalysed by the enzyme lipase *M.miehei* (MML) was chosen as a test system. While the free enzyme exhibited higher selectivity towards the longer chain fatty acid ethyl ester ( $C_8$ -ethyl ester upward) and toward butanol, the enzyme encapsulated in the pAAm-Alg microcapsules showed a greater preference for the conversion of the short chain fatty acid ethyl ester ( $C_4$  and  $C_6$ -ethyl ester) with methanol. This was shown to be a consequence of the hydrophilic properties of the pAAm-Alg microcapsule membrane.

To fine-tune the permselective characteristics of the pAAm-Alg microcapsule membrane, a hydrophobic co-monomer, isopropyl acrylamide (IPPAAm) was added to the polymer solution at various levels, yielding pAAm-IPPAAm-Alg microcapsules. The multi-competitive enzymatic reactions were then repeated with these modified microcapsules. The results demonstrated that the permselectivity characteristics of the microcapsule membrane could be modified with only slight variations in the IPPAAm concentrations. At lower concentrations of IPPAAm, the encapsulated enzyme revealed a preference towards short chain fatty acid ethyl ester ( $C_4$  ethyl ester); while at concentrations of IPPAAm higher than 2.5%, the specificity of the encapsulated enzyme shifted to long chain fatty acid ethyl ester ( $C_8$  ethyl ester upward), as a result of the hydrophobic nature of the IPPAAm monomer. The modified microcapsule with IPPAAm concentration up to 10 % exhibited a high selectivity towards the smallest alcohol molecule, methanol.

This work has thus clearly demonstrated that, in particular, the precise composition of the polymeric microcapsule membrane can be used as a powerful tool to modify the effective selectivity behaviour of an encapsulated enzyme in comparison to that of the free enzyme.

The reusability of the immobilised enzyme was evaluated by performing multiple reaction cycles for enzyme encapsulated in pAAm-Alg microcapsules. The encapsulated enzymes retained about 90% of the initial catalytic activity even after being used for 5 reaction cycles, over a total of 240 hours, indicating the excellent stability of both the immobilised enzyme and the microcapsules.

## Kurzfassung

Mikrokapseln sind Partikel mit Abmessungen im Mikro- bzw. Millimeterbereich, in denen eine aktive Substanz in einer schützenden Hülle oder Matrix eingeschlossen wird. Die Mikroverkapselung ist eine besondere Methode zur Verkapselung dieser neuartigen, kleinen Partikel. Sie dient entweder der Stabilisierung, der Immobilisierung, der geregelten Freisetzung oder dem verbesserten Handling der aktiven Komponente. Des Weiteren ermöglicht die Mikroverkapselung eine gezielte Manipulation der Selektivität von immobilisierten, mikroverkapselten Katalysatoren durch die Einstellung des Permselectivitätsverhaltens der Mikrokapselmembran. Damit können solche „Mikromembranreaktoren“ als ein permselectives Tool zur Prozessintensivierung verwendet werden. Die Mikroverkapselung findet ihre Anwendung in einem großen Bereich der Industrie, Ingenieurwissenschaft, Medizin, Biotechnik und Forschung. Ihre aktuelle Entwicklung konzentriert sich auf detaillierte Untersuchungen der permselectiven Eigenschaften der Mikrokapseln.

In der vorliegenden Arbeit werden permselective Polyacrylamid-Alginat-(pAAm-Alg)-Mikrokapseln untersucht, die eine flüssige Kern-Lösung enthalten. Zur Herstellung der hohlen Mikrokapseln kam eine doppelkonzentrische Düse mit verschiedenen intrinsischen und extrinsischen Parametern zum Einsatz. Der äquivalente Durchmesser und die Kreisform der Mikrokapseln wurden unter Verwendung der Bildanalyse-Software *ImageJ* bestimmt, wobei ihre Membrandicke mithilfe eines Stereo-Mikroskops beobachtet und gemessen worden ist.

Es hat sich herausgestellt, dass die mittlere Größe und die Anzahl der hergestellten Mikrokapseln mit einer Zunahme von Vernetzer- und Monomer-Konzentration abnahmen, während der äquivalente Durchmesser mit einer Zunahme der Initiator-Konzentration zunahm. Der Einfluss von unterschiedlichen Konzentrationen an Vernetzer, Monomer und Initiator auf die Kreisform der Mikrokapseln war geringfügig. Mit Zufuhr von Druckluft in das System sank der äquivalente Durchmesser der Mikrokapseln dramatisch, wobei die Anzahl der erzeugten Mikrokapseln erheblich anstieg. Die Membrandicke der Mikrokapseln erhöhte sich proportional zur Zunahme des äquivalenten Durchmessers der Mikrokapseln.

Um die Transporteigenschaften (Durchlässigkeit) und den Molekulargewichtsschwellenwert (Molecular weight cut-off MWCO) der pAAm-Alg-Mikrokapselmembranen zu bestimmen,

die Informationen über die Porosität und indirekt auch über die Struktur der Mikro kapseln zu liefern, sind Diffusionsexperimente durchgeführt worden. Der Einfluss auf den Diffusionskoeffizienten von Dextran T1 und Glucose wurde für verschiedene Konzentrationen des Monomers Acrylamid (AAM), des Vernetzers N,N-Methylen-Bis-Acrylamid (Bis-AAM), des Initiators und des Silica-Additivs ermittelt. Die Diffusionskoeffizienten wurden mittels der Crank-Methode bestimmt, um die instationäre Diffusion aus einer endlich verdünnten Lösung in die Mikro kapseln zu untersuchen. Es ist beobachtet worden, dass die Diffusionskoeffizienten mit Zunahme von AAM-, Bis-AAM- und Silica-Additiv-Konzentrationen abnahmen, wobei die Veränderung der Initiator-Konzentration nur eine mäßige Auswirkung zeigte. Dementsprechend konnte die Porengröße der pAAM-Alg-Mikro kapselmembran allein durch die Einstellung der vorher erwähnten Parameter manipuliert werden.

Ein breites Spektrum gelöster Stoffe – Glucose, Maltose, Dextran T1, Insulin,  $\alpha$ -Lactalbumin und Trypsin – wurde verwendet, um den Molekulargewichtsschwellenwert der pAAM-Alg-Mikro kapseln zu ermitteln. Es hat sich ergeben, dass der Molekulargewichtsschwellenwert einer pAAM-Alg-Mikro kapsel 1 bis 5,7 kDa beträgt. Dieses deutet darauf hin, dass die pAAM-Alg-Mikro kapsel als eine grö ßenselektive Mikro kapsel für Substrate in diesem Molekulargewichtsbereich angewendet werden kann.

Zur Bestimmung der spezifischen und selektiven Eigenschaften verkapselter Enzyme in einer pAAM-Alg-Mikro kapselmembran wurden multi-kompetitive enzymatische Reaktionen durchgeführt. Die von der Lipase *M.Miehei* (MML) katalysierte Umesterung verschiedener Kettenlängen von Fettsäureethylestern ( $C_2$ - $C_{14}$ ) und Alkoholen mit unterschiedlichen Größen, wurde als Testreaktionssystem gewählt. Während das freie Enzym eine hohe Selektivität für den Fettsäureethylester mit einer langen Kettenlänge (ab  $C_8$ -Ethylester) und Butanol aufwies, lieferte das verkapselte Enzym eine hohe Selektivität für den Fettsäureethylester mit einer kurzen Kettelänge ( $C_4$ - und  $C_6$ -Ethylester) und Methanol. Dies ist auf die hydrophilen Eigenschaften der pAAM-Alg-Mikro kapselmembran zurückzuführen.

Die Regelung der selektiven Eigenschaften der pAAM-Alg-Mikro kapselmembran erfolgte durch das Einbringen verschiedener Konzentrationen des hydrophoben Comonomers Isopropyl-Acrylamid (IPPAAM) in die Mikro kapselhülle. Dazu wurden die multi-kompetitiven enzymatischen Reaktionen wiederholt. Die Resultate zeigten, dass die

Eigenschaften der Mikrokapsel durch die Modifizierung der Mikrokapselmembran geringfügig beeinflusst wurden. Bei niedrigen Konzentrationen von IPPAAm wies das verkapselte Enzym eine hohe Selektivität für den Fettsäureethylester mit einer kurzen Kette (C<sub>4</sub>- und C<sub>6</sub>-Ethylester) auf, wobei ein höherer Prozentsatz an IPPAAm (höher als 2,5%) eine Umsetzung der langkettigen Fettsäureethylester (ab C<sub>8</sub>-Ethylester) begünstigt. Dies beruht auf den hydrophoben Eigenschaften des IPPAAm-Monomers. Die modifizierte Mikrokapsel mit einer 10%-IPPAAm-Konzentration zeigte eine hohe Selektivität für das kleine Alkohol-Molekül (Methanol).

Die Wiederverwendbarkeit wurde anhand der Durchführung mehrfacher Reaktionszyklen der verkapselten Enzyme in pAAm-Alg-Mikrokapseln getestet. Die verkapselten Enzyme wiesen sogar nach fünf Reaktionszyklen (insgesamt 240 Stunden) noch ca. 90% ihrer anfänglichen katalytischen Aktivität auf. Damit ist von einer hohen Stabilität der Mikrokapseln auszugehen.



---

## Table of Contents

<b>Abstract.....</b>	<b>I</b>
<b>Table of Contents.....</b>	<b>VII</b>
<b>List of Figures.....</b>	<b>XI</b>
<b>List of Tables.....</b>	<b>XIV</b>
<b>Nomenclature-Abbreviations-Greek symbols.....</b>	<b>XVI</b>
<b>1 Introduction.....</b>	<b>1</b>
<b>1.1 General Overview.....</b>	<b>1</b>
<b>1.2 Objective and Motivation .....</b>	<b>4</b>
<b>2 Theoretical Background .....</b>	<b>6</b>
<b>2.1 Polymer Selection .....</b>	<b>6</b>
2.1.1 Alginate.....	6
2.1.2 Acrylamide .....	9
2.1.3 Graft co-polymerisation of acrylamide-alginate.....	10
<b>2.2 Air-jet nozzle.....</b>	<b>11</b>
<b>2.3 Mass transport in gel.....</b>	<b>14</b>
<b>2.4 Multi-competitive lipase reaction .....</b>	<b>17</b>
<b>3 Materials and Methods .....</b>	<b>20</b>
<b>3.1 Materials.....</b>	<b>20</b>
<b>3.2 Characterisation of microcapsules .....</b>	<b>20</b>
3.2.1 Microcapsule photography .....	21
3.2.2 Image analysis .....	21
3.2.3 Membrane thickness.....	22
<b>3.3 Construction of nozzle .....</b>	<b>23</b>
<b>3.4 Determination of sugar and protein concentrations.....</b>	<b>25</b>
3.4.1 Quantitative sugar analysis.....	25
3.4.2 Quantitative protein analysis.....	25
<b>3.5 GC Analysis for lipase reaction .....</b>	<b>26</b>

---

<b>4</b>	<b>Experimental procedure .....</b>	<b>27</b>
<b>4.1</b>	<b>Preparation of microcapsules.....</b>	<b>27</b>
4.1.1	Preparation of polymer solution .....	27
4.1.2	Preparation of gelling bath .....	28
4.1.3	Apparatus for microcapsule preparation.....	29
4.1.4	Variation of operating parameters .....	30
4.1.5	Microcapsule preparation.....	31
<b>4.2</b>	<b>Diffusion and MWCO experimentation.....</b>	<b>32</b>
4.2.1	Effect of monomer, cross-linker and initiator concentration on diffusion coefficient.....	32
4.2.2	Effect of Silica HS-30 on diffusion coefficient.....	33
4.2.3	MWCO of pAAm-Alg microcapsules .....	33
4.2.4	Preparation of DNS Solution .....	33
<b>4.3</b>	<b>Loading efficiency test .....</b>	<b>34</b>
<b>4.4</b>	<b>Multi-competitive lipase reaction assay .....</b>	<b>34</b>
<b>4.5</b>	<b>Reusability test.....</b>	<b>36</b>
<b>5</b>	<b>Results and Discussion .....</b>	<b>37</b>
<b>5.1</b>	<b>Characterisation of pAAm-Alg microcapsules.....</b>	<b>37</b>
5.1.1	The effect of physicochemical properties on microcapsule preparation ..	38
5.1.2	Extrinsic parameters in microcapsule preparation.....	44
5.1.3	Membrane thickness.....	50
5.1.4	Summary .....	52
<b>5.2</b>	<b>Diffusion and MWCO of pAAm-Alg microcapsules .....</b>	<b>53</b>
5.2.1	Influence of AAm monomer concentration on sugar diffusion.....	54
5.2.2	Influence of Bis-AAm cross-linker concentration on sugar diffusion .....	55
5.2.3	Influence of initiator concentration on sugar diffusion .....	57
5.2.4	Influence of silica additive on sugar diffusion.....	59
5.2.5	MWCO of pAAm-Alg microcapsules .....	61
5.2.6	Summary .....	64
<b>5.3</b>	<b>Multiple substrate competitive reactions: the determination of the specificity of lipase encapsulated in permselective microcapsules .....</b>	<b>65</b>
5.3.1	Loading efficiency of lipase MML in pAAm-Alg microcapsules .....	65
5.3.2	Competitive reaction of fatty acid ethyl esters toward free and encapsulated lipase MML in pAAm-Alg microcapsules.....	66

---

5.3.3 Competitive reaction of alcohols toward free and encapsulated lipase MML in pAAm-Alg microcapsules.....	67
5.3.4 Competitive reaction among the most selective fatty acid ethyl esters and alcohols toward free and encapsulated lipase MML in pAAm-Alg microcapsules .....	69
5.3.5 Summary .....	71
<b>5.4 Modification of pAAm-Alg microcapsules with hydrophobic IPPAAm monomer .....</b>	<b>71</b>
5.4.1 Characterisation of modified pAAm-IPPAAm-Alg microcapsules .....	71
5.4.2 Loading efficiency of encapsulated lipase MML in pAAm-IPPAAm-Alg at different concentrations .....	73
5.4.3 Competitive reaction of fatty acid ethyl esters toward free and encapsulated enzyme lipase MML in pAAm-IPPAAm-Alg microcapsules .....	74
5.4.4 Competitive reaction of alcohols toward free and encapsulated enzyme lipase MML in pAAm-IPPAAm-Alg microcapsules .....	76
5.4.5 Competitive reaction of the most selective fatty acid ethyl esters and alcohols toward free enzyme and encapsulated enzyme lipase MML in pAAm-IPPAAm-Alg microcapsules .....	78
5.4.6 Competitive reaction of fatty acid ethyl esters (C <sub>6</sub> and C <sub>8</sub> ) and two alcohols toward free enzyme and encapsulated enzyme lipase MML in pAAm-IPPAAm-Alg microcapsules .....	81
5.5 Reusability.....	83
<b>6 Mass transfer enhancement by encapsulated magnetic nanoparticles in the liquid core of microcapsules .....</b>	<b>86</b>
6.1 Background.....	86
6.2 Materials and Methods .....	86
6.2.1 Preparation of Ca-Alg microcapsules.....	87
6.2.2 Preparation of magnetic nanoparticles and magnetic microcapsules .....	87
6.2.3 Influence of magnetic field on magnetic microcapsules.....	88
6.2.4 Diffusion of dextran T1 from bulk liquid into microcapsules .....	88
6.2.5 Dextranase reaction activity .....	89
6.3 Results and Discussion .....	89
6.3.1 Characterisation of Ca-Alg and magnetic microcapsules.....	89
6.3.2 Influence of a magnetic field on magnetic microcapsules.....	90
6.3.3 Diffusion coefficient of dextran T1 into Ca-Alg and magnetic microcapsules .....	91

6.3.4 Loading efficiency of dextranase in full and hollow Ca-Alg microcapsules  
94

6.3.5 Enzyme activity of full and hollow-magnetic Ca-Alg microcapsules..... 94

6.4 Conclusions ..... 95

7 Summary and Outlook.....97

8 Literature.....99

9 Appendix A..... 109

9.1 Analytical Equipment ..... 109

9.1.1 Light microscopy and Stereo-microscopy ..... 109

9.1.2 Rotational Viscometer ..... 110

9.1.3 Tensiometer ..... 111

9.2 Calibration of peristaltic pump and micro-gear pump ..... 112

---

## List of Figures

Figure 1-1: Morphology of microcapsules .....	2
Figure 1-2: Concentration profile due to transport resistances .....	3
Figure 2-1: M-block, G-block, and the alginate chain structure [40] .....	7
Figure 2-2: Formation of calcium-alginate network at low/high concentrations [43] .....	8
Figure 2-3: Polymerisation and cross-linking of AAm [48] .....	10
Figure 2-4: Schematic of graft co-polymer .....	10
Figure 2-5: Reaction scheme for synthesis of pAAm graft alginate co-polymer.....	11
Figure 2-6: Double nozzle concentric air-jet.....	12
Figure 2-7: Droplet formation .....	12
Figure 3-1: Steps in image analysis.....	21
Figure 3-2: Illustration of circularity shape descriptor.....	22
Figure 3-3: Comparison the microcapsule picture taken with: (a) light microscope and (b) stereo-microscope.....	23
Figure 3-4: Schematic representation of air-jet nozzle .....	23
Figure 3-5: Nozzle structure.....	24
Figure 3-6: DNS reduction reaction according to Miller .....	25
Figure 4-1: Flow-sheet of the encapsulation device and nozzle details.....	29
Figure 5-1: Histograms of equivalent diameter (0.03 mm intervals) and circularity (0.01 intervals).....	37
Figure 5-2: Average equivalent diameter and circularity for various core solution volumetric flow rates .....	40
Figure 5-3: Images of microcapsules under light microscope with (a) 1%, (b) 2%, (c) 4% Bis-AAm.....	43
Figure 5-4: Images of microcapsules taken by stereo-microscope .....	50
Figure 5-5: Membrane thicknesses of various microcapsules .....	51

---

Figure 5-6: Change in membrane thickness during the gelling process .....	51
Figure 5-7: Concentration profiles of glucose and dextran T1 diffusing into pAAm-Alg microcapsules at different AAm concentrations. The points are the experimental data and the solid curves represent the results calculated using eq.2-16.....	54
Figure 5-8: Concentration profiles of glucose and dextran T1 diffusing into pAAm-Alg microcapsules at different Bis-AAm concentrations. The points are the experimental data and the solid curves represent the results calculated using eq. 2-16.....	56
Figure 5-9: Concentration profiles of glucose and dextran T1 diffusing into pAAm-Alg microcapsules at different initiator concentrations. The points are the experimental data and the solid curves represent the results calculated using eq. 2-16.....	58
Figure 5-10: Concentration profile of glucose diffusing into pAAm-Alg microcapsules with different concentrations of silica HS30 additive. The points are experimental data and the solid curves represent the results calculated using Eq. 2-16.....	60
Figure 5-11: Diffusion curves of different probe molecules in pAAm-Alg microcapsules. The points are the experimental data and the solid curves represent the results calculated using Eq. 2-16.....	62
Figure 5-12: Diffusion coefficients versus molecular weights of glucose 180 Da, maltose 360 Da, dextran T1 1.1 kDa, Insulin 5 kDa, $\alpha$ -lactalbumin 15 kDa and Trypsin 23 kDa .....	63
Figure 5-13: Concentrations of propyl esters of different chain lengths from free enzyme and encapsulated enzyme in pAAm-Alg microcapsules.....	66
Figure 5-14: Concentrations of C <sub>8</sub> ester with different acyl groups from free enzyme and encapsulated enzyme in pAAm-Alg microcapsules.....	68
Figure 5-15: Concentrations of C <sub>4</sub> methyl ester, C <sub>4</sub> butyl ester, C <sub>8</sub> methyl ester and C <sub>8</sub> butyl ester from free enzyme and encapsulated enzyme in pAAm-Alg microcapsules.....	70
Figure 5-16: Concentrations of propyl ester for different chain lengths with free and encapsulated enzyme in pAAm-Alg and pAAm-IPPAAm-Alg microcapsules.....	74
Figure 5-17: Concentration of C <sub>8</sub> ester with different alkyl groups for free and encapsulated enzyme in pAAm-Alg and pAAm-IPPAAm-Alg microcapsules .....	76

---

Figure 5-18: Concentrations of C <sub>4</sub> methyl ester, C <sub>4</sub> butyl ester, C <sub>8</sub> methyl ester and C <sub>8</sub> butyl ester for free enzyme and encapsulated enzyme in pAAm-Alg and pAAm-IPPAAm-Alg microcapsules .....	78
Figure 5-19: Relative activity of the encapsulated enzymes in pAAm-Alg and pAAm-IPPAAm-Alg microcapsules with respect to the free enzymes .....	81
Figure 5-20: Concentrations of C <sub>6</sub> methyl ester, C <sub>6</sub> butyl ester, C <sub>8</sub> methyl ester and C <sub>8</sub> butyl ester for free enzyme and encapsulated enzymes in pAAm-Alg and pAAm-IPPAAm-Alg microcapsules .....	82
Figure 5-21: Relative activity of reused enzyme lipase encapsulated in pAAm-Alg microcapsules .....	84
Figure 6-1: Images of a full (left) and a hollow (right) microcapsule.....	89
Figure 6-2: Images of magnetic nanoparticles (15-20 nm) and a magnetic microcapsule.....	90
Figure 6-3: Displacement of magnetic microcapsules at various magnetic field frequencies .	91
Figure 6-4: Concentration profiles of dextranT1 diffusing into full, hollow, and magnetic microcapsules with encapsulated magnetic nanoparticles at concentrations of 1, 2, and 3 mg/ml. The points are the experimental data and the curves represent the results calculated using the “Analysis data fitting (ExpDec1)” function from the “Origin” programme. ....	92
Figure 6-5: Isomaltose concentration generated by free and encapsulated dextranase.....	94
Figure 9-1: (a) Transmitted light microscope (b) Reflected light microscope.....	109
Figure 9-2: A LEICA MZ-95 stereo microscope [3] .....	110
Figure 9-3: Schematic diagram of the ring method tensiometer [4] .....	111
Figure 9-4: Calibration curves for micro-gear and peristaltic pumps with water .....	112

---

## List of Tables

Table 4-1: Variation of intrinsic operating parameters .....	30
Table 4-2: Variation of extrinsic operating parameters .....	31
Table 5-1: Classification criteria for qualitative characterisation of microcapsules .....	38
Table 5-2: Density and viscosity of the polymer solution at various monomer and cross-linker concentrations, and surface tension of the gelling bath for various initiator concentrations ...	39
Table 5-3: Ratios of volumetric flow rates.....	41
Table 5-4: Equivalent diameter, circularity, membrane thickness, and production rate of pAAm-Alg microcapsules at different parameters.....	42
Table 5-5: Equivalent diameter, circularity, quality classification, and production rate of pAAm-Alg microcapsules for different numbers of rings .....	45
Table 5-6: Equivalent diameter, circularity, quality classification, and production rate of pAAm-Alg microcapsules for different nozzle outlet types .....	47
Table 5-7: Equivalent diameter, circularity, quality classification, and production rate of pAAm-Alg microcapsule for different needle lengths.....	48
Table 5-8: Equivalent diameter, circularity, quality classification, and production rate of pAAm-Alg microcapsules at different nozzle ring inner diameters .....	49
Table 5-9: Diffusion coefficients ( $D_m$ , $D_1$ , and $S$ ) of pAAm-Alg microcapsules at different AAm concentrations.....	55
Table 5-10: Diffusion coefficients ( $D_m$ , $D_1$ , and $S$ ) of pAAm-Alg microcapsules at different cross-linker Bis-AAm concentrations .....	57
Table 5-11: Diffusion coefficients ( $D_m$ , $D_1$ , and $S$ ) of pAAm-Alg microcapsules at different initiator concentrations.....	58
Table 5-12: Diffusion coefficients ( $D_m$ , $D_1$ , and $S$ ) of pAAm-Alg microcapsules at different silica HS-30 concentrations.....	60
Table 5-13: Diffusion coefficients ( $D_m$ , $D_1$ , $D_2$ , and $S$ ) for different probe molecules in pAAm-Alg microcapsules.....	62



---

Table 5-14: Specificity constant values for transesterification of different acyl donors C <sub>2</sub> to C <sub>14</sub> ethyl ester with n-propanol toward free and encapsulated lipase MML in pAAm-Alg microcapsules .....	67
Table 5-15: Specificity constant values for transesterification of C <sub>8</sub> ethyl octanoate with different alcohol acceptors: methanol, n-propanol, n-butanol, n-propanol in pAAm-Alg microcapsules .....	68
Table 5-16: Specificity constant values for transesterification of C <sub>4</sub> , C <sub>8</sub> ethyl ester with methanol, n-butanol in pAAm-Alg microcapsules .....	70
Table 5-17: Diameter and membrane thickness of pAAm-Alg and pAAm-IPPAAm-Alg microcapsules at different IPPAAm concentrations .....	72
Table 5-18: Loading efficiency of encapsulated lipase MML in pAAm-IPPAAm-Alg microcapsules at different IPPAAm concentrations .....	73
Table 5-19: Specificity constant values for transesterification of different acyl donors C <sub>2</sub> to C <sub>14</sub> ethyl ester with n-propanol in various media/microcapsules.....	75
Table 5-20: Specificity constant values for transesterification of C <sub>8</sub> ethyl octanoate with different alcohol acceptors; methanol, n-propanol, n-butanol, n-propanol in various media ..	77
Table 5-21: Specificity constant values for transesterification of C <sub>4</sub> , C <sub>8</sub> ethyl ester and methanol, n-butanol.....	79
Table 5-22: Specificity constant values for transesterification of C <sub>6</sub> and C <sub>8</sub> ethyl ester with methanol and n-Butanol .....	82
Table 6-1: D <sub>m</sub> and S of dextran T1 diffusing into full, hollow, and magnetic microcapsules with encapsulated magnetic nanoparticles at concentrations of 1, 2, and 3 mg/ml .....	93

## Nomenclature

Symbol	Description	Units
J	Flux	mol/(m <sup>2</sup> ·s)
A	Area of diffusion	m <sup>2</sup>
A <sub>E</sub>	Peak area of the ethyl esters under GC analysis	-
A <sub>P</sub>	Peak area of the propyl esters under GC analysis	-
D	Diffusion coefficient	m <sup>2</sup> /s
C	Concentration	g/ml
Z	Distance	m
$\partial c/\partial z$	Concentration gradient in z direction	mol/m <sup>4</sup>
C (%)	Cross-linking ratio	%
C <sub>o</sub>	Initial concentration of bulk solution	mol/m <sup>3</sup>
C <sub>L</sub>	Concentration of bulk solution	mol/m <sup>3</sup>
D <sub>m</sub>	Combined diffusion coefficient	<sup>2</sup> /s
D <sub>1</sub>	Diffusion coefficient in the membrane of the capsule	m <sup>2</sup> /s
D <sub>2</sub>	Diffusion coefficient in the liquid core of the capsule	m <sup>2</sup> /s
D <sub>w</sub>	Diffusion coefficient in pure water	m <sup>2</sup> /s
q <sub>n</sub>	Nonzero positive roots of Eq.(4)	-
PM <sub>P</sub>	Molecular weight of propyl ester	g/mol
PM <sub>E</sub>	Molecular weight of ethyl ester	g/mol
R	Distance from the sphere core	m
R	External radius of the solid sphere	m
r <sub>a</sub>	Internal radius of the microcapsule	m
r <sub>b</sub>	External radius of the microcapsule	m
T	Time	second
A	Ratio of the liquid volume to the capsule volume	-
S	Sum of error square	-
rpm	Revolutions per minute	min <sup>-1</sup>
mm	Millimeter	10 <sup>-3</sup> m
nm	Nanometer	10 <sup>-9</sup> m
μm	Micrometer	10 <sup>-6</sup> m

<b>Symbol</b>	<b>Description</b>	<b>Units</b>
$D_{eq.}$	Equivalent diameter	m
F	Friction factor	
P	Perimeter	m
U	Fluid velocity inside the pipe	m/s
$\dot{V}$	Core solution volumetric flow rate	ml/min
$k_A$	Reaction rate of substrate A	IU/g
$k_B$	Reaction rate of substrate B	IU/g
$[A]_t$	Concentration of A at time t	mol/l
$[A]_0$	Concentration of A at time 0	mol/l
$[B]_t$	Concentration of B at time t	mol/l
$[B]_0$	Concentration of B at time 0	mol/l
C	Conversion	-
$C_i$	initial protein concentration	g/cm <sup>3</sup>
$V_i$	the initial volume of enzyme solution	cm <sup>3</sup>
$C_e$	protein concentration encapsulated in microcapsule	g/cm <sup>3</sup>
$V_e$	volume of encapsulated enzyme solution	cm <sup>3</sup>
$d_p$	Droplet diameter	m
$d_{Cap}$	Capillary diameter	m
$F_G$	Gravitation force	N
$F_B$	Buoyancy force	N
$F_R$	Resistance force	N
$F_\sigma$	Interfacial tension force	N
$F_{Max}$	Maximum force	
$F_V$	Weight of volume of liquid lifted	
$V_P$	Particle volume	M <sup>3</sup>
G	Gravitational acceleration	m/s <sup>2</sup>
$v_{Air}$	Air flow velocity	m/s
$c_w$	Flow resistance	
$Re_p$	Reynold number	
$D^*$	Cross section	m <sup>2</sup>

## Abbreviation

Symbol	Description	Units
AAM	Acrylamide	
Alg	Alginate, Alginic acid sodium salt	
Bis-AAM	N,N-methylene-bis-acrylamide	
IPPAAM	Isopropyl Acrylamide	
pAAM	Polyacrylamide	
pIPPAAM	Polyisopropyl acrylamide	
pAAM-Alg	Polyacrylamide-Alginate	
pAAM-IPPAAM-Alg	Polyacrylamide-Isopropylamide-Alginate	
TBHP	Tert-butyl hydroperoxide	
MML	Lipase M.Miehei	
Tris	Tris(hydroxymethyl) aminomethane	
DNS	3,5- dinitrosalicylic acid	
M	Mole	
L	Liter	
L	Wetted length	
Da	Daltons	
K	Kilo	
kDa	Kilodalton	
MWCO	Molecular weight cut-off	
cPS	Centi poise second	
rpm	Revolutions per minute	
E	Enzyme	
Prod.	Production	

## Greek Symbol

Symbol	Description	Units
$\rho_{\text{Sol}}$	Density of solution	kg/m <sup>3</sup>
$\rho_c$	Density of continuous phase	kg/m <sup>3</sup>
$\Sigma$	Surface tension	N/m
H	Dynamic viscosity	Pa·s
$\dot{\gamma}$	Shear rate	s <sup>-1</sup>
$\tau$	Shear stress	N/m
$\dot{n}$	Number of rotations	
$\Theta$	Contact angle	
$\Delta p$	Pressure drop	Pa
$\alpha$	Competitive factor	

# 1 Introduction

## 1.1 General Overview

Immobilisation is a technique primarily used to facilitate catalyst recovery and reuse, but which can also improve stability, enhance substrate selectivity, and diminish susceptibility to inhibition. The technique of immobilisation used for chemical or physical fixation of cells, enzymes, organelles or other proteins, catalysts on to a solid support, into a solid matrix or by membrane retention, in order to increase the stability and make possible the repeated and continuous use of the active component [1-8].

Encapsulation along with covalent binding, entrapment, electrostatic interaction and adsorption are the most common methods for catalyst immobilisation based on an interaction between the catalyst and the support [9-16]. Covalent binding uses modification of the catalyst ligand to bind it on to a carrier such as nylon, bentonite, cellulose, and dextran. Adsorption relies on the interaction of van der Waals interactions between catalyst and support, while electrostatic interaction involves ionic association between the catalyst and support. Both of these methods cause the catalyst being in close proximity to the support, which may affect the ligand conformation and electronic properties. Moreover, the support material used in traditional immobilisation approaches can, however, lead to mass transfer resistances, resulting in lower selectivity and conversions as well as distortions in the catalysts. Catalyst immobilisation by encapsulation is the only method that does not require any interaction between the catalyst and the support [11, 17,18].

Encapsulating a catalyst or enzyme entails confinement of liquid solution within small microcapsules enclosed by a polymer shell. To prevent loss of catalyst into the solution during the course of reaction, the size of the catalyst must be larger than the pores of the support material. On the other hand, the support material must be able to provide a good mass transfer between the catalyst and substrate. The supported catalyst is prepared either by i) assembling the catalyst within the pores of the support or ii) assembling the support around the catalyst [11,17]. The method for encapsulating a catalyst is known as microencapsulation.

Microencapsulation is the process of enclosing micron-sized particles/active components of solids or droplets of liquid or gas bubbles in an inert shell, which in turn isolate and protects them from the atmosphere. Microencapsulation provides the possibility of combining the

properties of different materials - a process that is difficult to achieve using other techniques. The products of microencapsulation – microcapsules, with a diameter in the range of 1 micron to 1,000 microns, have a spherical or irregular shape consisting of a core containing the active ingredient and a shell that protects the core temporarily or permanently. The compatibility of the shell and the core material is crucial for the efficiency of microencapsulation. Various natural and man-made polymers provide a wide choice for shell material, being permeable, semi-permeable or impermeable depending on the application. Based on their morphology, microcapsules can be classified as mononuclear, polynuclear, and matrix types (Figure 1-1). Mononuclear or *hollow microcapsules* have a membrane around the core material, while polynuclear microcapsules have many distinct cores within the shell. In matrix encapsulation, the core material is distributed homogeneously into the shell material. In this case one can refer to *full microcapsules* [19-23].

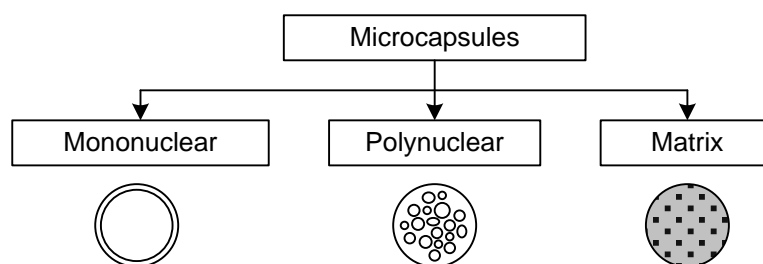


Figure 1-1: Morphology of microcapsules

With respect to mass transfer, within full microcapsules which the active material is bounded to the support material exhibits higher mass transfer resistances than hollow microcapsules where the active component is free to move around inside the liquid core.

The desired properties of the microcapsule required to achieve the functionalities and mass transfer characteristics sought are, good resistance to mechanical stress, long-time stability, thin walls (to minimize the mass transfer resistances), spherical and concentric inner-outer core structure, small size (micrometer range) to increase the specific surface area and a uniform, narrow size distribution. The key factor is the choice of an appropriate membrane that allows complete retention of the catalyst and unhindered passage of the desired substrates and products.

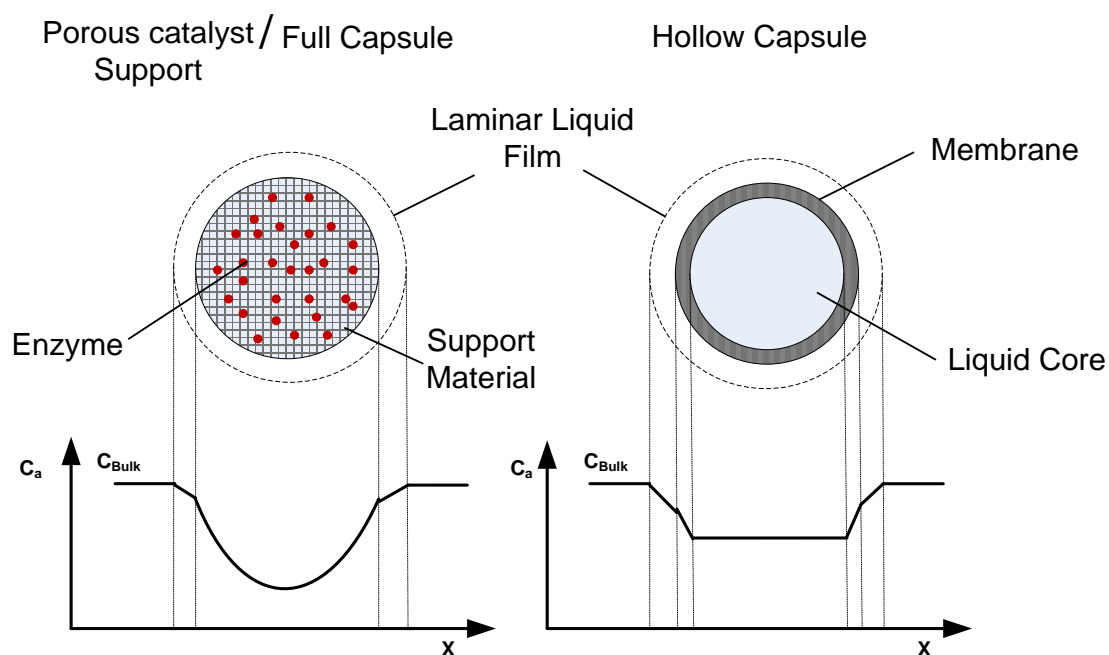


Figure 1-2: Concentration profile due to transport resistances

Both natural and/or synthetic polymers are used as shell material in these immobilisation procedures. Some well-known of natural biopolymers applied in microcapsule production are calcium alginate, chitosan, agarose, cellulose etc. The distinct advantages of the natural biopolymers lie in their biocompatibility and availability. However, biopolymers possess poor mechanical stability and may break down under harsh condition. Synthetic polymers are employed to overcome these shortcomings. Examples of some of the synthetic polymers applied in microencapsulation technique are polylysine, polyurethane, polyethyleneimine, polyacrylic acid, polystyrene, polyester, polystyrene sulfonate, etc. [24-27].

The physiochemical properties of such shell materials can have an effect on the reactions of the active material enclosed. The pore size is the critical parameter affecting the diffusion of substrate and products and limiting the reaction rates of the active material. The membrane pore size must be small enough to retain the catalyst enclosed, allowing the diffusion of substrates into and products out of the core. The viscosity of the carrier and/ or its concentration is reflected by the pore size of the gel, which gives the technique a distinct advantage controlling the pore size [28].

For efficient mass transfer, the surface area to volume ratio of the capsules should be high and the capsules should have a uniform size. Diffusion plays a major role in the mass transfer mechanism of microcapsules, since the substrate diffuses through the outer gel membrane to reach the active core. The gel membrane introduces an additional mass transfer resistance



giving rise to the major mass transfer limitation in the microcapsule system [29]. The evaluation of the mass transport properties of microcapsule membranes and microcapsules as a whole is often investigated by determination of molecular weight cut-off (MWCO) values and the diffusion coefficient of appropriate substrates able to freely enter the microcapsules, and of the reaction products which can be transported out. The MWCO value gives an insight into the minimum size of the active material that can be encapsulated using the membrane, where-as the value of diffusion coefficient gives an idea of the rate of substrate diffusion into the microcapsules.

Apart from the simple retention of the catalyst within the microcapsule, the membrane can also act as a permselective barrier that only allows certain substrates access to the catalyst. For example, size and charge selective retention of aromatic compounds have been controlled by poly(allylamine hydrochloride)/poly(sodium styrenesulfonate) membranes [30], silicon membranes [31], polystyrene/polyacrylamide [32] and in poly(diallyldimethylammonium chloride) membranes [33]. The permselectivity of a membrane can be controlled by manipulating properties such as composition, pore size and even thickness.

According to Buonomenna et al., 2008 [34], a microcapsule can be classified as a volume enclosed by a catalytically inert membrane, which serves as a selective barrier to reactants that diffuse into and products that diffuse out of the microcapsule core solution containing the catalyst. Moreover, microcapsules can be considered as multifunctional catalytic micro-membrane reactors, in the sense that the membrane shell mediates the transport of substrate and product, while the catalyst provides the reactive functionality. Thus, microencapsulation can also be regarded as a process intensification measure by virtue of the extremely high specific surface area it provides for permeation. While the manipulation of microcapsule permeation has been exploited extensively for the purposes of controlled release, its use to regulate access to immobilised catalysts, in analogy to the powerful tool of zeolitic catalysis, has attracted little attention.

## **1.2 Objective and Motivation**

The aim of this thesis is to prepare microcapsules having permselective properties for industrial application. In previous work, the microcapsules were produced from calcium alginate, which offers biocompatibility and facile gelation. However, it exhibits relatively poor mechanical stability. This research presented here is focussed on applying

polyacrylamide, a synthetic polymer to co-polymerize with the biopolymer alginate in order to achieve both good biocompatibility and mechanical stability whilst permitting manipulation of the permselective properties of the microcapsules.

The research work starts with the preparation and quantitative characterisation of pAAm-Alg microcapsules using an air-jet nozzle with varying both the intrinsic and extrinsic parameters involved. The mass transfer of different solutes and molecular weight cut-off of the microcapsule membrane, which represents the size selective property of the microcapsule were then studied. Next, the permselective properties of pAAm-Alg membrane were investigated for the encapsulated enzyme lipase MML inside microcapsules and the selectivity of free enzyme and encapsulated enzyme towards substrates in a multi-competitive reaction were compared. Finally, the pAAm-Alg microcapsule membrane was modified by a hydrophobic co-monomer isopropyl acrylamide (IPPAAm), yielding pAAm-IPPAAm-Alg microcapsule membranes, which permit fine tuning of the hydrophobic-hydrophilic property of the original pAAm-Alg membranes. Additional study on the influence of an encapsulation of magnetic nanoparticles inside the liquid core, which induced by the external alternating magnetic field, to generate the convection within calcium alginate microcapsules, was presented in the last section.

## 2 Theoretical Background

### 2.1 Polymer Selection

The type of polymer used plays a decisive role in the properties of a microcapsule membrane. The driving force for the transport of solutes across the polymer membrane can be either a gradient in pressure, concentration, electric potential or temperature, depending on the properties of the membrane material selected. The pore size of the polymer membrane allows for tuneable permselectivity towards solutes. The potential deficiencies in microcapsules also depend on the properties of membrane material. The design of a microcapsule membrane should consider the premature failure of the microcapsule shell insuring service [23].

The selection of the polymeric material for the membrane is crucial to achieve the desired membrane structure, which in turn determines its application. The mechanical, thermal and chemical stability under reaction conditions is the major issue in the polymer selection. A high catalyst loading should be possible without causing brittleness of the film. The polymer should exhibit excellent film forming properties. Apart from the stability, the polymer should possess good transport properties for the reactants and products [23].

Even though a myriad of polymeric materials exist, it should be stressed that there is no general polymeric membrane material for all applications in catalysis and organic syntheses. Every polymer has its individual drawbacks, such as poor chemical stability, unwanted polarity etc. Combinations of polymers, including blends of natural and synthetic polymers are used to achieve the desired functionality in many applications [23,35-37].

#### 2.1.1 Alginate

In this study, alginate was selected as a suitable encapsulating polymer due to its biocompatibility and excellent gelation properties under mild conditions, especially for the immobilisation of particular enzymes and living cells. 'Alginate' is a term used for the salts of alginic acid, and to all the derivatives of alginic acid and alginic acid itself [6,7,38,39]. Alginate is present in the cell wall of brown algae as the sodium, calcium and magnesium salts of alginic acid. The structure of alginate is a linear anionic co-polymer composed of 1, 4'- linked  $\beta$ -D mannuronic acid (M) and  $\alpha$ -L-guluronic acid (G) in different proportions and sequential arrangement (MMMMMMM, GGGGGG and GMGMGMGM) and with different

conformational behaviour. The monomer composition of alginate and its chain is illustrated in Figure 2-1.

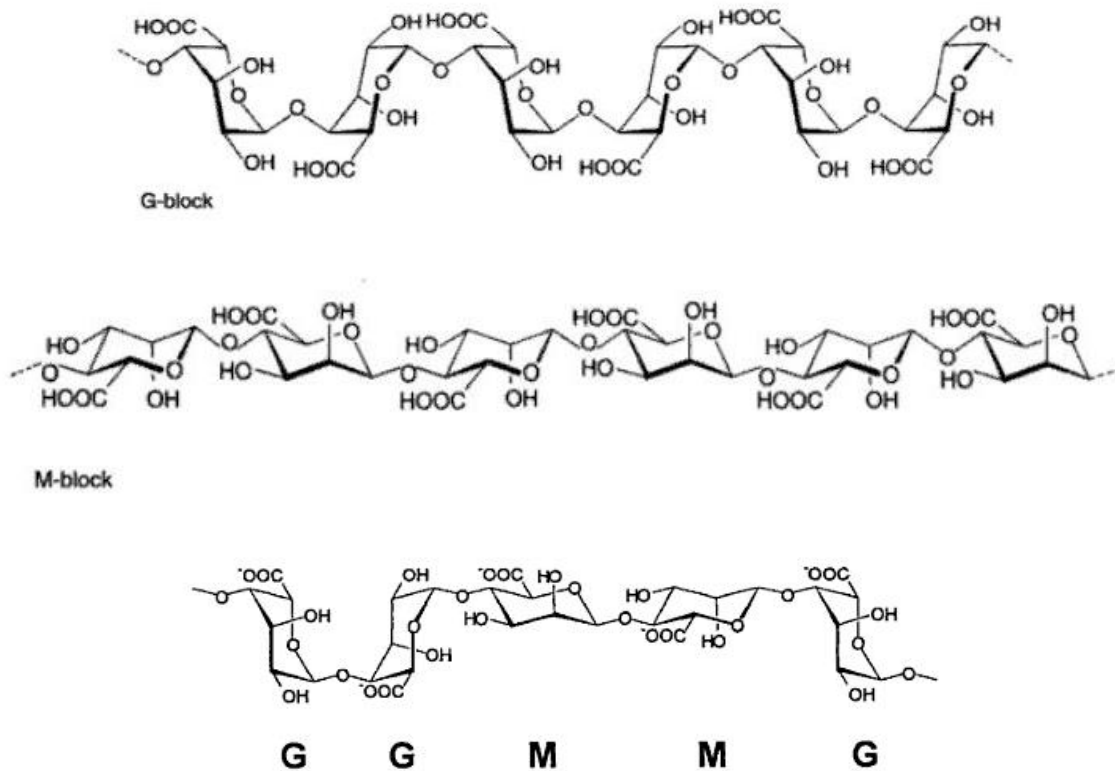


Figure 2-1: M-block, G-block, and the alginate chain structure [40]

The gelling of alginate occurs when the carboxyl groups of the polymers are cross-linked with the di/multivalent cations (e.g.  $\text{Ca}^{2+}$ ,  $\text{Ba}^{2+}$ , and  $\text{Fe}^{3+}$ ). The intrinsic inflexibility of the alginate molecules in solution increases in the order  $\text{MG} < \text{MM} < \text{GG}$ , whilst its viscosity is mainly a function of the molecular size. The exchange of sodium ions from the  $\alpha$ -L-guluronic acids block with divalent ions and the stacking of these guluronic groups in a highly co-ordinated manner forms the so-called egg box structure (Zipper mechanism) [40,41].

Alginate gel has a remarkably higher affinity towards  $\text{Ca}^{2+}$  ions than the Na-alginate solution [40,42]. The ion exchange process between sodium and calcium is almost 50% complete in the first 5 minutes and subsequently the calcium concentration in the gel slowly increases to reach a maximum. The cations combine quickly with the biopolymer to link the chains together and further diminishing the cation diffusion and substitution process. After about 10 minutes in the  $\text{CaCl}_2$  bath, the cations concentration is constant, with only 10 % of sodium ions remaining in the film as shown in Figure 2-2.

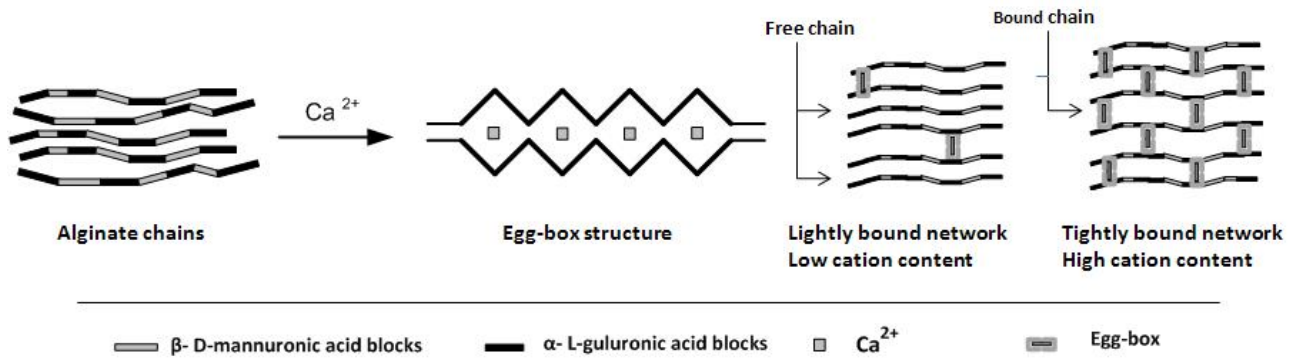


Figure 2-2: Formation of calcium-alginate network at low/high concentrations [43]

Considering the properties of calcium alginate matrix, chemical composition and molecular weight of alginate affect the diffusion and mechanical properties of the calcium alginate gel, which are the critical parameters in selection of an immobilisation matrix. Depending on the nature of the cross-linking cations, the length of the polymeric chains, the M:G ratio and the percentage of the block structures, hydrogels of varying mechanical strength, elasticity and swelling characteristics can be generated. High-M alginates can produce elastic microcapsules when they are cross-linked with  $\text{Ba}^{2+}$ , whereas microcapsules based on high G-alginates exhibit high mechanical strength. Combining high-M and high-G alginates can yield flexible microcapsules with the desired mechanical strength. The pore size of the calcium alginate gel, which is influenced by the M:G concentration ratio and gelation time, can be used to regulate the diffusion of various substrates or products and the retention of active catalytic components within the microcapsule. The temperature and pH under gelling conditions also influences the diffusion and mechanical properties [24,25,41,42].

However, due to the inherent nature of the alginate molecule as a biodegradable polydisperse material, and the properties of the gel as a reversible ionic network alginate-based microencapsulation has some limitations. As a consequence of the latter, substances with high affinity for calcium ions such as phosphate and citrate will remove the cross-linking calcium ions and destabilise the gel. Since the calcium ions can be exchanged with other cations, the gel will also be destabilised by high concentrations of non-gelling ions, such as sodium and magnesium. Therefore, much research has been devoted to improving the stability of alginate gels through the covalent cross-linking with polyethyleneimine (and glutaraldehyde), polyvinyl alcohol, polyacrylamide, propylene glycol, and proteins [44-47].

### 2.1.2 Acrylamide

In this study, polyacrylamide (pAAm) was chosen to co-polymerise with alginate membrane to overcome the deficiencies of alginate gels. In general, polyacrylamide gels are formed by the co-polymerisation of an acrylamide (AAm) monomer and N,N-methylene-bis-acrylamide (Bis-AAm) cross-linker via a vinyl addition polymerisation reaction initiated by a free radical. A traditional pair of radical initiation are ammonium persulfate as the reducing agent and N,N,N,N'-tetramethylethylenediamine (TEMED) as the oxidizing agent. TEMED accelerates the rate of formation of persulfate free radicals, which in turn induce polymerisation. Persulfate free radicals convert AAm monomers to free radicals that then react with other monomers to form the polymer chain [48]. Another possible initiator pair is the use of tert-butyl hydroperoxide (TBHP) as the activator and sodium metabisulfite ( $\text{Na}_2\text{S}_2\text{O}_5$ ) as the acceptor. This redox pair yields a faster rate of polymerisation than the first mentioned one and was thus used in this study. The Bis-AAm crosslinks the elongating polymer chain randomly to form the gel [47-49].

Various factors such as the initiator system and concentration, monomer concentration and their purity along with temperature, time of gelation and presence of inhibitors, have an effect on the polymerisation process and its reproducibility. Poor quality AAm can contain contaminants like acrylic acid, linear pAAm and ionic contaminants that inhibit gel polymerisation, lead to loss of reproducibility of gel porosity and affect local pH changes in the gel. Contaminants in the Bis-AAm and buffer reagents used can cause the same deleterious effects [48]. The concentration of the initiators used affects the properties of the gel. An increase in initiator concentration leads to a decrease in the average polymer chain length, gel elasticity and an increase in gel turbidity. Excess initiator can produce a gel solution that does not appear to polymerise at all and lead to changes in the buffer pH. Decreases in initiator concentration lead to slower polymerisation resulting in longer polymer chain lengths, greater elasticity and lower turbidity. However, slower polymerisation results in the inhibition of the polymerisation with oxygen entering the monomer solution, leading to porous gels that are mechanically weak [48,50].

A faster polymerisation was found to result from increasing the monomer concentration. The practical range of total monomer of AAm and cross-linker Bis-AAm concentration varied from 3 to 30%. Temperature also plays a part in the rate of gel polymerisation and the properties of the resultant gel. Hence, it is important to control the temperature of the

polymerisation for the reproducibility of AAm polymerisation [48]. The polymerisation of monomer AAm and cross-linker Bis-AAm is depicted in Figure 2-3.

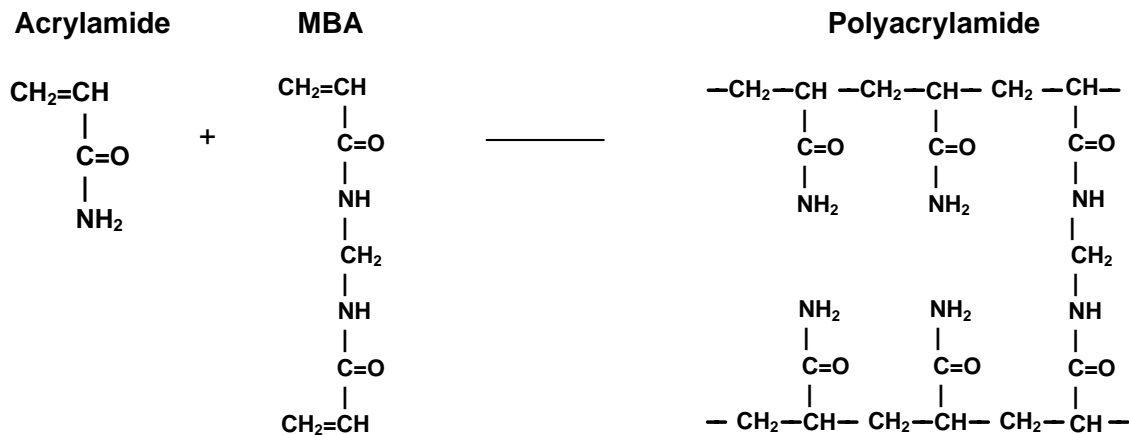


Figure 2-3: Polymerisation and cross-linking of AAm [48]

### 2.1.3 Graft co-polymerisation of acrylamide-alginate

Two or more different polymeric entities may unite chemically to form a high polymer termed a graft co-polymer. These comprise of molecules with one or more species of block connected to the main chain as side chains and having constitutional or configurational features that differ from those of the main chain, independent of the branching locations [49]. Figure 2-4 shows the simplest case of a graft co-polymer.

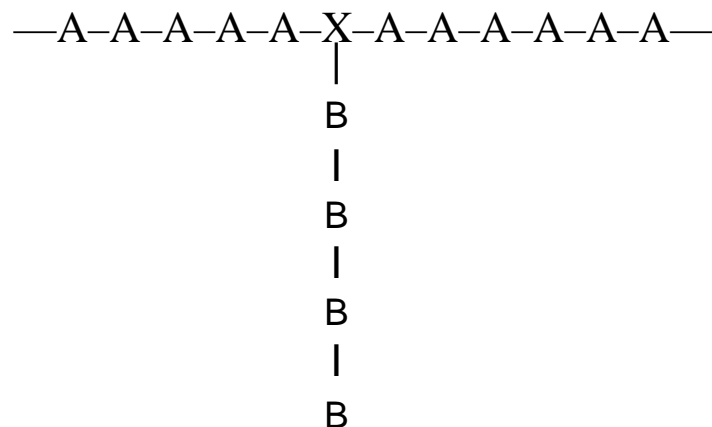


Figure 2-4: Schematic of graft co-polymer

A: represents the main chain, or the backbone, while B is the side chain or the graft. X is the unit in the main chain to which graft is attached. A and B can both be homo-polymers or A homo-polymer and B a co-polymer. Cross-linking can occur in one or more stages. Grafting is

a common method for modifying polymer properties. Graft co-polymerisation improves the properties of natural and synthetic polymers to impart new properties. Upon grafting, the host polymers gain some of the properties of the monomer used for grafting [51].

Free radical polymerisation methods are the oldest and the most widely used procedures for the synthesis of graft polymers, because they are relatively simple [49].

The grafting of polyacrylamide on sodium alginate is of great importance in developing new materials combining the properties of both natural and synthetic polymers. Figure 2-5 shows a reaction scheme adapted from Kulkarni et al [54], for the synthesis of pAAm graft alginate using TBHP as the initiator.

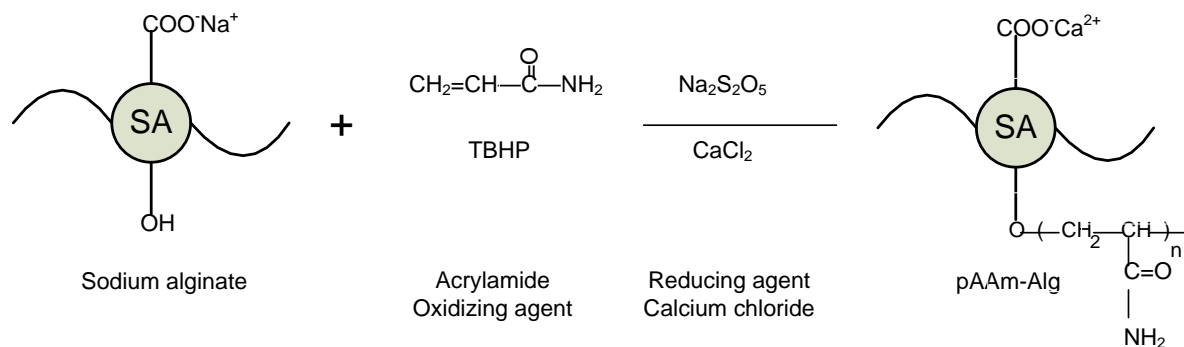


Figure 2-5: Reaction scheme for synthesis of pAAm graft alginate co-polymer

The interaction between two kinds of molecules: the  $-\text{COO}^-$ ,  $-\text{OH}^-$  groups of sodium alginate and  $-\text{CONH}_2$  groups of pAAm establish an inter-chain hydrogen bond that has been shown to increase the thermal stability and improve the mechanical properties of the graft co-polymer pAAm-Alg [52-54].

## 2.2 Air-jet nozzle

A variety of methods have been proposed to prepare microcapsules such as spray coating, droplet generation by inverse emulsion polymerisation, droplet generation using a spray dryer, droplet formation by extrusion with gas followed by coating and many others.

In this work, the microcapsules were prepared in an air-jet nozzle, in which the droplet formation takes place by co-extrusion of the polymer solution and active core. A double liquid nozzle is utilised to prepare the smaller hollow microcapsules. This equipment consists of two concentric capillaries, which release the droplets (Figure 2-6). In the inner capillary, the core solution is supplied and the outer provides the surrounding wall materials. The



droplets formed can be directly dropped into a gelling bath, where the outer part of droplets harden and form the microcapsules. With the aid of compressed air, the microcapsules produced become smaller, depending on the volumetric flow rate of air used.

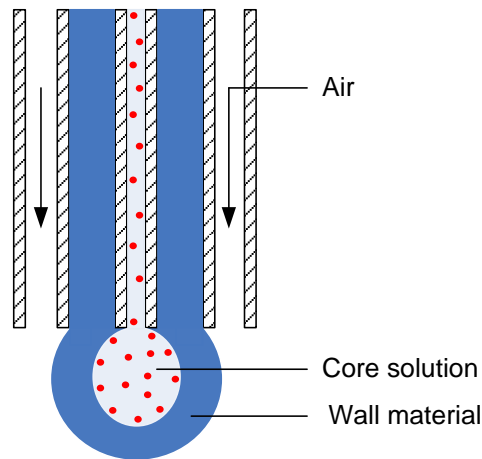


Figure 2-6: Double nozzle concentric air-jet

The principles of the air-jet process can be simply summarised with the aid of the following two assumptions [55]. Firstly, a quasi-static consideration means that the momentum of the solution at the exit of the capillary can be neglected. Consequently, the viscosity of the solution does not influence the dripping mechanism. Secondly, only primary droplets are considered, meaning that only droplets are considered with diameters  $d_P$ , larger than that of the capillary,  $d_{Cap}$ . (Rule of thumb:  $d_P \approx d_{Cap}$ , without air flow).

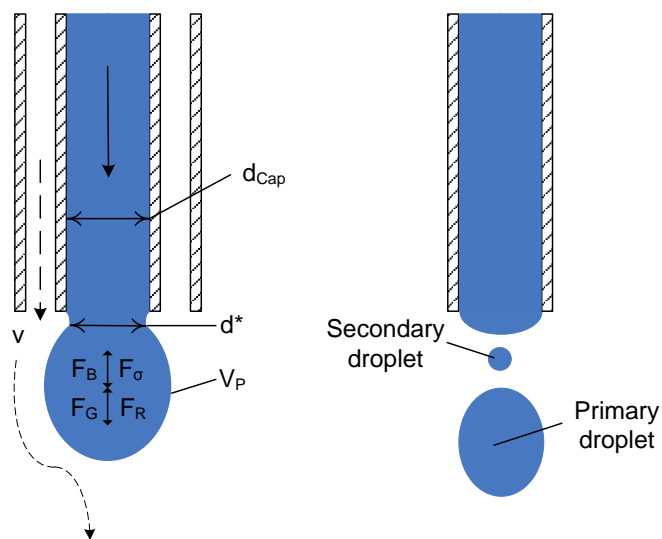


Figure 2-7: Droplet formation

Forces affecting droplet formation are gravitation force ( $F_G$ ), buoyancy force ( $F_B$ ), resistance force ( $F_R$ ), and interfacial tension force ( $F_\sigma$ ). The forces balance according to the following equation:

$$F_G + F_R = F_B + F_\sigma \quad (\text{eq. 2-1})$$

The gravitational force is a result of the particle volume ( $V_P$ ), the density of solution ( $\rho_{Sol}$ ), and the gravitational acceleration ( $g$ ). The buoyancy force is analogous to the weight force. In this case, the density of the continuous phase  $\rho_c$  (air) is used instead of the density of a solution. The forces mentioned above can be described as follows:

$$F_G = V_P \cdot \rho_P \cdot g \quad (\text{eq. 2-2})$$

$$F_B = V_P \cdot \rho_c \cdot g \quad (\text{eq. 2-3})$$

$$F_G - F_B = V_P \cdot (\rho_P - \rho_c) \cdot g \quad (\text{eq. 2-4})$$

$$= \frac{4}{3} \cdot \pi \cdot \frac{d_P^3}{8} \cdot (\rho_P - \rho_c) \cdot g = \frac{1}{6} \cdot \pi \cdot d_P^3 (\rho_P - \rho_c) \cdot g$$

The interfacial tension force  $F_\sigma$ , which acts in the opposite direction to the gravitational force, is a result of surface tension  $\sigma$  and the perimeter  $P$  of the smallest cross section of constriction  $d^*$ . This cross section is a function of the capillary diameter  $d_{Cap}$ , the droplet volume  $V_P$ , and the air flow velocity  $v_{Air}$ . Since the cross section  $d^*$  can be assumed to be maximal at the capillary diameter  $d_{Cap}$ , the equation for interfacial tension force with the aid of correction factor  $a$  can be derived. The correction factor  $a$ , is assumed to be 1 as a first approximation.

$$F_\sigma = P \cdot \sigma = \pi \cdot d \cdot \sigma \quad (\text{eq. 2-5})$$

$$F_\sigma = \pi \cdot d_{Cap} \cdot \sigma \cdot a \quad \text{with } a = f(d_{Cap}, V_P, v_{Air}) \quad (\text{eq. 2-6})$$

The resistance force  $F_R$  is a result of the flow resistance to the moving surface  $A^*$  opposite to the air flow velocity  $v_{Air}$ . Since the flow of the droplet through the capillaries is intermittent, there is no pressure difference on the upper side of the particles. The basic assumption for the air-jet process is thus taken to be a complete sphere.

$$F_W = cw \cdot A \cdot \rho_c \cdot \frac{1}{2} \cdot v^2 = cw \cdot \frac{\pi}{8} \cdot d_P^2 \cdot \rho_c \cdot v^2 \quad (\text{eq. 2-7})$$

The value of flow resistance factor  $cw$  is a function of Reynold number  $Re_p$ . The dimensionless Reynold number is associated with the smoothness of fluid flow. According to this definition,  $cw$  can finally be expressed as follows:

$$Re_p = \frac{v \cdot d_p \cdot \rho_c}{\eta_c} \quad (\text{eq. 2-8})$$

$$cw = \frac{24}{Re_p} \quad \text{for } Re_p < 0.5 \quad (\text{eq. 2-9})$$

$$cw = 0.44 \quad \text{for } 10^3 < Re_p < 2.5 \cdot 10^5 \quad (\text{eq. 2-10})$$

From the rearrangement and combination of equation 2-1, 2-4, 2-6, 2-7, and 2-10, the particle (droplet) diameter  $d_p$  can be finally given as follows:

$$\frac{1}{6} \cdot \pi \cdot d_p^3 \cdot (\rho_p - \rho_c) \cdot g + cw \cdot \frac{\pi}{8} \cdot d_p^2 \cdot \rho_c \cdot v^2 - \pi \cdot d_{cap} \cdot \sigma = 0 \quad (\text{eq. 2-11})$$

$$d_p = \sqrt[3]{6 \cdot \frac{\left( d_{cap} \cdot \sigma - \left( \frac{cw \cdot d_p^2 \cdot \rho_c \cdot v^2}{8} \right) \right)}{(\rho_p - \rho_c) \cdot g}} \quad (\text{eq. 2-12})$$

Pressure drop in the capillary ( $\Delta p$ )

Theoretically, the pressure drop  $\Delta p$  in a pipe (or channel) is a function of density and viscosity of the fluid, length and diameter of the pipe, and fluid flow rate in the pipe. It can be calculated using following formula [56]

$$\Delta p = 8 \cdot f \cdot \left( \frac{L}{d_i} \right) \cdot \frac{\rho \cdot u^2}{2} \quad (\text{eq. 2-13})$$

where  $f$  is the friction factor,  $L$  is the pipe length (m),  $d_i$  is the inner diameter of pipe (m),  $\rho$  is the fluid density ( $\text{kg/m}^3$ ), and  $u$  is the fluid velocity inside the pipe (m/s).

### 2.3 Mass transport in gel

Usually, the diffusion characteristics of microcapsule systems have been analysed by an expression based on Fick's law with the assumption that the mass transfer rate is proportional to the concentration gradient of solutes and that all the microcapsules are of identical size [57-

60]. The diffusion coefficients of a microcapsule or sphere have been determined by applying Crank's solution of the unsteady-state diffusion equation.

In general, gels can be looked upon as semisolid material which are 'porous'. The pores or open spaces in gels are filled with water. Mass transport in microcapsules is mainly based on diffusion. The transport processes based on biological interactions are negligible [61]. Diffusion is the process responsible for movement of matter from one location to another due to random molecular motions [62]. Diffusion processes in gases are fast compared to those in liquids and are slowest in solids. Diffusion in polymers is a complex process and the diffusion rates lie between those in liquids and solids, depending mainly on the concentration and degree of polymer swelling. It is therefore a challenge to understand, predict and regulate diffusion in polymer systems [63].

Adolf Fick established the first mathematical treatment of diffusion in a one dimensional system [61].

$$J = -Aj = -AD \frac{\partial c}{\partial z} \quad (\text{eq. 2-14})$$

where J is the overall diffusion, j the flux, A the area available to diffusion, D the diffusion coefficient, c the concentration, z the distance and  $\partial c/\partial z$  the concentration gradient in the z direction. This equation is known as the Fick's first law. For diffusion without convection and over a unit cross-sectional area eq. 2-14 can be written as:

$$j = -D \frac{\partial c}{\partial z} \quad (\text{eq. 2-15})$$

Eq.2-15 is the starting point for all models of diffusion in polymer systems. The theoretical description of diffusion of solvents and/or solutes in polymer solution, gels and solids are based on different physical concepts; the obstruction effect, the hydrodynamic interaction and free volume [68]. The polymer chains are regarded as motionless relative to the diffusing molecules in the obstruction effect. The polymer is represented as fixed and impenetrable segments immersed in the solution that lead to an increase in the mean path length for the diffusing molecules [64].

The hydrodynamic theories consider hydrodynamic interactions such as the friction between the solute and the polymer, solute and solvent and between the solvent and the polymer. The hydrodynamic theory finds applications in concentrated regimes, where the polymer tends to

overlap. The free volume theory assumes that the free volume contributed by solute, solvent and polymer is the major factor controlling the diffusion rates of molecules [63].

According to Crank J. 1975 and A. Nguyen and J.H.T. Luong 1986 [62,65], when spherical beads that are free of substrate are immersed in a bulk solution with an initial concentration,  $C_0$ , the substrate diffuses into the beads. Under the assumptions that a capsule is a homogenous sphere and that liquid film resistance can be ignored due to effective stirring, the change in the bulk solution concentration with time is described as followed:

$$C_l(t) = C_{r=R}(t) = \frac{\alpha C_0}{1 + \alpha} \left[ 1 + \sum_{n=1}^{\infty} \frac{6(1 + \alpha) e^{-\frac{Dq_n^2 t}{R^2}}}{9 + 9\alpha + q_n^2 \alpha^2} \right] \quad (\text{eq. 2-16})$$

where  $r$  is the distance from the core;  $R$  is the external radius of a bead;  $t$  is the time;  $D$  is the diffusion coefficient of the bead and  $\alpha$  is the ratio between the liquid volume and the bead volume which can be described by:

$$\alpha = \frac{V}{N \left( \frac{4}{3} \pi R^3 \right)} \quad (\text{eq. 2-17})$$

where  $V$  is the volume of the bulk solution and  $N$  is the total number of beads;  $C_0$  is the initial concentration of the bulk solution; and  $q_n$  are the non-positive roots of the following equation:

$$\tan q_n = \frac{3q_n}{3 + \alpha q_n^2} \quad (\text{eq. 2-18})$$

The  $D$  value was calculated using the non-linear fitting and sum of least squares method.  $C_l(t)$  was calculated using eq.2-15 by assuming a value for  $D$  that corresponds to  $S$ , the smallest sum of the squares of the differences between the experimentally measured values and the calculated ones. However, the diffusion of the substrate in hollow microcapsules is more complex than that in a homogeneous microcapsule since the transport of the substrate through the microcapsule membrane  $D_1$  is different from that through the liquid core  $D_2$ . In eq.2-15  $D$  becomes  $D_m$  which is a combination of diffusivity of the microcapsule membrane and the diffusivity of the liquid core. The relationship between  $D_m$ ,  $D_1$ , and  $D_2$  can be defined as

$$D_m = \frac{r_b}{\frac{r_b - r_a}{D_1} + \frac{r_a}{D_2}} \quad (\text{eq. 2-19})$$

where  $r_a$  is the internal radius and  $r_b$  is the external radius of the microcapsule. The solution used in this study is so dilute that the diffusion in the liquid core of the microcapsule,  $D_2$  can be considered the same as that in pure water.

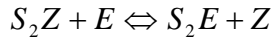
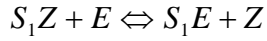
## 2.4 Multi-competitive lipase reaction

Lipases (triacylglycerol ester hydrolases EC3.1.1.3) are enzymes that catalyse the breakdown of fats and oils with releasing free fatty acids, diglycerides, monoglycerides and glycerol. They also catalyse esterification and transesterification reactions. Consequently, they are widely employed in industrial applications such as the oil processing, dairy industry, production of surfactants, flavour and aroma compounds and pharmaceuticals [66-68]. Since most lipase substrates are hydrophobic lipids, organic solvents are commonly used as reaction media for lipase catalysed reactions in order to increase the substrate solubility. However, lipases exhibit decreased activity and a limited stability in organic solvents compared to that in aqueous medium because of the rigidity of the protein structure in organic solvents. Immobilisation method has been applied to improve the lipase activity, stability and reusability [69-72]. Polyacrylamide and calcium alginate have been among the media used for immobilisation lipase. Nevertheless, a co-polymer of pAAm-Alg has never been studied before in this context.

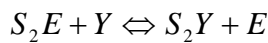
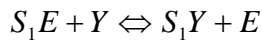
In order to study the selective properties of lipase immobilised in pAAm-Alg microcapsules, the transesterification of fatty acid ethyl ester of different chain lengths with various alcohols and vice versa was applied as a test system. Multi-competitive behaviour among fatty acid ethyl esters with chain lengths from  $C_2$  to  $C_{14}$  was observed by reacting them with alcohols which competed for an active site on the free enzyme lipase MML, or when the enzyme was encapsulated in pAAm-Alg microcapsules, the fatty acid ethyl esters were selected by the pAAm-Alg membrane.

It has been reported that the initial reaction rate of a lipase catalysed reactions in organic media follows Michaelis-Menten kinetics, with the formation of an intermediate acyl-enzyme. The theory of substrate competition can thus be applied to these reactions [73-75]. The classical mechanism of transesterification reactions catalysed by lipase is described as follows [76-78]:

Acyl enzyme formation; where  $S_1Z$  and  $S_2Z$  are two acyl donors (fatty acid ethyl ester) with the same transfer group  $Z$  (ethyl) and two different acyl groups ( $S_1$  and  $S_2$ : fatty acid acyl group)



Acyl enzyme solvolysis: where  $Y$  is a nucleophile or alcohol acceptor



This approach has been developed by M. Rangheard et al. [73] for the determination of fatty acid specificity and is generalised here for the determination of substrate specificity for the free and encapsulated enzyme. The term specificity refers to an enzyme's discrimination between several substrates competing for an enzyme active site which can be represented by a simple parameter, the competitive factor [79]. When more than two potential substrates are presented, competitive factors for any pair can be determined from simple initial rate measurements. For a mixed system where substrate A and B are competing for the same active site, the competitive factor ( $\alpha$ ) is defined by the following equation:

$$\alpha = \frac{(k_A/[A]_t)}{(k_B/[B]_t)} \quad (\text{eq. 2-20})$$

where  $k_A$  and  $k_B$  are the reaction rate constants for substrate A and B respectively.  $[A]_t, [B]_t$  are the molar concentrations of A and B at time  $t$ . From eq. 2-20 it is apparent that the competitive factor is equal to the ratio of the reaction rates of two substrates when they are present at identical concentrations. A practical estimate of the competitive factor is obtained by the integration of eq. 2-20 resulting in:

$$\alpha = \frac{\log([A]_t/[A]_0)}{\log([B]_t/[B]_0)} \quad (\text{eq. 2-21})$$

where  $[A]_0, [B]_0$  and  $[A]_t, [B]_t$  are molar concentrations of A and B at times zero and  $t$  respectively. This analysis of competitive behaviour can be extended to multiple competitions amongst several substrates. The substrate with the highest reaction rate is taken as the reference [A] and relative competitive factors are calculated for all the other substrates. To facilitate the interpretation of the result, the specificity constant ( $1/\alpha$ ) is generally used. The

specificity constant of the reference is 1, while the value for the other substrates ranges between 0 and 1. Under the assumption that the rate of acyl enzyme formation is the rate limiting step and that excess of nucleophile is present, the specificity constant can be adapted to a pseudo-first order kinetic constant. Consequently, the specificity constant can be used to represent the substrate reactivity towards the enzyme. In a mixture of multiple substrates with the same functional group, the higher the specificity constant value, the higher the reaction rate of this substrate compared to that of the reference compounds.



## 3 Materials and Methods

### 3.1 Materials

Alginate sodium salt (Alg) from brown algae-viscosity at 25°C: ~250cP, acrylamide (AAm) A9099, N, N'-methylene-bis-acrylamide (Bis-AAm) 99% 146072, LUDOX<sup>®</sup> HS-30 colloidal silica 30% (w/w) 420824, Bradford reagent B6916, Trypsin 23.8 kDa from porcine pancreas-activity ~90units/mg 93613,  $\alpha$ -lactalbumin 14.2 kDa from bovine milk TYPEIII Calcium depleted > 85% PAGE L6010, Insulin 5.7 kDa from bovine pancreas I6634 powder bioreagent, Isopropyl acrylamide (IPAAm), n-pentane, n-methanol, n-propanol, n-butanol, n-pentanol, ethyl acetate (C<sub>2</sub>), ethyl butyrate (C<sub>4</sub>), ethyl hexanoate (C<sub>6</sub>), ethyl octanoate (C<sub>8</sub>), ethyl decanoate (C<sub>10</sub>), ethyl dodecanoate (C<sub>12</sub>), ethyl myristate (C<sub>14</sub>), lipase from *M. Miehei* (MML) 1 U/mg (1 U corresponds to the amount of enzyme which liberates 1  $\mu$ mol oleic acid per minute at pH 8.0 and 40°C) from Sigma Aldrich; dextran T1 clinical grade MW 1.1 kDa from Pharmacosmos, Denmark; D+-maltose monohydrate 360Da, D+-glucose 180Da minimum 99.5 % purity from Fluka Analytical; tert-butyl hydroperoxide 70% solution in water (TBHP), anhydrous Calcium chloride (CaCl<sub>2</sub>), potassium sodium tartrate tetrahydrate from Merck; 3,5-dinitrosalicylic acid, 98% from Aldrich Chemistry; sodium metabisulfite (Na<sub>2</sub>S<sub>2</sub>O<sub>5</sub>), Tris(hydroxymethyl) aminomethane (TRIS), 99.8-100.1% from Alfa Aesar; sodium hydroxide pellets BDH from Prolabo.

### 3.2 Characterisation of microcapsules

The diameter and circularity of microcapsules were determined by photographing samples and later analysing the photographs with image analysis software, ImageJ 1.43u (free download software from <http://www.soft82.com/version/download/windows/imagej-1-43u/>). A camera (CANON DIGITAL IXUS 80 IS) was used to take photographs of the microcapsules under UV light (Type NV-8KL series 5321003 Benda Laborgeräte U. Ultravioletstrahler D-69168 Wiesloch), in night-snapshot mode and without flash. The photographs were transferred and further analysed by the ImageJ software. The thickness of the microcapsule membrane was measured using a stereo microscope LEICA MZ95 interfaced to a PC operating with image analysis software (LEICA IM50 version 4.0 Release 132). The average diameter, circularity, and membrane thickness with standard deviations

(S.D.) were determined for the investigated microcapsules. The detail of LEICA MZ95 stereo microscope is given in Appendix A.

### 3.2.1 Microcapsule photography

In order to produce a contrasting picture, around 200 microcapsules were suspended in an 8% w/w  $\text{CaCl}_2$  solution with addition of small amount of a fluorescent dye (Merck KGaA, Darmstadt, Germany) and left to stand for 10 minutes. The fluorescent dye is a yellow-colouring agent that makes the capsules visible and coloured when exposed to an ultraviolet (UV) light. The coloured capsules were then filtered and washed with a small amount of deionised water. Finally, the capsules were dried with laboratory tissue paper and arranged regularly on a black background. The number of capsules to be photographed had to be arranged with some spaces between them, so as to enable ImageJ to analyse each capsule separately. This procedure should be completed within 10 minutes; otherwise the capsules will dry up and shrunk at room temperature. A ruler or a coin was placed on the plate as a reference for the image analysis. The camera (CANON DIGITAL IXUS 80 IS) was used to take the picture under UV light, in night-snapshot mode and without a flash. The pictures were then transferred to and further analysed on a computer.

### 3.2.2 Image analysis

The pictures of microcapsules were analysed using the IMAGEJ software. Initially, the picture was converted from colour into the 8-bit or grey-scale one. A black-and-white or monochrome picture was then obtained as shown in Figure 3-1a. Furthermore, the binary function of the software results the microcapsules appearing as grey-coloured particles on the grey or black background (Figure 3-1b). Finally, each particle was transformed into a black dot with a white background (Figure 3-1c).

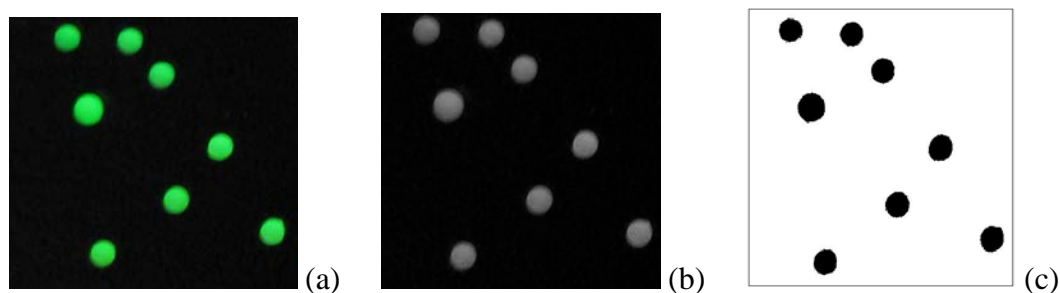


Figure 3-1: Steps in image analysis

The properties of particle, such as area, circularity, Feret diameter, and perimeter were ascertained. The Feret diameter is the largest distance between two parallel lines or points that do not intersect the particle. After the area (A) and perimeter (P) of microcapsules were determined, the equivalent diameter and circularity were calculated. Circularity is determined by comparing the area with the perimeter of a particle. It can actually be described as a deviation from a perfect circle. It has values in the range 0–1. A perfect circle has a circularity of 1 while a very irregular object has a circularity value close to 0. The circularity of a particle is defined as follows:

$$Circ. = \frac{4\pi A}{P^2} \quad (\text{eq. 3-1})$$

where, A is the particle area and P is its perimeter.

Figure 3-2 illustrates circularity for different shapes. However, circularity is not an appropriate parameter for characterising highly irregular and elliptical particles.



Figure 3-2: Illustration of circularity shape descriptor

The equivalent diameter of microcapsules is defined as follows:

$$A = \frac{\pi \cdot D^2}{4} \quad (\text{eq. 3-2})$$

$$Deq. = \sqrt{\frac{4 \cdot A}{\pi}} \quad (\text{eq. 3-3})$$

### 3.2.3 Membrane thickness

The membrane which separates the core solution from the alginate wall inside microcapsules cannot be easily observed with a conventional microscope. A stereo microscope LEICA MZ95

was therefore employed in order to examine the membrane. This microscope is interfaced to a PC operating with LEICA IM50 version 4.0 Release 132 (LEICA MICROSYSTEMS Ltd) as image analysis software. The comparison of pictures taken with the light microscope ZEISS STEMI 2000-C and the stereo microscope LEICA MZ95 is shown in Figure 3-3.

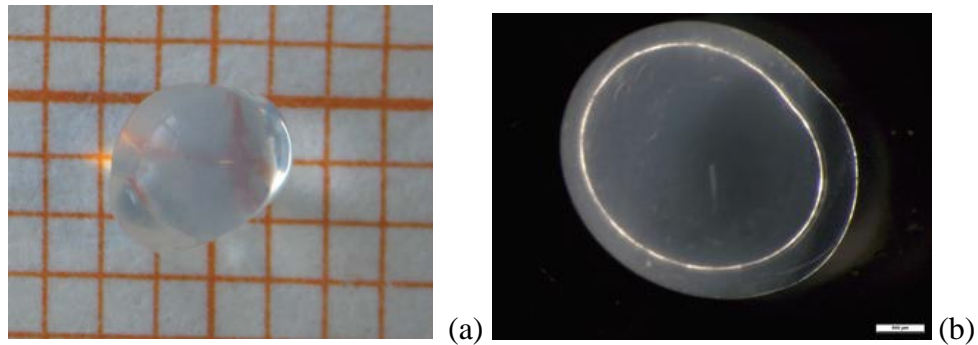


Figure 3-3: Comparison the microcapsule picture taken with: (a) light microscope and (b) stereo-microscope

### 3.3 Construction of nozzle

The head of the air-jet nozzle consists of three inlet sections for polymer solution, core solution, and air as depicted in Figure 3-4.

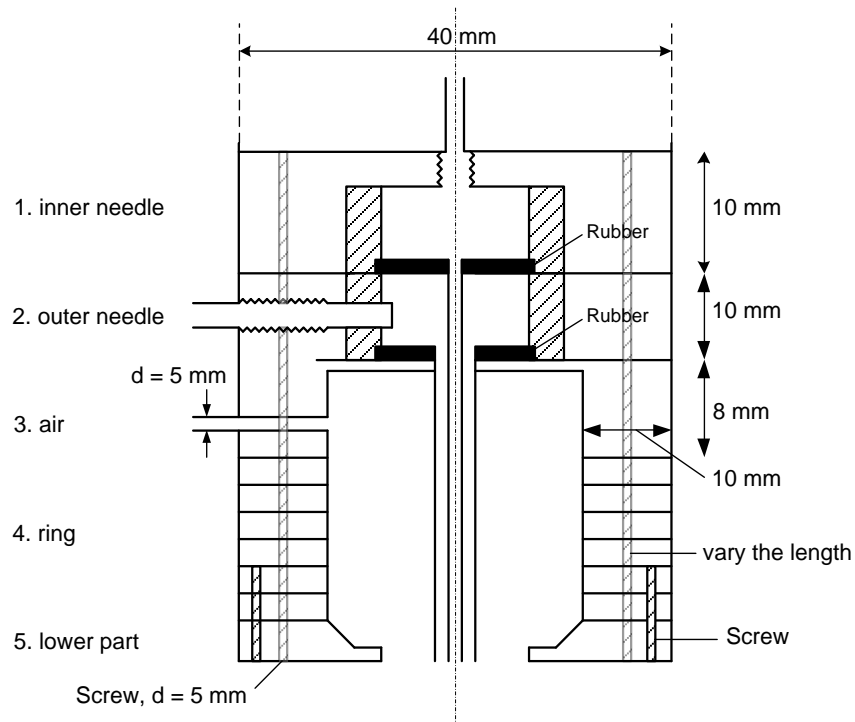


Figure 3-4: Schematic representation of air-jet nozzle

The nozzle itself comprises of two needles or capillaries with different diameters which are connected to peristaltic and micro-gear pumps. The core solution is introduced at the top part of the nozzle head (1); the polymer solution and the compressed air are supplied laterally from the connections (2) and (3) respectively. The inner and outer needles are adjusted in such a way that they are aligned concentrically. The screws (4) have to be tightened in order to avoid leakage of both solutions within the nozzle. The number of rings in the lower part of nozzle can be varied to obtain the various heights of the air chamber inside the nozzle structure. The volume of the air chamber can be adjusted by changing the ring diameters.

The inner diameter of the inner needle is 0.75 mm with a wall thickness of 0.1 mm. The outer needle, which acts as the inlet for the polymer solution has an inner diameter of 1.5 mm with a wall thickness of 0.1 mm. A constructional diagram of the rings and needles is shown in Figure 3-5.

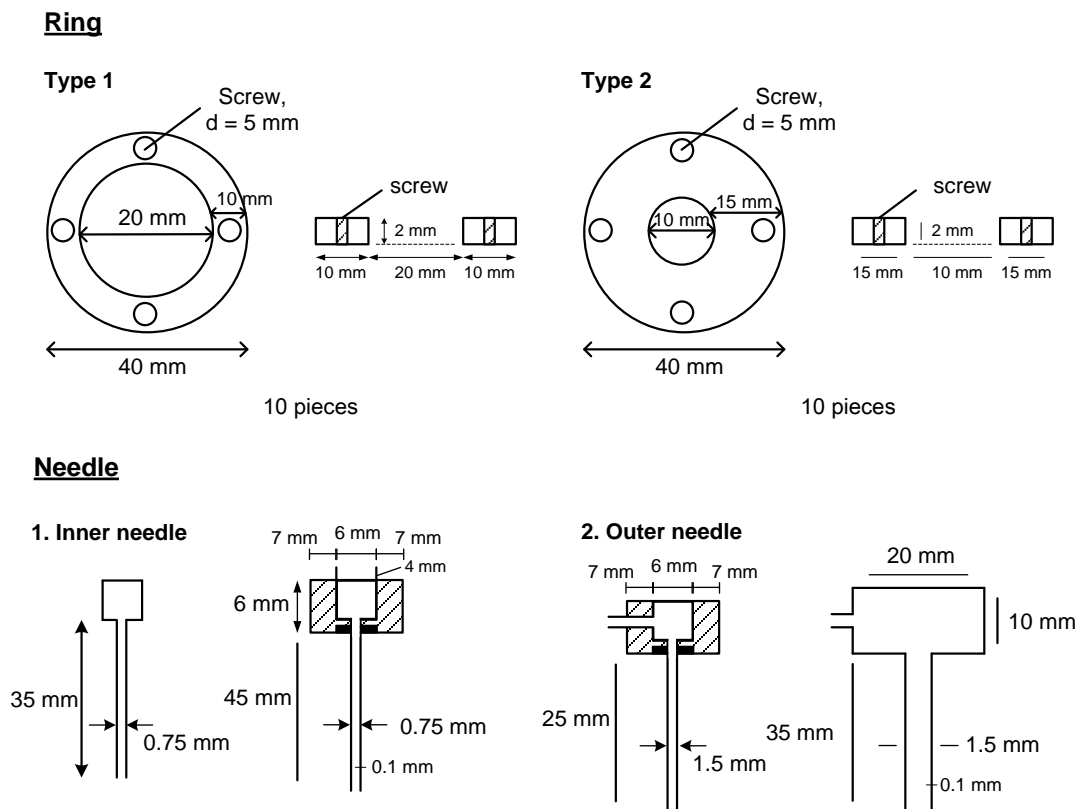


Figure 3-5: Nozzle structure

## 3.4 Determination of sugar and protein concentrations

### 3.4.1 Quantitative sugar analysis

The concentrations of glucose and dextran T1 solutions were measured using dinitrosalicylic (DNS) colorimetric method. This method tests for the presence of a free aldehyde group (H=O) in the so-called reducing sugars. It involves a colour transition reaction from yellow to red-brown at 575 nm. The reducing sugar reduces 3,5-dinitrosalicylic acid to 3-amino,5-nitrosalicylic acid under alkaline conditions. DNS absorbs maximally at yellow wavelengths. Upon reduction there is a shift in the absorption spectrum to red/brown at 575 nm. The amount of absorbance is directly proportional to the amount of sugar present [80].

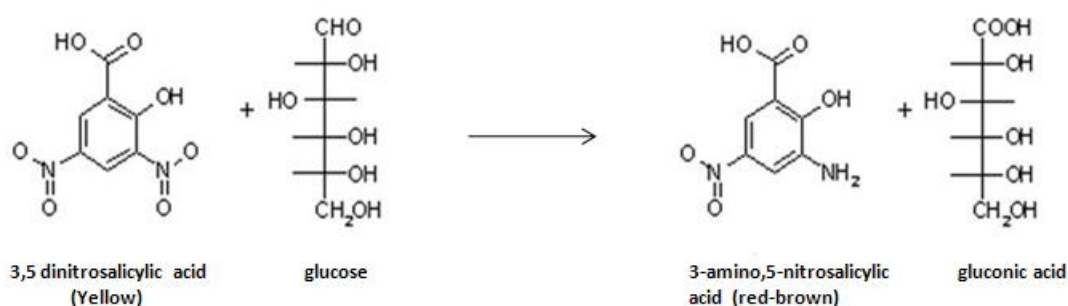


Figure 3-6: DNS reduction reaction according to Miller

### 3.4.2 Quantitative protein analysis

The concentrations of protein in solution were determined with the Bradford reagent. The Bradford protein assay is a simple procedure that depends on the change of absorbance based on proportional binding of the dye coomassie brilliant blue G 250 to proteins. The dye forms a complex with the protein and causes a shift in the absorption maximum of the dye from 465 nm to 595 nm. The absorption is proportional to the amount of protein present. Both hydrophobic and ionic interactions of the anionic form of the dye give rise to a visible colour change [81].

Unlike many other assays, the Bradford assay is not susceptible to interference by a wide range of chemicals present in the samples, but the assay is less accurate for basic or acidic proteins (Applichem GmbH 2010).

### 3.5 GC Analysis for lipase reaction

Fatty acid ester and alcohol composition were determined by gas-liquid chromatography using a HP 6890 Series apparatus equipped with a flame ionisation detector (300°C) and a split injector (270°C). The fatty acid ethyl esters were separated using a CP-Sil-8 column from ChromPack / VARIAN Agilent with helium as carrier gas. A split ratio of 100:1 was used and a column temperature of 50°C was maintained for 4 minutes before being increased at 10°C/min to 270°C.

Quantitative data were obtained by integration of the peak areas. The molar response factors for the ethyl and propyl esters for the same fatty acid were found to be identical. The kinetics of the reaction was monitored using the degree of conversion of the ethyl ester into the propyl ester using the following equation.

$$C_n = \frac{A_p / PM_p}{A_p / PM_p + A_E / PM_E}$$

where  $A_p$  and  $A_E$  are the areas of the propyl and ethyl esters peaks respectively and  $PM_p$  and  $PM_E$  are the corresponding molecular weights of the esters.

## **4 Experimental procedure**

### **4.1 Preparation of microcapsules**

#### **4.1.1 Preparation of polymer solution**

To prepare the various polymer solutions, a 20 mM Tris-HCl buffer solution prepared from 2.4 g of Tris was used as a base stock. Distilled water was later added until the volume of solution was approximately 1000ml. 1M HCl solution was then added slowly to adjust the pH to 7. The solution was poured into a 1 litre bottle and distilled water was added to make up the volume. The bottle was closed and shaken gently to make the solution homogenous.

##### **4.1.1.1 AAm-Alg solution**

A stock of polymer-alginate solution was prepared from 3.5% w/w Alg, 19% w/w AAm, and 1% w/w Bis-AAm in 30 ml Tris-HCl buffer. First 5.7 g AAm and 0.3 g Bis-AAm were first poured into a glass measuring cylinder and the Tris-HCl buffer solution was added until the total volume of the solution was 30 ml. The solution was then gently stirred for about five minutes until all reagents completely dissolved. The solution was poured into a 100-ml beaker glass and stirred gently, using a magnetic stirrer. The stirring rate was set at a low speed and the alginate powder was added gradually while the stirring rate was slowly increased to its maximum value. Parafilm was put over the beaker to prevent any spillage during stirring. The solution was stirred for about two to three hours, depending on the concentration of solution, until it was homogenous. About five minutes before running the experiment, TBHP, was added as an oxidant to the polymer solution. Due to the nature of the solution, each experiment employed fresh polymer solution.

##### **4.1.1.2 AAm-Alg solution with silica additive**

AAm-Alg solution with silica additive was prepared by the same procedure described in 4.1.1.1, except that the Tris-HCl was replaced by silica solution. Silica solution at various concentrations (1 to 5% w/w) was diluted from LUDOX<sup>®</sup> HS-30 colloidal silica 30% (w/w). Then, 5.7 g AAm (19% w/w) and 0.3 g Bis-AAm (1% w/w) were dissolved in the silica solution in a measuring cylinder. The solution was agitated and homogenised using a magnetic stirrer. 1.05 g Alg (3.5% w/w) was added to this solution in a beaker little by little



whilst stirring. The solution was kept stirred for two hours to ensure homogenisation. Parafilm was placed over the beaker to prevent the loss of water during stirring. 0.06 ml TBHP was added to the polymer solution shortly before start of the microcapsule preparation.

#### **4.1.1.3 AAm-Alginate solution with modified IPPAAm**

In order to modify the membrane properties of pAAm-Alg microcapsules, hydrophobic IPPAAm monomer was selected to co-polymerise with AAm during the formation of the polymer solution to prepare pAAm-IPPAAm-Alg microcapsules. Since pAAm-Alg membrane exhibits hydrophilic properties, it is selective toward hydrophilic substrates. IPPAAm, which is a hydrophobic co-monomer of AAm, was introduced to co-polymerise with AAm in order to manipulate the water affinity properties of pAAm-Alg microcapsule membranes.

Polymerisation of AAm-IPPAAm was done by free radical cross-linking of IPPAAm and AAm with TBHP and  $\text{Na}_2\text{S}_2\text{O}_5$  initiator. Different concentrations of IPPAAm were employed in the polymer solution. To prepare 30ml polymer solution, the following amounts of IPPAAm were added while dissolving of AAm and Bis-AAm 0.15, 0.3, 0.75, 1.05, 1.5 and 3 g to produce 0.5%, 1%, 2.5%, 3.5%, 5% and 10% w/w of IPPAAm in pAAm-IPPAAm-Alg microcapsule respectively. The amounts of alginate as well as of the other chemicals remained the same as in section 4.1.1.1. The characterisation of pAAm-IPPAAm-Alg microcapsules followed the same procedure as that for pAAm-Alg microcapsules.

#### **4.1.2 Preparation of gelling bath**

The gelation solution was prepared by dissolving 80 g  $\text{CaCl}_2$  in distilled water until the volume was approximately 1000 ml. The solution was poured into a 1-l calibrated flask and distilled water was added until the volume of the solution was exactly 1000 ml. The solution was shaken gently to render the solution homogeneous. In this study, the  $\text{CaCl}_2$  concentration was prepared at 8% w/w for all experiments, since lower amounts of  $\text{CaCl}_2$  leads to slow gelation and leaching of AAm, while concentrations of more than 8% w/w do not yield any significant improvement [47].

The cationic gelling bath was composed of 8% w/w  $\text{CaCl}_2$  solution, 20 mM Tris and 0.2% w/w (0.5 g) sodium metabisulfite, 0.605 g tris(hydroxymethyl)aminomethane was added to 250 ml of 8%  $\text{CaCl}_2$  to prepare the gelling bath.. The gelling bath was kept stirred throughout the microcapsule preparation to prevent Tris attaching to the surface of the microcapsules.

### 4.1.3 Apparatus for microcapsule preparation

A schematic diagram of the apparatus used in the microcapsule production is presented in Figure 4-1. Polymer and enzyme solutions were supplied by a peristaltic pump (Watson Marlow 205U, Falmouth, Cornwall, England) and a micro-gear pump (MZR-4605 HNP, Mikrosysteme GmbH, Parchim, Germany) respectively to the concentric nozzle. The nozzle is comprised of two capillaries fed separately with the shell and a core solution. The inside diameter of the inner capillary is 0.55 mm with a wall thickness of 0.1 mm. The outer capillary has an inside diameter of 1.3 mm and wall thickness of 0.1 mm. The shell solution envelops the core solution at the tip of the nozzle and forms the droplet. When the weight of the droplet exceeds the surface tension forces, it falls into the gelling bath. The solutions were extruded through the nozzle outlet with a regulated air stream in order to control the size of the droplets. The droplets fell into the gelation solution and the microcapsules kept submerged in the solution for 30 minutes.

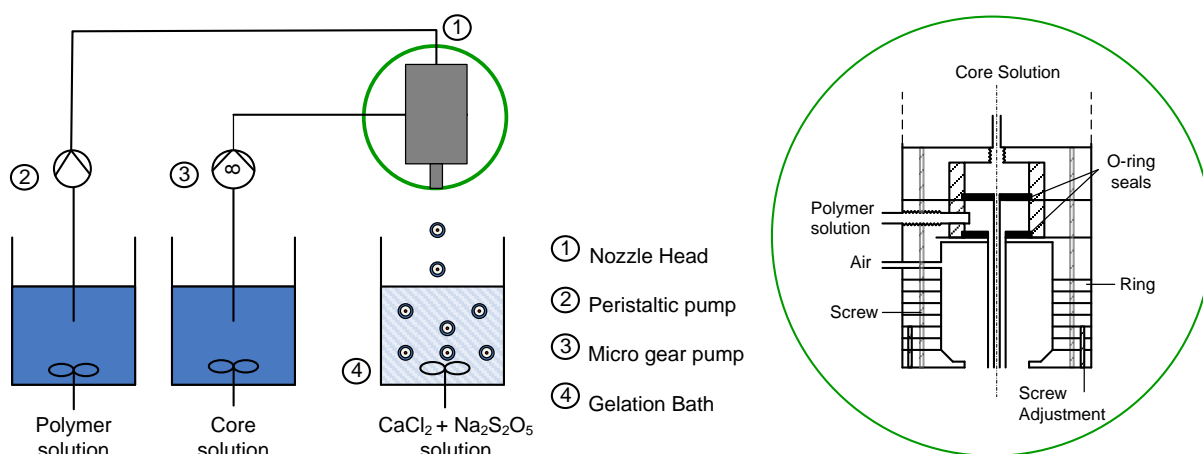


Figure 4-1: Flow-sheet of the encapsulation device and nozzle details

The calibration of the peristaltic pump and the micro-gear pump is given in Appendix A. Before commencing the microcapsule preparation, the nozzle was rinsed with bi-distilled water. The rotation speed for the micro-gear and peristaltic pumps were adjusted to their maximum speed for 5 minutes in order to rinse the inner and outer needles thoroughly and ensure that no blockages occurred in the nozzle.

The preparation of microcapsules was begun by running both the micro-gear and peristaltic pumps at the desired velocity until the operation became stable and regular droplets were generated. The droplets that came out of the nozzle were first allowed to fall into a small beaker glass with approximately 80 ml of 8 %  $\text{CaCl}_2$  solution, to ensure that the droplets were

not breaking up. The beaker glass was then replaced with the gently-stirred gelling bath and the preparation of microcapsules was finally implemented. For experiments using compressed air, the air valve was first opened at a higher volumetric flow rate and throttled back to the desired flow with the help of a rotameter.

#### 4.1.4 Variation of operating parameters

Microcapsules were prepared with different intrinsic physicochemical and extrinsic parameters in order to obtain the best microcapsules with optimal operating conditions. The physicochemical or intrinsic parameters comprise the properties of both the polymer solution and the gelling bath solution, i.e. the level of monomer and cross-linker, initiator concentration, the density and viscosity of the polymer solution and the surface tension of the gelling bath. The extrinsic parameters are related to the geometry of nozzle, i.e. the nozzle configuration (short and long), the number of rings inside the nozzle, the inner diameter of the ring and the outlet type. The variation in intrinsic and extrinsic operating parameters is summarised in Table 4-1 and Table 4-2 respectively.

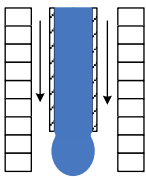
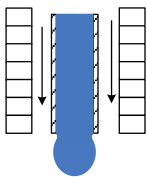
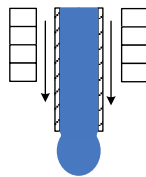
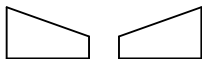
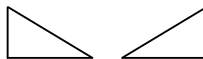
Table 4-1: Variation of intrinsic operating parameters

Parameter	Variation range	Unit
<b>Monomer concentration</b>	19 23 27	w%
<b>Cross-linker concentration</b>	0.5 1 2 4	w%
<b>Initiator concentration</b>	0.2 0.4 0.6	w%
<b><math>\dot{V}</math> core solution</b>	1.337 1.904 2.5	ml/min
<b>or <math>\dot{n}</math> micro-gear pump</b>	10 15 20	rpm

The density and viscosity of polymer solution were measured with the aid of a pycnometer (BRAND DURAN) and a rotational viscometer (ROTOVISCO RV 20, HAAKE) respectively. The surface tension of the gelling bath was measured with a tensiometer (KRÜSS). Details of the viscometer and the tensiometer were given in Appendix A.

When microcapsule preparation was finished, the experimental set-up was rinsed again with bi-distilled water. The nozzle was completely dismantled, washed, and dried, in order to prevent formation of dried polymer solution inside the nozzles.

Table 4-2: Variation of extrinsic operating parameters

Parameter	Variation		
			
<b>Position:</b>	A	B	C
<b>Number of rings:</b>	9	7	4
<b>Outlet type:</b>			
	1	2	
<b>Ring diameter (mm):</b>	10	20	
<b>Nozzle length:</b>	Short	Long	
$\dot{V}$ air (l/h)	150	300	500

#### 4.1.5 Microcapsule preparation

In order to prepare microcapsules for characterisation and diffusion purpose, a polymer solution and water as core solution were supplied by a peristaltic pump and a micro-gear pump respectively to the concentric nozzle arrangement. The rotation rate of the peristaltic pump was set up at 70 rpm while that of micro-gear pump was varied. Microcapsules were kept submerged in the solution for 30 minutes, to ensure that the gelation process was complete. Thereafter, the microcapsules were filtered and washed with deionised water and stored in a closed sample glass filled with 8%  $\text{CaCl}_2$  to await further analysis. All these experimental procedures were conducted at room temperature.

To prepare microcapsules for enzyme reaction studies, on the other hand, an enzyme solution replaced water solution as the core solution. The other procedures remained unchanged.

To characterise the microcapsules, microscopic photographs of the microcapsules were taken using a Canon PowerShot A 640 digital camera through the light microscope (ZEISS STEMI 2000-C) and a stereo microscope Leica MZ95, which were interfaced to a PC operating with

Leica IM50 version 4.0 Release 132 (Leica Microsystems Ltd) as image analysis software to evaluate the microcapsule diameter and shell thickness.

## **4.2 Diffusion and MWCO experimentation**

The diffusion study was performed at room temperature in a 200ml vessel with a Teflon stirrer. Predefined amounts (20 g) of microcapsules (~1600 microcapsules) were added to 100ml of the well-stirred substrate solution and samples were withdrawn at regular intervals. Adequate stirring of the substrate solution was ensured to negate the liquid film resistance around the microcapsules.

Glucose, maltose and dextran T1 concentration were determined using the DNS method [80] to ascertain the sugar concentration. Briefly, 1 ml of the sample was placed into a cuvette followed by the same amount of the DNS solution. The sample was then heated in a thermostat heating bath to a temperature of 80°C with a cover to prevent the dehydration of the solution. 0.5 ml of bi-distilled water was then added to the solution for dilution of the colouration, due to the high concentration of sugar in the sample. The solution was cooled in a water bath at room temperature for 15 minutes and the sample then analysed by a UV spectrophotometer (GENESYS 10 UV Scanning) at a wavelength of 575 nm.

Insulin,  $\alpha$ -lactalbumin and trypsin concentration were determined using the Bradford reagent [81]. Briefly, 1 ml of sample was placed into a cuvette followed by the same amount of Bradford reagent and left standing for 15 minutes at room temperature. The sample was then analysed using the same UV spectrophotometer but at a wavelength of 595 nm.

The same procedure was followed for all samples to determine the concentration of the bulk solution with time. Samples were withdrawn after 2, 4, 6, 8 and 10 minutes and then every 5 minutes up to 60 minutes. The change in substrate concentration with time was plotted and the diffusion coefficient was determined with the help of Crank's method. Diffusion and MWCO experiments for each variable were repeated three times under the same condition

### **4.2.1 Effect of monomer, cross-linker and initiator concentration on diffusion coefficient**

A series of diffusion experiments was conducted to investigate the influence of the variation of AAm concentrations (19, 23, 27% w/w), Bis-AAm concentrations (1, 2, 4% w/w), and initiator concentrations (0.2, 0.4, 0.6% w/w) on the diffusion coefficient. The concentration of

Alg was maintained at 3.5% w/w, because at concentrations below 3.5% acrylamide diffuses too rapidly into the gelling bath, while concentrations above 3.5% lead to high viscosity of the polymer solution, which are inappropriate for air-jet nozzles [47]. Glucose and dextran T1 were selected as substrates with initial concentrations of 3 g/l and the diffusion coefficients corresponding to each particular set of experimental condition were determined.

#### **4.2.2 Effect of Silica HS-30 on diffusion coefficient**

It is known that silica particles can be used to enhance the mechanical stability and modify the transport properties of the alginate membranes [82,83]. In this study, silica HS-30 was selected to investigate the effect of silica particles on the transportation of glucose into pAAm-Alg microcapsules. The concentration of silica particles was varied from 1-5% w/w in the polymer solution, since concentration above this level will cause too high a viscosity of the polymer solution, which is unsuitable for the nozzle. The polymer solution was composed of 19% w/w AAm, 1% w/w Bis-AAm, and 3.5% w/w Alg with 0.2% w/w initiator concentration and was blended with various amounts of the silica HS30 additive. The initial concentration of glucose solution was 3g/l.

#### **4.2.3 MWCO of pAAm-Alg microcapsules**

The pAAm-Alg microcapsules consisting of 19% w/w AAm, 1% w/w Bis-AAm, and 3.5% w/w Alg with 0.2% w/w initiator concentration were selected as the benchmark to study the MWCO. Substrates with different molecular weights and initial concentrations: glucose (180 Da) 3 g/l, maltose (360 Da) 3 g/l, dextran T1 (1.1 kDa) 3 g/l, insulin (5.7 kDa) 1 g/l,  $\alpha$ -lactalbumin (14.2 kDa) 1 g/l, and trypsin (23.8 kDa) 3 g/l were tested to establish the MWCO of the pAAm-Alg microcapsules. The concentration of the substrates glucose, maltose, and dextran concentrations were determined by the DNS method, while those of insulin,  $\alpha$ -lactalbumin, and trypsin concentrations were determined by the Bradford reagent. The MWCO study followed the same procedure as given for the diffusion experiment.

#### **4.2.4 Preparation of DNS Solution**

500 ml of DNS reagent solution was prepared by dissolving 150 g potassium sodium tartrate tetrahydrate (Rochelle salt), 8 g sodium hydroxide (NaOH), 0.23 g sodium sulfite (Na<sub>2</sub>SO<sub>3</sub>) in a 500 ml calibrated flask. 5 g DNS was slowly added into the flask while stirring, in order to dissolve the substance completely and the solution was then made up to 500ml.

Rochelle salt stabilises the colour developed. Sodium sulfite absorbs the dissolved oxygen that can interfere through the glucose oxidation. Sodium hydroxide (at low concentrations) aids in obtaining the maximum colour intensity without concomitant loss of glucose. It is necessary to heat the sugar-DNS solution for 15 minutes to obtain linear calibration data, protect the glucose and stabilise the colour [80].

Calibration experiments for both glucose and dextran T1 at various concentrations and volume ratios determined the linear concentration range and maintained the absorbance below 1.0 using the spectrometer (Genesys 10UV scanning).

### 4.3 Loading efficiency test

The purpose of the loading efficiency study was to examine the ability of the polymer and the microcapsule preparation technique to retain the enzyme within the polymeric shell. The content of the enzyme was quantified by the Bradford assay [81]. The loading of the enzyme solution in the microcapsules was determined following the method of Ma et al. 2009 and Wang et al. 2009 [84,85]. Briefly, 10 grams of microcapsules were grounded up and transferred into 5 mM Bis-Tris-HCl buffer at pH 6.5 to completely release the protein. The mixture was then filtered and the protein content in the supernatant was determined. To this end, 1 ml of sample was placed into a cuvette followed by the same amount of the Bradford reagent and left standing for 15 minutes at room temperature. The sample was then analysed using the UV spectrometer (GENESYS 10 UV Scanning) at a wavelength of 595 nm. The loading efficiency of the enzyme solution was calculated using the following formula

$$\text{Loading efficiency (\%)} = \frac{C_e V_e}{C_i V_i} \times 100$$

where  $C_i$  and  $V_i$  are the initial protein concentration and the initial volume of the enzyme solution during the microcapsule preparation respectively.  $C_e$  and  $V_e$  are the protein concentration and the volume of the enzyme solution entrapped or encapsulated in the microcapsule. The results were expressed as mean  $\pm$  standard deviation for 3 replicate measurements.

### 4.4 Multi-competitive lipase reaction assay

The transesterification reaction of fatty acid ethyl ester and alcohol catalysed by lipase MML was selected as a test system for both free and encapsulated enzyme in microcapsules. The

determination of substrate specificity of lipase MML followed the method developed by Rangheard et al 1989 [73]. The investigation of the lipase specificity was divided into three parts, namely the specificity towards chain length of fatty acid ethyl esters (mixed C<sub>2</sub> to C<sub>14</sub> ethyl ester), the specificity towards linear aliphatic primary alcohols (mixed n-methanol, n-propanol, n-butanol and n-pentanol) and the specificity toward both high selectivity fatty acid ethyl esters and alcohols for both the free and encapsulated enzyme.

In the first instance, the specificity of lipase MML towards the chain length of fatty acid ethyl ester was studied. Seven ethyl esters of fatty acid from C<sub>2</sub> to C<sub>14</sub> containing an even number of carbon atoms, each at a concentration of 0.1M, i.e. a total of 0.7M, were mixed in n-pentane in the presence of 2M n-propanol as a nucleophile. The total amount of substrate solution is 20ml. The lipase as either free or encapsulated enzyme was then added to the reaction system. For the free enzyme, 5mg (5U) of lipase MML was dissolved in 3ml distilled water, while for the encapsulated enzyme, 5mg of lipase MML dissolved in 3ml Tris-HCl was used as core solution and encapsulated in pAAm-Alg microcapsules. In both cases, the lipase was insoluble in the reaction mixture. The reaction was carried out at room temperature and aliquots were withdrawn from the reaction at predetermined intervals (0, 1, 2, 3, 4, 6, 24 and 48 hours) and analysed by gas chromatography.

For the second set of experiments, the alcohol specificity of lipase MML was examined. The reaction mixture contained equal molarities of 0.7M of ethyl octanoate (C<sub>8</sub> ethyl ester) as acyl donor and the alcohol acceptors; methanol, n-propanol, n-butanol and n-pentanol in pentane. The enzyme preparations, reactions conditions and sampling procedure were as in the first approach.

The third study was conducted to confirm the highest specificity for the free and encapsulated lipase MML. 0.7M of the highest specificity of chain length ethyl ester and alcohol for the free enzyme and encapsulated enzyme were chosen as competitive substrates. In our initial studies, the free enzyme exhibited the highest specificity for ethyl octanoate (C<sub>8</sub>) and n-butanol, while the encapsulated enzyme in pAAm-Alg microcapsules showed the greatest preference toward ethyl butanoate (C<sub>4</sub>) and methanol. 0.7M of each of ethyl octanoate, ethyl butanoate, n-butanol and n-methanol was prepared in pentane. Enzyme preparation, reaction conditions and sampling followed the procedures given for the first investigation.

All reactions were performed in triplicate and mean values are reported. It should be pointed out that the number of competing acyl donors, the nature of the alcohol acceptor and substrate



concentrations do not influence the competitive factor [73]. These parameters were therefore not studied.

#### **4.5 Reusability test**

The reproducibility of enzyme activities in the pAAM-Alg microcapsule was ascertained in reusability tests. The leaching of the encapsulated lipase was determined by measuring the residual activity after an interval of 48 hours. After each cycle, the microcapsules were washed twice with n-pentane and then reintroduced into the fresh reaction medium. The reaction was conducted for a total of 6 cycles with activity being measured at the end of each cycle. The highly competitive reaction was selected and the reaction conditions were the same as those described above.

## 5 Results and Discussion

### 5.1 Characterisation of pAAm-Alg microcapsules

In general, the formation of spherical droplets of polymer solutions results from the dynamic interaction between an axisymmetric flow of fluids with free surface forces [86]. In this study, the preparation of microcapsules was carried out by co-extrusion, using a jet break-up technique involving the concentric, two-fluid nozzle described in section 2.2 [87]. The preparation may be influenced by physicochemical properties, such as viscosities, densities, and the chemical compositions of the polymer and by parameters such as the apparatus configuration, for example, the diameter of the ring, the length of the needle, the number of rings, and the type of air-outlet. Each parameter was examined independently in order to understand its effect on the characteristics of a cross-linked, co-polymerised pAAm-Alg microcapsule. Thus, in order to determine the optimal conditions and composition for the synthesis of pAAm-Alg microcapsules, the effects of the physicochemical properties and operating parameters were investigated.

To assess the quality of each batch of microcapsules, two critical characteristics were measured: the equivalent diameter ( $D_{eq.}$ ) and the circularity. Example of histograms illustrating the frequency and the cumulative distribution of different equivalent diameters and circularities of pAAm-Alg microcapsules produced in each batch are presented in Figure 5-1.

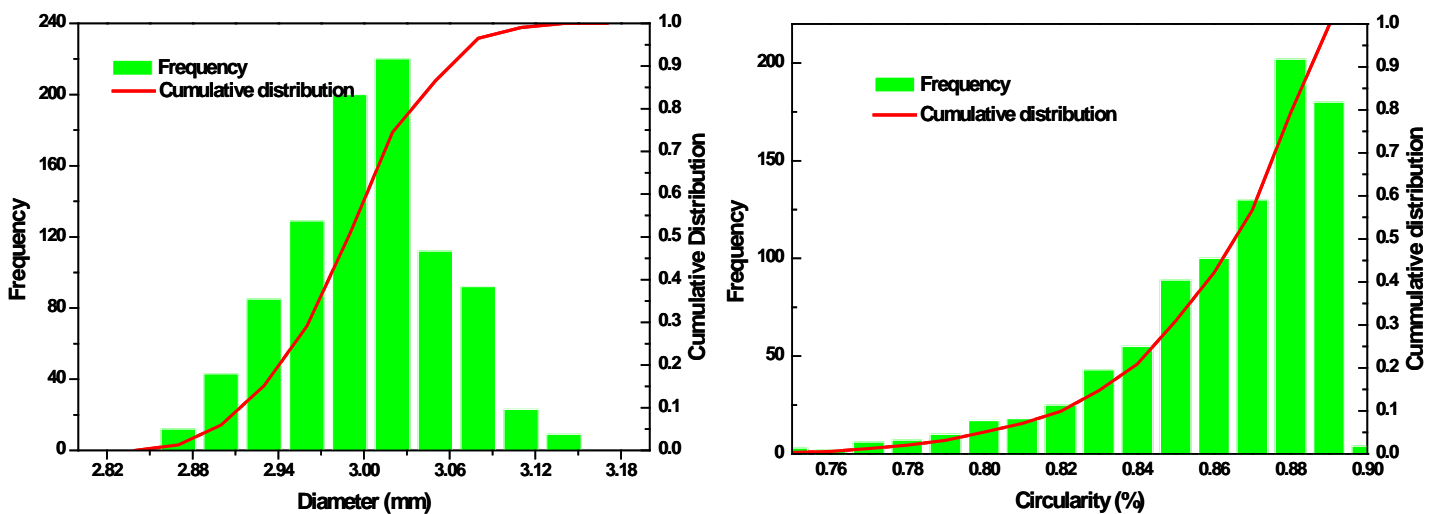


Figure 5-1: Histograms of equivalent diameter (0.03 mm intervals) and circularity (0.01 intervals)

The histogram presents an overview of the distribution of the equivalent diameter and circularity on an abscissa giving size and circularity respectively. In addition, the values of the maximum and minimum  $D_{eq}$  and circularity were obtained together with their relative standard deviations. The line represents the cumulative distribution of the microcapsules. The steep curve indicates a relatively tight uni-modal distribution. The standard deviation of the mean equivalent diameter is related to the slope of the cumulative distribution and is thus high for a flat curve.

In addition, to simplify the qualitative characterisation of the microcapsules prepared, criteria for their classification were set-up as detailed in Table 5-1.

Table 5-1: Classification criteria for qualitative characterisation of microcapsules

<b>Quality Classification</b>	$D_{eq}$ Standard deviation	Mean	Circularity Standard deviation	Sum of particles with min. 0.85
<b>Good</b>	< 7%	$\geq 0.82$	< 8%	$\geq 30\%$
<b>Acceptable</b>	< 9%	$\geq 0.80$	< 10%	$\geq 15\%$
<b>Bad</b>	when two or more criteria of the categories are not fulfilled.			

### 5.1.1 The effect of physicochemical properties on microcapsule preparation

The physicochemical or intrinsic properties consist of the properties of both the polymer and the gelling bath solution. The polymer solution comprises of alginate, an AAm monomer, a Bis-AAm cross-linker and a TBHP oxidant; while the gelling bath solution consists of calcium chloride ( $\text{CaCl}_2$ ) and a sodium metabisulfite ( $\text{Na}_2\text{S}_2\text{O}_5$ ) reductant. A series of microcapsules were prepared by varying the monomer, the cross-linker, and the initiator concentrations. It should be noted that the concentration of the alginate in the polymer solution and the concentration of the  $\text{CaCl}_2$  in the gelling bath were kept constant at 3.5% and 8% w/w respectively, because reducing the concentration of the alginate would have caused leakage of the AAm monomer, which in turn would have led to the formation of microcapsules with a tail, whilst lowering the concentration of the  $\text{CaCl}_2$  below 8% would also have resulted in leakage of the AAm monomer [47]. The influence of these quantities on the quality of microcapsules, in terms of the equivalent diameter, and the circularity, are given in the following sections.

### 5.1.1.1 The density and the viscosity of the polymer solution and the surface tension of the gelling bath

The polymer solution with various concentrations of monomer and cross-linker was prepared and the density was measured with the aid of a pycnometer (BRAND DURAN). The viscosity of the polymer solutions was determined using a rotational viscometer (ROTOVISCO RV 20, HAAKE). The tensiometer (KRÜSS) was used to measure the surface tension of the gelling bath containing the 8% CaCl<sub>2</sub> solution, the sodium metabisulfite reductant and Tris. The pH of the gelling bath was kept constant around 5 by balancing the amount of Tris against that of sodium metabisulfite. The temperature was kept constant at 25 °C. The density, viscosity, and surface tension are given in Table 5-2.

Table 5-2: Density and viscosity of the polymer solution at various monomer and cross-linker concentrations, and surface tension of the gelling bath for various initiator concentrations

<b>Microcapsule (%Alg-%Aam-%Bis-AAm-%initiator)</b>	<b>Density [g/cm<sup>3</sup>]</b>	<b>Dynamic Viscosity <math>\eta</math> [mPa.s]</b>	<b>Surface Tension <math>\sigma</math> [mN/m]</b>
<b>3.5%Alg.-19%Aam-1%Bis-AAm-0.2% initiator</b>	1.026	491.75	56.1
<b>3.5%Alg.-23%Aam-1%Bis-AAm-0.2% initiator</b>	1.092	1153.62	56.1
<b>3.5%Alg.-27%Aam-1%Bis-AAm-0.2% initiator</b>	1.139	1235.12	56.1
<b>3.5%Alg.-19%Aam-2%Bis-AAm-0.2% initiator</b>	1.057	848.11	56.1
<b>3.5%Alg.-19%Aam-4%Bis-AAm-0.2% initiator</b>	1.084	1040.53	56.1
<b>3.5%Alg.-19%Aam-1%Bis-AAm-0.4% initiator</b>	1.026	491.75	62.4
<b>3.5%Alg.-19%Aam-1%Bis-AAm-0.6% initiator</b>	1.026	491.75	70.2

From these results, the density of the polymer solutions at various monomer and cross-linker concentrations clearly exhibited no great difference to the density of water at 25 °C (0.997 gr/cm<sup>3</sup>). Hence, the density of the polymer solution has no significant influence on the size of droplets formed during preparation of the microcapsules. In contrast, the viscosity of the polymer solutions rose with an increase in either the monomer or the cross-linker concentration. The viscosity of the polymer solution plays an important role in the output flow rate of the peristaltic pump. However, by operating the pump at a lower rotational speed, the influence could be kept at a negligible level.

The surface tension of the gelling bath solution was increased with increasing sodium metabisulfite concentration. Too large surface tension can cause the microcapsules to be deformed. To reduce this effect, the distance between the nozzle outlet and the liquid surface of the gelling bath should be adjusted to an appropriate value.

### 5.1.1.2 Core solution volumetric flow rate

In the preparation of microcapsules, the volumetric flow rate of the encapsulated core solution plays an important part in determining the characteristics of the microcapsules. The core content of the microcapsules is determined by the volumetric flow rate of the core solution. To study the effect of the core solution volumetric flow rate, the pumping speed of the polymer solution, which consisted of 3.5% Alg, 19% AAm, 1% Bis-AAm, and 0.2% initiator, was maintained at 70 U/min (0.232 ml/min) while the volumetric flow rate of the core solution (water) was varied. It was also important to suppress unwanted air flow, so that the optimum volumetric flow ratio between the core and the polymer-alginate solution could be determined. The equivalent diameter and circularity of the microcapsules produced were measured and presented in Figure 5-2.

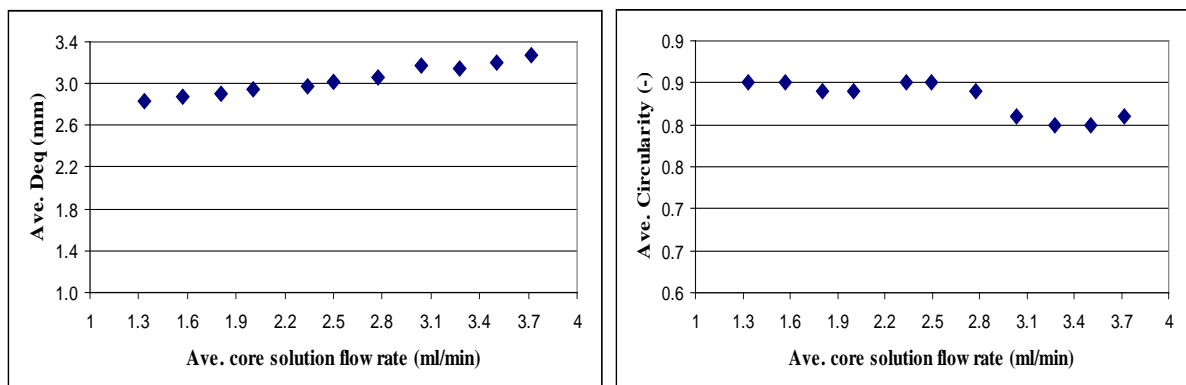


Figure 5-2: Average equivalent diameter and circularity for various core solution volumetric flow rates

The figures show that the size of the microcapsules increased with an increase in the core solution volumetric flow rate. The proportion of polymer to core solution decreased with an increase in the volumetric flow rate of the core solution, and thus the thickness of the microcapsule membrane diminished accordingly. At a core solution volumetric flow rate of 22-26 U/min (2.78-3.27 ml/min), some microcapsules broke due to the reduced proportion of gel, which decreased the mechanical stability of the microcapsules. The maximum threshold

for the core solution volumetric flow rate was 32 U/min (4.0 ml/min), at which speed all the microcapsules ruptured when dropped into the gelling bath.

Moreover, at high core solution volumetric flow rates, the structure of the microcapsules was deformed and their circularity decreased. During subsequent experiments, core solution volumetric flow rates of 10, 15, and 20 U/min (1.34, 1.90 and 2.5 ml/min respectively) were used. The ratios of volumetric flow rates of the alginate-polymer solution to those of the core solution are given in Table 5-3.

Table 5-3: Ratios of volumetric flow rates

<b>Pump speed ratio [U/min : U/min]</b>	<b>Ratio of volumetric flow rate</b>	
<b>(Peristaltic pump : Micro gear pump)</b>	$\frac{\dot{V}_{\text{polymer-alginate-solution}}}{\dot{V}_{\text{core-solution}}}$	$= \frac{\dot{V}_{\text{polymer-alg.}}}{\dot{V}_{\text{core}}}$
<b>70 : 10</b>	$\frac{0.232 \text{ ml/min}}{1.337 \text{ ml/min}}$	$\frac{1.0}{5.7}$
<b>70 : 15</b>	$\frac{0.232 \text{ ml/min}}{1.904 \text{ ml/min}}$	$\frac{1.0}{8.2}$
<b>70 : 20</b>	$\frac{0.232 \text{ ml/min}}{2.5 \text{ ml/min}}$	$\frac{1.0}{10.7}$

### 5.1.1.3 Effects of AAm monomer, Bis-AAm cross-linker, and initiator concentrations

Generally, the physical properties of the polymer microcapsules depend strongly on the amounts of the monomer and the cross-linker [88]. pAAm-Alg microcapsules were prepared with different reactant concentrations, at a polymer solution volumetric flow rate and a core solution volumetric flow rate of 70 and 20 U/min (0.232 and 2.5 ml/min) respectively. The equivalent diameter and circularity of the microcapsules were determined by photographing them and then interpreting the photographs using image analysis software (Image J). 200 microcapsules in each production batch were used to determine the mean diameter and circularity. The influences of the monomer, the cross-linker, and the initiator on the microcapsule characteristics are shown in Table 5-4. The values reported are the average values of five production batches.

The influence of monomer concentrations on microcapsule production was established by keeping the Alg (3.5%), Bis-AAm (1%), and initiator (0.2%) concentrations constant while varying the concentration of AAm from 19% to 27%. The average microcapsule equivalent

diameter and circularity for each of the batches varied from 2.843 to 3.353 mm and 0.842 to 0.883 respectively.

Table 5-4: Equivalent diameter, circularity, membrane thickness, and production rate of pAAm-Alg microcapsules at different parameters

<b>Microcapsule (%Alg-%Aam-%Bis-AAm-%initiator)</b>	<b>Equivalent Diameter (mm)</b>	<b>Circularity (-)</b>	<b>Membrane Thickness (mm)</b>	<b>No. of Capsules (min<sup>-1</sup>)</b>
<b>3.5%Alg.-19%Aam-1%Bis-AAm-0.2% ini.</b>	3.020	0.877	0.234	28
<b>3.5%Alg.-23%Aam-1%Bis-AAm-0.2% ini.</b>	2.967	0.868	0.228	22
<b>3.5%Alg.-27%Aam-1%Bis-AAm-0.2% ini.</b>	2.773	0.857	0.211	18
<b>3.5%Alg.-19%Aam-2%Bis-AAm-0.2% ini.</b>	2.857	0.860	0.205	21
<b>3.5%Alg.-19%Aam-4%Bis-AAm-0.2% ini.</b>	2.843	0.883	0.191	19
<b>3.5%Alg.-19%Aam-1%Bis-AAm-0.4% ini.</b>	3.233	0.851	0.263	28
<b>3.5%Alg.-19%Aam-1%Bis-AAm-0.6% ini.</b>	3.353	0.842	0.272	28

The standard deviation of the microcapsule equivalent diameter was less than 0.12 mm or 4% of the average while that of circularity was less than 0.05 or 6% of the average value. The results showed that an increase in the monomer concentration leads to an increase in the polymer viscosity, forming a denser gel and raising flow resistance. Hence the average diameter and membrane thickness as well as the production rate were all reduced. These results are also in accordance with work of Shigeri et al. 1970 [89], who reported that an increase in monomer concentration results in a reduction in the microcapsule size, probably through a change in the polymerisation characteristics. This is attributed to the diameter of the primary polymer particles when they are formed from the polymerisation of monomer droplet [90]. Hence, particle size can be controlled by the monomer concentration.

The number of microcapsules produced per minute decreased with an increase in the monomer concentration. This was the result of increasing viscosity which is proportional to the increasing monomer concentration as mentioned above.

The effect of cross-linker density on the microcapsule characteristics, which is an important factor in controlling the size of membrane pore and pore volume fractions [47], was

investigated. The influence of cross-linker concentrations was examined by varying Bis-AAm concentrations between 1% and 4% while maintaining a constant concentration of the Alg (3.5%), AAm (19%), and the initiator (0.2%). The structure of the microcapsules produced at different cross-linker concentrations is shown in Figure 5-3

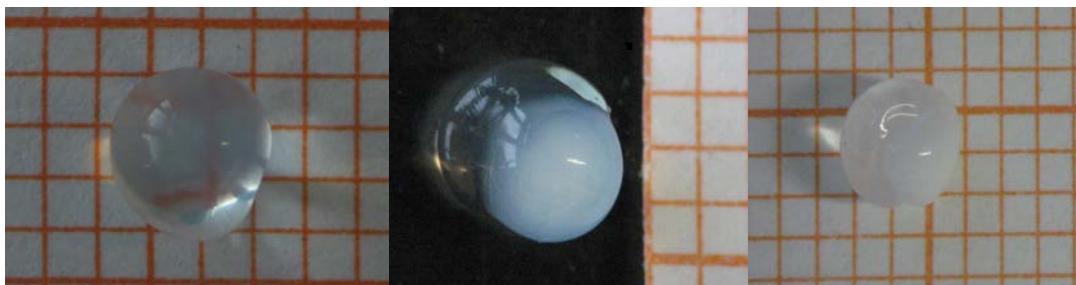


Figure 5-3: Images of microcapsules under light microscope with (a) 1%, (b) 2%, (c) 4% Bis-AAm.

The equivalent diameter and membrane thickness of the microcapsules were reduced with increasing cross-linker Bis-AAm concentration. This is attributed to a higher degree of cross-linking of the AAm leading to a dense polymer network in the microcapsule membrane and, as a result, the formation of a denser gel. In addition, it was observed that the microcapsules that were formed with a higher concentration of the cross-linker became opaque, which could be the result of micro precipitation causing the microcapsule to lose transparency. If the concentration of cross-linker is above 6%, the encapsulation deteriorates due to the alteration mechanism and the inability of the cross-linker to integrate into the polymer network, even with the addition of excess reagents [47]. However, an increase in cross-linker concentration does not exert a significant influence on the circularity of microcapsules. The number of microcapsules produced per minute decreases with an increase in the cross-linker concentration, which is attributed to the higher viscosity of the polymer solution yielding, a higher flow resistance.

The influence of the initiator on the characteristics of the microcapsules was studied by varying the concentration of the redox pair from 0.2-0.6% while the concentrations of the other reactants were kept constant at 3.5% Alg, 19% AAm, and 1% w/w Bis-AAm respectively. The results show that both the microcapsule diameter and the membrane thickness increased with higher concentrations of initiator, which could be due to the effect of an increase in the level of polymerisation of AAm, since the rate of polymerisation varies with the square root of the initiator concentration and the monomer concentration [32,34,91]. Since increasing the reductant (sodium metabisulfite) causes a reduction in the pH of the



gelling bath, Tris was added to the gelling bath to maintain the pH at around 5 in order to maintain the stability of the microcapsules. It was found that the microcapsules produced from a gelling bath with a low pH were dissolved in the protein solution (result not shown). Although an increase in the initiator concentration leads to a higher rate of polymerisation, it is important to note that the higher initiator concentration also leads to higher surface tension in the gelling bath which can affect the quality of the microcapsules because a high surface tension results in microcapsule rupture.

With regard to the qualitative analysis, microcapsules prepared with 3.5% Alg, 19% AAm, 1% Bis-AAm, and 0.2% initiator exhibited the highest mechanical stability of all concentrations. This could be because microcapsules produced at high monomer or cross-linker concentrations had thinner membranes, due to the high viscosity of the polymer solution, while the amount of encapsulated core solution increased, which reduces the mechanical stability of the microcapsules.

From the above results, it is clear that the optimum composition of pAAm-Alg microcapsules is 19% AAm monomer, 1% Bis-AAm cross-linker, 0.2% initiator, and 3.5% w/w Alg. The production rate of standard pAAm-Alg microcapsules is 1800 microcapsules/hr and the microcapsule-specific surface area is approximately 2000 m<sup>2</sup>/m<sup>3</sup>.

## **5.1.2 Extrinsic parameters in microcapsule preparation**

Apart from the physicochemical properties, the effects of extrinsic parameters, such as the geometry of the nozzle used in microcapsule production, on the characteristics of the microcapsules were investigated. The geometric features of the nozzle, which is expected to play a role in the characteristics of the microcapsules, are the number of rings, the inner diameters of the rings, and the length of the needle. The experiments were conducted using the standard composition: 3.5% alginate, 19% AAm, 1% Bis-AAm, and 0.2% initiator to prepare the microcapsules.

### **5.1.2.1 Number of rings**

Since the rings constitute the air chamber of the nozzle, the number of rings determines the height of the air chamber and the position of the tip of the needle. The number of rings was designed to arrange the air chamber in three different categories: the last ring is above the tip of the needle (position A, 4 rings), the last ring is at the same position as the tip of the needle (position B, 7 rings), and the last ring is below the tip of the needle (position C, 9 rings). It is

expected that the drag force of the air at different positions of the tip of the needle will influence the characteristics of the microcapsules. The effect of the number of rings (4, 7, or 9) at various air (300l/h and 500l/h) and inner core solution (1.337 ml/min and 1.904 ml/min) volumetric flow rates was investigated. The other geometric features of the nozzle used were a short needle, a small diameter ring (10 mm), and a sharp outlet end. The influence of the number of rings at various air and core solution volumetric flow rates on the characteristics of the microcapsules and production rates are shown in Table 5-5.

Table 5-5: Equivalent diameter, circularity, quality classification, and production rate of pAAm-Alg microcapsules for different numbers of rings

<b>Position:</b>	<b>A</b>	<b>B</b>	<b>C</b>
<b>Number of rings:</b>	<b>9</b>	<b>7</b>	<b>4</b>
$\dot{V}$ core: 1.337 ml/min; $\dot{V}$ air: 300 l/h	$D_{eq}$ : 2.557 mm Circ. : 0.863 quality : good Prod. Rate. : 25	$D_{eq}$ : 2.667 mm Circ. : 0.850 quality : good Prod. Rate: 23	$D_{eq}$ : 2.753 mm Circ. : 0.843 quality : good Prod. Rate: 22
$\dot{V}$ core: 1.337 ml/min; $\dot{V}$ air: 500 l/h	$D_{eq}$ : 2.233 mm Circ. : 0.880 quality : acceptable Prod. Rate: 34	$D_{eq}$ : 2.32 mm Circ. : 0.853 quality : good Prod. Rate: 32	$D_{eq}$ : 2.633 mm Circ. : 0.86 quality : good Prod. Rate: 28
$\dot{V}$ core: 1.904 ml/min; $\dot{V}$ air: 300 l/h	$D_{eq}$ : 2.680 mm Circ. : 0.847 quality : good Prod. Rate: 29	$D_{eq}$ : 2.727 mm Circ. : 0.850 quality : good Prod. Rate: 27	$D_{eq}$ : 2.807 mm Circ. : 0.847 quality : good Prod. Rate: 24
$\dot{V}$ core: 1.904 ml/min; $\dot{V}$ air: 500 l/h	$D_{eq}$ : 2.387 mm Circ. : 0.877 quality : acceptable Prod. Rate: 38	$D_{eq}$ : 2.633 mm Circ. : 0.850 quality : good Prod. Rate: 35	$D_{eq}$ : 2.730 mm Circ. : 0.833 quality : good Prod. Rate: 33

The maximum threshold for the air flow rate was 600 l/h at which rate all the microcapsules produced became incompletely encapsulated. The results show that as air is introduced to the system, the diameter of the microcapsules decreases but that the number of microcapsules produced per minute increases.

It could be seen that the microcapsules produced were of a smaller size and had a moderately decreased circularity at higher numbers of rings or for increased height of the air chamber. This result could be attributed to the effect of the drag force of the air on the microcapsule droplets. At position C, with the tip of the needle below the air chamber, the pressure of the air on droplet formation is less than at position A, where the air is expected to drag the droplet out of the tip of the needle, or at position B, where the air is expected to push the droplet from the tip of the needle.

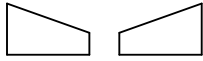
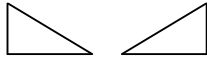
In the absence of air flow, the force for detaching the droplet from the nozzle is simply the droplet weight which slightly exceeds its surface tension. When air flow is applied, the polymer solution is forced through the outlet needle, and droplets are formed at the end of the needle, which extends into the gas stream. A droplet detaches when the drag force of the air flow and the weight of the droplet slightly exceeds the surface tension forces that hold the droplet on to the nozzle. A gradual increase in air flow through the air sheath increases the drag forces on the droplets and decreases the diameter of the resultant microcapsules. However, fragmentation of droplets occurs when a certain air flow rate, dependent on each particular nozzle's characteristics, is exceeded. As a consequence, not only normally sized, but also very small droplets (sub-micro beads), are generated.

From the results given above, the number of rings in the air chamber was selected to be 7 (position B), where the position of the tip of the needle is at the same position as the air chamber, for further experimentation.

#### **5.1.2.2 Nozzle outlet type**

When air flow is applied to the preparation system, the outlet of the nozzle serves as a 'cutter' for microcapsules at the needle tip. Two types of nozzle outlets, blunt-end and sharp-end, were used to assess the effect of the air outlet on the characteristics of the microcapsules. The tip of the needle was set at position B, with a ring diameter of 10 mm and a short needle. The effects of the nozzle outlet type at various air and inner core solution volumetric flow rates on the characteristics of the microcapsules and production rates are shown in Table 5-6.

Table 5-6: Equivalent diameter, circularity, quality classification, and production rate of pAAm-Alg microcapsules for different nozzle outlet types

Outlet type:	Blunt-end	Sharp-end
		
$\dot{V}$ core: 1.337 ml/min;	$D_{eq}$ : 2.727 mm	$D_{eq}$ : 2.667 mm
$\dot{V}$ air: 300 l/h	Circ. : 0.857	Circ. : 0.850
	Remark : good	Remark : good
	Prod.Rate: 23	Prod.Rate: 23
$\dot{V}$ core: 1.337 ml/min;	$D_{eq}$ : 2.440 mm	$D_{eq}$ : 2.320 mm
$\dot{V}$ air: 500 l/h	Circ. : 0.853	Circ. : 0.853
	Remark : good	Remark : good
	Prod.Rate: 28	Prod.Rate: 32
$\dot{V}$ core: 1.904 ml/min;	$D_{eq}$ : 2.787 mm	$D_{eq}$ : 2.727 mm
$\dot{V}$ air: 300 l/h	Circ. : 0.877	Circ. : 0.850
	Remark : good	Remark : good
	Prod.Rate: 26	Prod.Rate: 27
$\dot{V}$ core: 1.904 ml/min;	$D_{eq}$ : 2.683 mm	$D_{eq}$ : 2.633 mm
$\dot{V}$ air: 500 l/h	Circ. : 0.870	Circ. : 0.850
	Remark : good	Remark : good
	Prod.Rate: 32	Prod.Rate: 35

The results show that the microcapsules produced from a nozzle outlet with a sharp-end have comparable diameters and circularities to those produced from a nozzle outlet with a blunt-end. However, the number of microcapsules produced per minute from a sharp-end outlet was higher than that from a blunt-end outlet. This could be the result of higher air pressure at the air outlet, detaching the microcapsules more easily from the tip of the needle. For further experimentation involving air flow, the sharp-end outlet was used.

### 5.1.2.3 Length of the needle

Since the pressure drop varies with the length of the needle, the effects of the length of needle on the characteristics of the microcapsules and production rates were studied. Two types of needles were used in the nozzle head: a short and a long needle with the same diameter. The location of the tip of the needle was set at position B with a ring diameter of 10 mm. The effects of the length of the needle at various inner core solution volumetric flow rates on the characteristics of the microcapsules and production rates are shown in Table 5-7.

Table 5-7: Equivalent diameter, circularity, quality classification, and production rate of pAAm-Alg microcapsule for different needle lengths.

Needle length	Short	Long
$\dot{V}$ core: 1.337 ml/min	$D_{eq}$ : 2.83 mm	$D_{eq}$ : 2.86 mm
	Circ. : 0.850	Circ. : 0.843
	Remark : good	Remark : good
	Prod.Rate: 22	Prod.Rate: 18
$\dot{V}$ core: 1.904 ml/min	$D_{eq}$ : 2.88 mm	$D_{eq}$ : 2.91 mm
	Circ. : 0.86	Circ. : 0.840
	Remark : good	Remark : good
	Prod.Rate: 24	Prod.Rate: 21

The results show the expected trend. Microcapsules produced with a short needle had a diameter comparable to those produced with a long needle. The circularity of the microcapsules produced with a short needle was slightly better than those produced with a long needle. However, the production rate of the short needle was higher than that of the longer needle. This could be attributed to the higher pressure drop and increase in flow resistance in the long needle. It is therefore, preferable to keep the needle as short as possible in order to achieve a higher production rate.

### 5.1.2.4 Nozzle ring diameter

When the outer diameter of the nozzle ring is fixed, it is the inner diameter of the nozzle ring that determines the volume of the air chamber. It is predicted that a smaller volume of the air chamber will give rise to a higher air pressure than a larger one. Two different inner

diameters of the nozzle ring, 10 mm and 20 mm, were used to configurate the air chamber. The effect of nozzle ring diameter at various air flow rates (300l/h and 500l/h) and inner core solution (1.337 ml/min and 1.904 ml/min) on the characterisation and production rate of microcapsules were investigated. The rings of the needle were at position B, with a short needle and a sharp-end outlet. The influence of the inner diameter of nozzle ring at various air and inner core solution volumetric flow rates on the characteristics of the microcapsules are presented in Table 5-8.

Table 5-8: Equivalent diameter, circularity, quality classification, and production rate of pAAm-Alg microcapsules at different nozzle ring inner diameters

<b>Ring inner diameter (mm):</b>	<b>10</b>	<b>20</b>
<b><math>\dot{V}</math> core: 1.337 ml/min;</b>	$D_{eq}$ : 2.667 mm	$D_{eq}$ : 2.737 mm
<b><math>\dot{V}</math> air: 300 l/h</b>	Circ. : 0.850	Circ. : 0.863
	Remark : good	Remark : good
	Prod.Rate: 23	Prod.Rate: 21
<b><math>\dot{V}</math> core: 1.337 ml/min;</b>	$D_{eq}$ : 2.320 mm	$D_{eq}$ : 2.460 mm
<b><math>\dot{V}</math> air: 500 l/h</b>	Circ. : 0.853	Circ. : 0.843
	Remark : good	Remark : good
	Prod.Rate: 32	Prod.Rate: 29
<b><math>\dot{V}</math> core: 1.904 ml/min;</b>	$D_{eq}$ : 2.727 mm	$D_{eq}$ : 2.817 mm
<b><math>\dot{V}</math> air: 300 l/h</b>	Circ. : 0.850	Circ. : 0.863
	Remark : good	Remark : good
	Prod.Rate: 27	Prod.Rate: 25
<b><math>\dot{V}</math> core: 1.904 ml/min;</b>	$D_{eq}$ : 2.633 mm	$D_{eq}$ : 2.717 mm
<b><math>\dot{V}</math> air: 500 l/h</b>	Circ. : 0.850	Circ. : 0.853
	Remark : good	Remark : good
	Prod.Rate: 35	Prod.Rate: 33

The results indicate that the inner diameter of the nozzle ring, which influences the volume of the air chamber, has an effect on the size and production rate of the microcapsules. At the same air and inner core solution volumetric flow rates, a larger inner diameter yielded a larger microcapsule diameter, but at a slightly lower rate of production. This could be attributed to a decrease in the drag force of the air stream on the polymer droplets. An increase in the diameter of the air sheath with an unchanged air flow rate is associated with a decrease in the air stream velocity, which enhances the formation of microcapsules with a larger diameter and reduces the rate of microcapsule production.

It should be noted that at a higher air flow rate, the distance between the needle tip and the surface of the gelling solution should be increased in order to prevent the formation of excessive ‘waves’ in the gelling bath.

### 5.1.3 Membrane thickness

The thickness of the membrane for various sizes of microcapsules was analysed with a stereo microscope (Leica MZ95) and with the help of image analysis software (Leica IM50 version 4.0 Release 132). With this software, each image of microcapsules was compared to a 500  $\mu\text{m}$  line as a reference. For each batch produced, 5 microcapsules were taken to be analysed. A sample of such images is shown in Figure5-4.

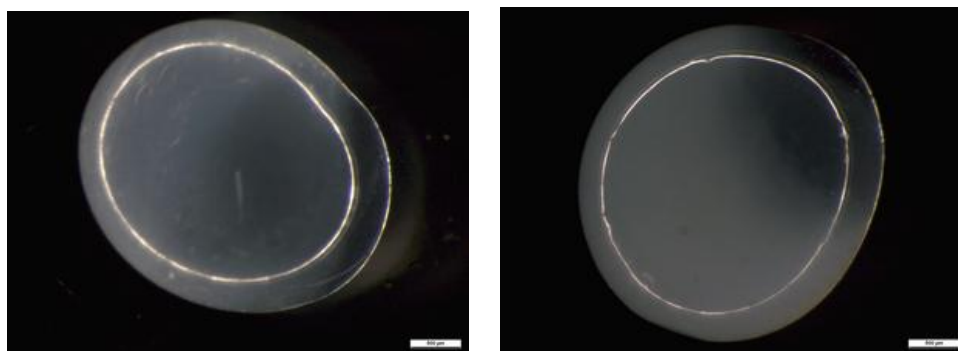


Figure 5-4: Images of microcapsules taken by stereo-microscope

The advantages in using a stereo-microscope to analyse the microcapsules are its simplicity and accuracy. The results of the analysis of membrane thickness for various equivalent diameters of microcapsules are depicted in Figure 5-5.

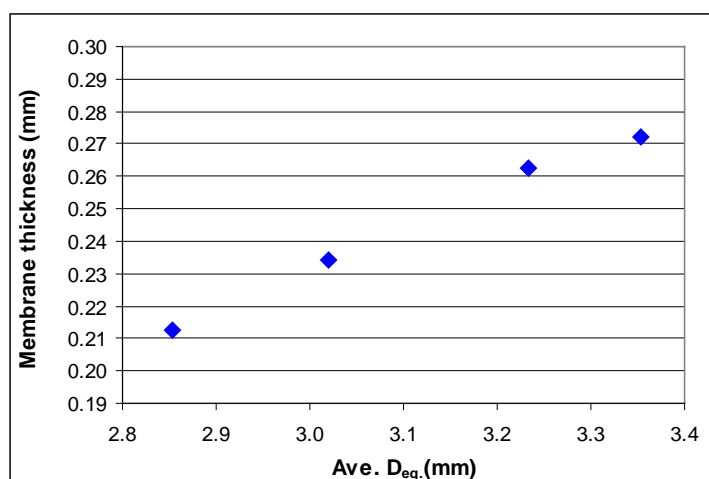


Figure 5-5: Membrane thicknesses of various microcapsules

The results show that the membrane thickness increased proportionally to the increase in the  $D_{eq}$  value of the microcapsule. The gelling velocity at the contacting surface between the polymer solution and the gelling solution in the gelling bath is very high, and since the outer surface of the microcapsules is directly fixed through a thin gel membrane, the outer radius of the microcapsules is constant. With the ‘shrinkage’ of the polymer solution, the thickness of the surrounding layer is reduced (Figure 5-6).

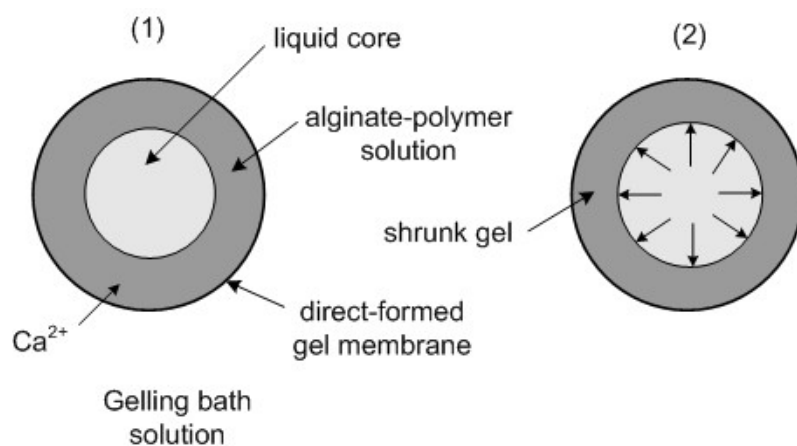


Figure 5-6: Change in membrane thickness during the gelling process

The term ‘shrinkage’ refers to a reduction in gel volume when compared to the polymer solution used. This is due to the networking and the denser arrangement of polymer chain [92]. This ‘shrinkage’ is accompanied by an increase in the inner core radius and the concentration of the core solution. However, data on the thickness of the membrane of the microcapsules is essential when interpreting the diffusion and permeability of the catalyst core solution inside the microcapsules.



### 5.1.4 Summary

Significant improvements in the mechanical stability of the liquid core in encapsulated hollow microcapsules using a polyacrylamide-alginate membrane were achieved. A suitable double nozzle, concentric air-jet for producing microcapsules with the desired characteristics was systematically designed and its performance evaluated. The preparation parameters which affect the basic properties of microcapsules and their optimum settings for reproducibly generating high quality microcapsules were investigated in detail. A qualitative analysis of the microcapsules was also conducted, in order to classify the microcapsules formed according to their 'quality'. Finally, the membrane thickness of the microcapsules was measured.

The microcapsules produced were mostly stable. When either the monomer or cross-linker concentration was increased, the average equivalent diameter of the microcapsules decreased. On the other hand, the size of microcapsules increased when the concentration of the initiator was increased. The equivalent diameter and circularity of the microcapsules, together with their relative standard deviation, were obtained using the Image J image analysis software, and the membrane thickness was analysed using a stereo-microscope.

Microcapsules with the best mechanical stability were produced with concentrations of 3.5% Alg, 19% AAm, 1% Bis-AAm, and 0.2% initiator. This 'recipe' was therefore used in further experiments. The distance between the needle tip and the surface of the gelling solution in the gelling bath was kept within 4 to 6 cm, to prevent the droplet breakage. The addition of Tris into the gelling bath improved the smoothness of microcapsules' surface and helped maintain a constant pH in the gelling bath solution.

The size of the microcapsules can be adjusted by varying the rate of compressed air flow into the system. The diameter of the microcapsules varies depending on the air flow rate, the number of rings (the size of the air chamber) inside the nozzle, the nozzle outlet type, the ring diameter, and the length of the nozzle. The use of compressed air gave a significant increase in the number of microcapsules produced. This significant increase in the production rate might prove beneficial in industrial applications.

Further work is still needed to analyse the mechanical resistance of microcapsules precisely. This can be done using a Texture Analyzer (Stable Micro Systems, Surrey, UK), in which the mean force needed to break a capsule is measured. A Bench Comparator (Ames, Waltham, USA.) can also be used to measure the deformation of microcapsules at a given load. This

measurement is important for the application of microcapsules in chemical reactors, where microcapsules serve as catalyst carriers and may rupture during the chemical reaction.

The effect of temperature on the microcapsules should also be examined. Further, one could envisage carrying out experiments using different types of initiators. The data for the equivalent diameter and circularity of the microcapsules could be improved if the microcapsules were analysed directly under a stereo-microscope as was done for the membrane thickness analysis. In addition, a Nuclear Magnetic Resonance (NMR) spectroscope, which has been widely used for studying the characteristics of molecules, could also be utilised to elucidate the chemical structure of the microcapsules [93].

## 5.2 Diffusion and MWCO of pAAm-Alg microcapsules

The first section explained about the parameters affecting the preparation and hence, characterisation of pAAm-Alg microcapsules. This section focuses on the study of the mass transport properties of pAAm-Alg microcapsules in term of diffusion coefficient. The diffusion characteristics of microcapsule systems were analysed according to kinetics based on Fick's law, with the assumption that the release rate is proportional to the concentration gradient of the solutes and that all the capsules are of identical size. The diffusion coefficients were determined applying Crank's solution to the diffusion equation [57-64]. The effects of different factors, such as monomer, cross-linker, initiator, and silica additive concentrations were tested. Subsequently, the molecular weight cut-off (MWCO) of the optimised microcapsules was determined.

To determine the diffusion coefficient, microcapsules were placed into substrate solutions of glucose and dextran T1 at initial concentrations of 3 g/l and the substrate was allowed to diffuse from the medium surrounding the microcapsules into the microcapsules core solution. The substrate diffusion curve was obtained by measuring the concentration of the substrate in the external medium; the combined diffusion coefficient value,  $D_m$ , and the diffusion coefficient of the microcapsule membrane,  $D_l$ , were calculated according to eq. 2-16 and eq. 2-19 respectively. Similar diffusion experiments were carried out to test the cut-off properties of a standard pAAm-Alg microcapsule. Substances with different molecular weights (sugar and protein) were employed as diffusion substrate probes and the MWCO was determined.

### 5.2.1 Influence of AAm monomer concentration on sugar diffusion

To study how the concentration of the AAm monomer influences the diffusion coefficients, microcapsules were prepared with different concentrations of AAm monomer (19%, 23%, and 27% w/w), and fixed concentrations of Bis-AAm (1%), Alg (3.5%), and initiator (0.2%). The microcapsules were placed into separate sugar solutions of glucose and dextran T1 and the sugar solutions were allowed to diffuse from the medium surrounding the microcapsules into the microcapsule core solutions. The sugar diffusion curves were obtained by measuring the concentration of sugar in the external medium. The observed experimental data fits the theoretical curve for eq.2-16 well. The calculated values of  $D_m$ ,  $S$ , and  $D_l$  for glucose and dextran T1 are listed in Table 5-9. The effects of the AAM concentration on the pAAm-Alg microcapsules with respect to the diffusivity of glucose and dextran T1 are depicted in Figure 5-7.

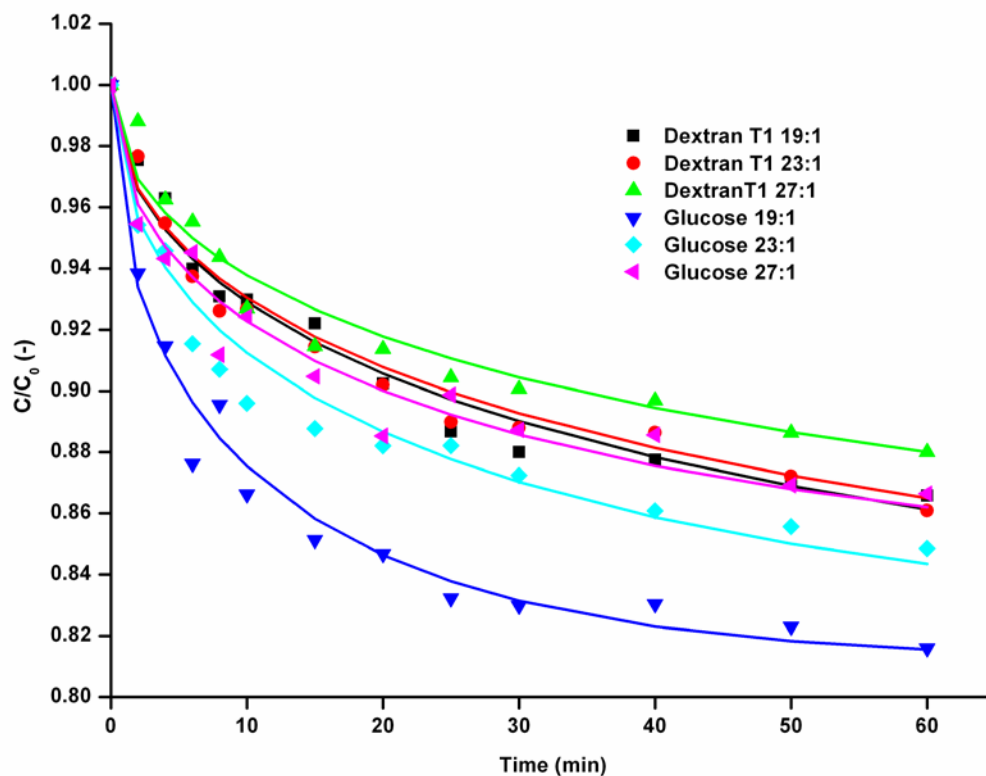


Figure 5-7: Concentration profiles of glucose and dextran T1 diffusing into pAAm-Alg microcapsules at different AAm concentrations. The points are the experimental data and the solid curves represent the results calculated using eq.2-16

Table 5-9: Diffusion coefficients ( $D_m$ ,  $D_1$ , and  $S$ ) of pAAm-Alg microcapsules at different AAm concentrations

Microcapsule (%Alg-AAm-Bis-AAm- initiator)	$D_m$ (m <sup>2</sup> /s) glucose	$S$ (%)	$D_1$ (m <sup>2</sup> /s) glucose	$D_m$ (m <sup>2</sup> /s) dextran T1	$S$ (%)	$D_1$ (m <sup>2</sup> /s) dextran T1
<b>Diffusion in water</b>	6.8x10 <sup>-10</sup> a			1.11 x10 <sup>-10</sup> b		
<b>3.5% -19% -1% -0.2%</b>	1.94x10 <sup>-10</sup>	0.079	3.98x10 <sup>-11</sup>	5.87 x10 <sup>-11</sup>	0.132	1.64 x10 <sup>-11</sup>
<b>3.5% -23% -1% -0.2%</b>	8.67x10 <sup>-11</sup>	0.080	1.50x10 <sup>-11</sup>	5.05 x10 <sup>-11</sup>	0.037	1.26 x10 <sup>-11</sup>
<b>3.5% -27% -1% -0.2%</b>	7.26x10 <sup>-11</sup>	0.085	1.22x10 <sup>-11</sup>	4.38 x10 <sup>-11</sup>	0.069	1.00 x10 <sup>-11</sup>

a) Value from H. Tanaka et al. [24]

b) Value from extrapolating diffusion coefficient of dextran T10, dextran T40 and dextran T70 [94]

The results demonstrate that sugar diffusivity decreases with an increase in the AAm monomer concentration, for which the gel becomes more homogeneous and a denser gel structure was probably formed [95]. Consequently, the resistance to sugar diffusion increased and the diffusion coefficient decreased.

It should be noted that glucose exhibited a more noticeable change in diffusion than did dextran T1. The value of the diffusion coefficient of glucose at 27% AAm was 60% less than that at 19% AAm while that of dextran T1 was only 30% less. Depending on the concentrations of AAm, the combined diffusion coefficient of glucose,  $D_m$ , was approximately 10-30% of the value for pure water, while the diffusion coefficient of the microcapsule membrane,  $D_1$ , was much smaller, only about 17-20% as large as the  $D_m$  value. These results indicate that the microcapsule membrane plays a decisive role in the permeability of the microcapsule and that the pore size of the microcapsule membrane can be adjusted by varying the monomer concentration.

### 5.2.2 Influence of Bis-AAm cross-linker concentration on sugar diffusion

Since the cross-linker is a key factor in controlling the size of the membrane pores, the pore volume fraction, and the cross-bonding [15], the effect of varying concentrations of the cross-linker, Bis-AAm, on diffusivity was studied. Microcapsules were prepared with different concentrations of cross-linker Bis-AAm (1%, 2%, and 4% w/w), for fixed concentrations of

Alg (3.5%), AAm (19%), and initiator (0.2%). Same experimental procedures and data analysis described earlier were repeated. The calculated values of  $D_m$ ,  $S$ , and  $D_l$  for glucose and dextran T1 are listed in Table 5-10. The effects of the cross-linker Bis-AAm concentrations on the pAAm-Alg microcapsules with respect to the diffusivity of glucose and dextran T1 are illustrated in Figure 5-8.

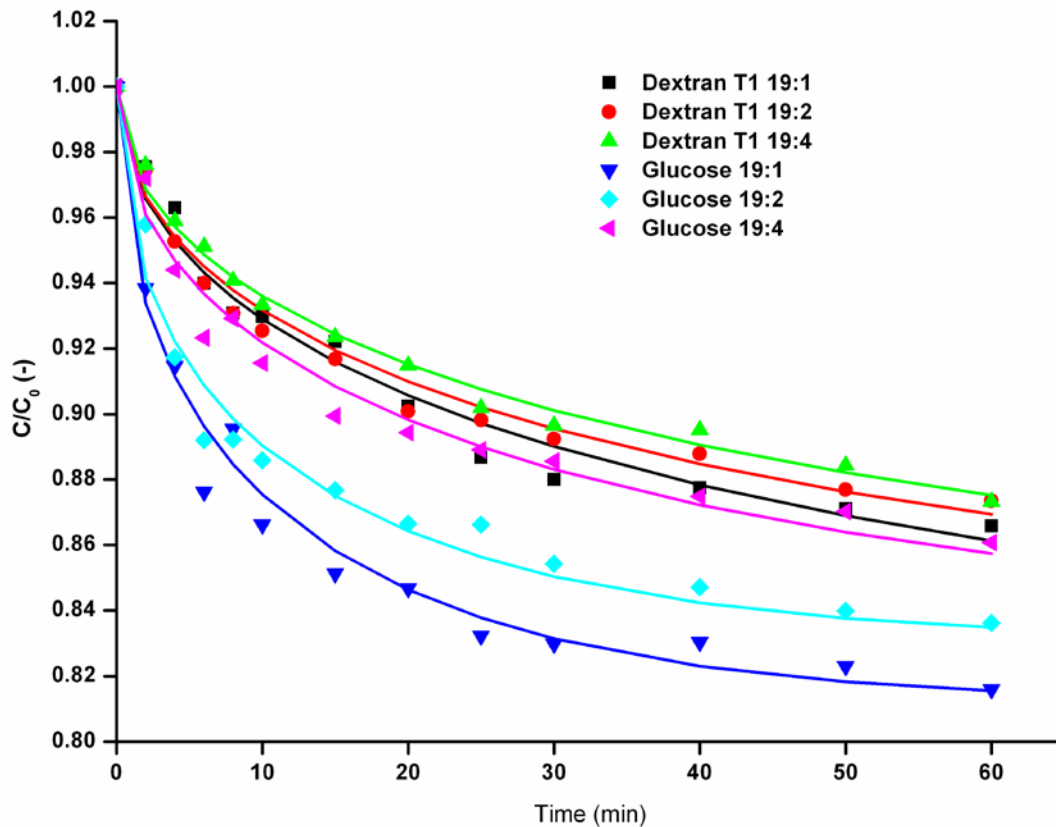


Figure 5-8: Concentration profiles of glucose and dextran T1 diffusing into pAAm-Alg microcapsules at different Bis-AAm concentrations. The points are the experimental data and the solid curves represent the results calculated using eq. 2-16

The sugar diffusivity decreased with an increase in the Bis-AAm concentration. This is the result of the minimal pore size which was generated from the 1-5% Bis-AAm concentrations [29]. Other concentrations of Bis-AAm resulted in larger pore sizes yielding in a denser alginate gel, and thus forming a denser membrane thickness. Therefore, the resistance to substrate diffusion rose with increasing in cross-linker concentration. It was observed that at higher concentrations of Bis-AAm, the microcapsule became opaque which may be the result of micro-precipitation causing the capsules to loose transparency [47].

Table 5-10: Diffusion coefficients ( $D_m$ ,  $D_1$ , and  $S$ ) of pAAm-Alg microcapsules at different cross-linker Bis-AAm concentrations

Microcapsule (%Alg-AAm-Bis-AAm-initiator)	$D_m$ (m <sup>2</sup> /s) glucose	$S$ (%)	$D_1$ (m <sup>2</sup> /s) glucose	$D_m$ (m <sup>2</sup> /s) dextran T1	$S$ (%)	$D_1$ (m <sup>2</sup> /s) dextran T1
<b>Diffusion in water</b>	$6.8 \times 10^{-10}$			$1.11 \times 10^{-10}$		
<b>3.5% -19% -1% -0.2%</b>	$1.94 \times 10^{-10}$	0.079	$3.98 \times 10^{-11}$	$5.87 \times 10^{-11}$	0.132	$1.64 \times 10^{-11}$
<b>3.5% -19% -2% -0.2%</b>	$1.60 \times 10^{-10}$	0.042	$2.88 \times 10^{-11}$	$5.08 \times 10^{-11}$	0.028	$1.20 \times 10^{-11}$
<b>3.5% -19% -4% -0.2%</b>	$6.38 \times 10^{-11}$	0.050	$9.34 \times 10^{-12}$	$4.32 \times 10^{-11}$	0.032	$8.45 \times 10^{-12}$

The value of the diffusion coefficient of glucose at 4% cross-linker Bis-AAm was approximately 70% less than at the 1% cross-linker level, while that of dextran T1 was 30% less. Depending on the concentrations of Bis-AAm, the combined diffusion coefficient of glucose,  $D_m$ , was approximately 10-30% of the value for pure water while the diffusion coefficient of the microcapsule membrane,  $D_1$ , was much smaller, only about 15-20% as large as the  $D_m$  value. As with the result from varying the monomer concentration in the microcapsules, the microcapsule membrane clearly controls the transport of substrate into the microcapsule and the pore size of the microcapsule membrane can be adjusted by varying the cross-linker concentration.

### 5.2.3 Influence of initiator concentration on sugar diffusion

Since the rate of polymerisation depends on the square root of the initiator concentration and the monomer concentration, [91] a change in the initiator concentration should have an effect on the level of polymerisation of the acrylamide and hence on the membrane formation process. To study the influence of initiator concentration on sugar diffusion, microcapsules were prepared with different concentrations of initiator (0.2%, 0.4%, and 0.6% w/w) for, fixed concentrations of Alg (3.5%), AAm (19%), and Bis-AAm (1%). Same experimental procedures and data analysis described earlier were repeated. The calculated values of  $D_m$ ,  $S$ , and  $D_1$  for glucose and dextran T1 are listed in Table 5-11. The effects of the initiator concentrations on the pAAm-Alg microcapsules with respect to substrate diffusion are presented in Figure 5-9.

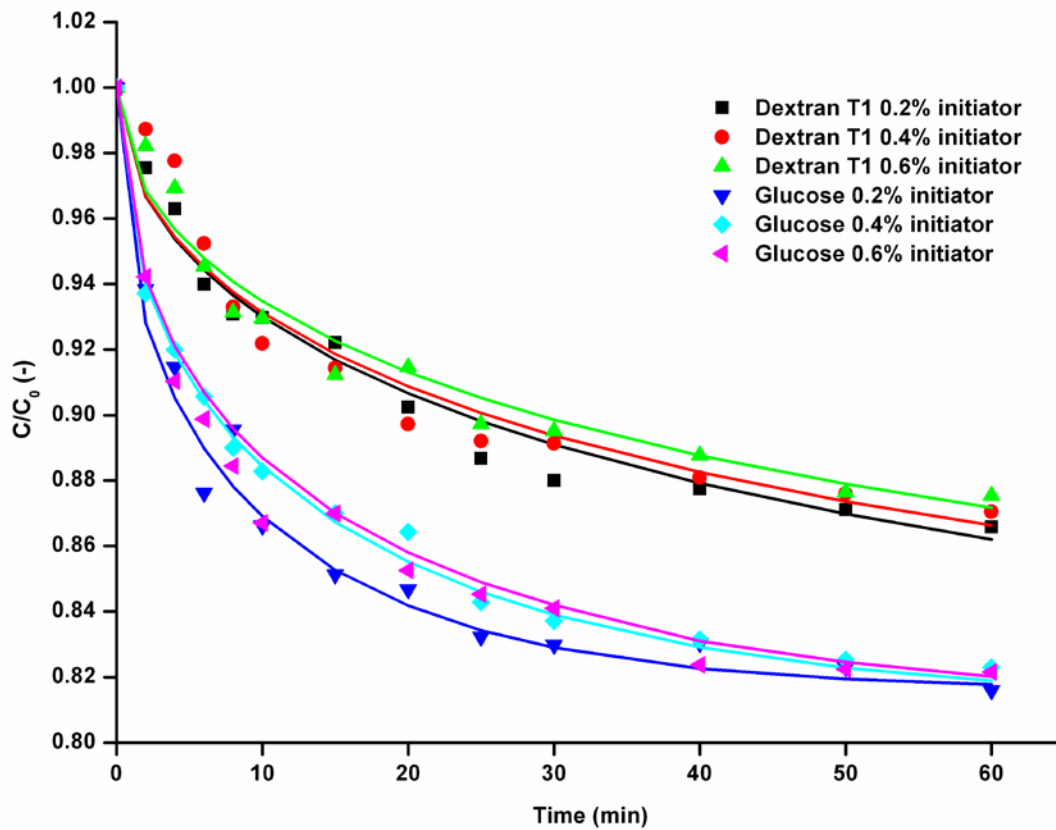


Figure 5-9: Concentration profiles of glucose and dextran T1 diffusing into pAAm-Alg microcapsules at different initiator concentrations. The points are the experimental data and the solid curves represent the results calculated using eq. 2-16

Table 5-11: Diffusion coefficients ( $D_m$ ,  $D_1$ , and  $S$ ) of pAAm-Alg microcapsules at different initiator concentrations

Microcapsule (%Alg-AAm-Bis-Aam- initiator)	$D_m$ (m <sup>2</sup> /s) glucose	$S$ (%)	$D_1$ (m <sup>2</sup> /s) glucose	$D_m$ (m <sup>2</sup> /s) dextran T1	$S$ (%)	$D_1$ (m <sup>2</sup> /s) dextran T1
<b>Diffusion in water</b>	$6.8 \times 10^{-10}$			$1.11 \times 10^{-10}$		
<b>3.5% -19% -1% -0.2%</b>	$1.94 \times 10^{-10}$	0.079	$3.98 \times 10^{-10}$	$5.87 \times 10^{-11}$	0.132	$1.64 \times 10^{-11}$
<b>3.5% -19% -1% -0.4%</b>	$1.57 \times 10^{-10}$	0.016	$3.16 \times 10^{-11}$	$3.48 \times 10^{-11}$	0.021	$7.68 \times 10^{-12}$
<b>3.5% -19% -1% -0.6%</b>	$1.47 \times 10^{-10}$	0.082	$2.91 \times 10^{-11}$	$2.95 \times 10^{-11}$	0.049	$6.16 \times 10^{-12}$

With an increase in initiator concentration, the diameter and membrane thicknesses of the microcapsules were higher, due to the greater rate of polymerisation. The substrate

diffusivity decreased with an increase in initiator concentration. This is because the greater membrane thickness resulted in a longer diffusion path for the substrate and thus more resistance to substrate diffusion, therefore reducing the diffusion coefficient. However the diffusivity of the substrate was only slightly affected by higher initiator concentrations (0.4% and 0.6%), which might be the result of initiator saturation in the membrane, yield roughly similar diffusion coefficients. The combined diffusion coefficient values for glucose and dextran T1,  $D_m$ , with 0.6% initiator concentration were 25% and 50% lower, respectively, than for a 0.2% concentration. Depending on the concentration of the initiator, the  $D_m$  value of glucose was approximately 22% to 30% of the value for pure water, while the diffusion coefficient of the microcapsule membrane,  $D_l$ , was much smaller, only about 20-25% as large as the  $D_m$  value. The results imply that, although with less sensitivity than for AAm and Bis-AAm, the pore size of the microcapsule membrane can be adjusted by varying the initiator concentration. Considering both the physical characteristics and the diffusion properties of the pAAm-Alg microcapsule, 3.5% of Alg, 19% of AAm, 1% of Bis-AAm, and 0.2% of initiator were selected as the optimum concentration for preparing the microcapsules.

#### 5.2.4 Influence of silica additive on sugar diffusion

Different concentrations of silica HS-30 additive (1%, 2.5%, and 5% w/w) were added to standard pAAm-Alg microcapsules (3.5% alginate, 19% acrylamide, 1% Bis-AAm, and 0.2% initiator) to study the influence of the silica particles on the diffusion coefficient. PAAm-Alg microcapsules prepared with different concentrations of additive silica HS-30 were placed into a glucose solution. The glucose solution was allowed to diffuse from the medium surrounding the microcapsules into the inner microcapsule core solutions. The sugar diffusion curves were obtained by monitoring the concentration of sugar in the external medium with time. The observed experimental data fits the value calculated from eq.2-16 well. The calculated values of  $D_m$ ,  $S$ , and  $D_l$  for glucose are listed in Table 5-12. The effects of the silica HS 30 additive on the pAAm-Alg microcapsules with respect to the glucose diffusion are shown in Figure 5-10.

The results show that the concentration of silica HS-30 of 1-5% w/w leads to a decrease in the combined diffusion coefficient of glucose to 60-80% of the value without the silica particles. This could be the result of the partial closure of the membrane pores with aggregated colloidal silica reducing the permeability for the substrate solution.



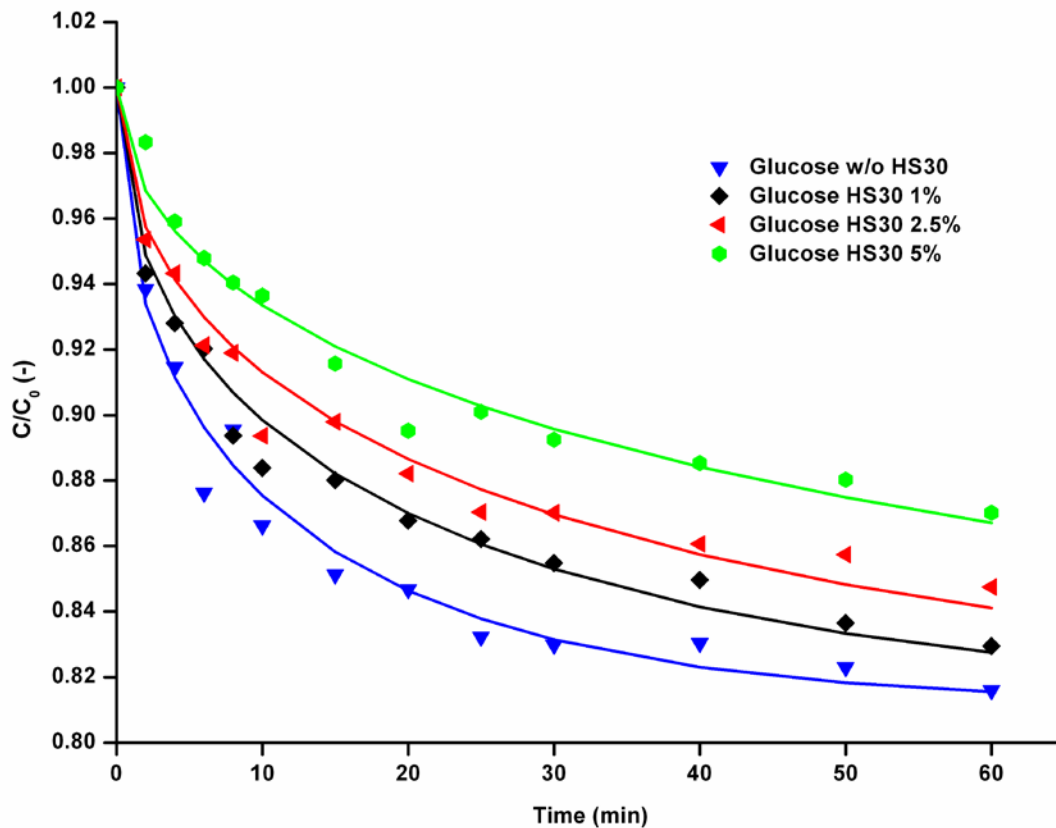


Figure 5-10: Concentration profile of glucose diffusing into pAAm-Alg microcapsules with different concentrations of silica HS30 additive. The points are experimental data and the solid curves represent the results calculated using Eq. 2-16

Table 5-12: Diffusion coefficients ( $D_m$ ,  $D_1$ , and  $S$ ) of pAAm-Alg microcapsules at different silica HS-30 concentrations

Microcapsule	$D_m$ (m <sup>2</sup> /s) glucose	$S$ (%)	$D_1$ (m <sup>2</sup> /s) glucose
Diffusion in water	$6.8 \times 10^{-10}$		
Standard pAAm-Alg microcapsule	$1.94 \times 10^{-10}$	0.079	$3.98 \times 10^{-11}$
Standard with HS30 1%	$1.16 \times 10^{-10}$	0.050	$2.10 \times 10^{-11}$
Standard with HS30 2.5%	$7.77 \times 10^{-11}$	0.064	$1.33 \times 10^{-11}$
Standard with HS30 5 %	$3.97 \times 10^{-11}$	0.056	$6.47 \times 10^{-12}$

The combined diffusion coefficient of glucose,  $D_m$ , was approximately 6-17% of the value for pure water, depending on the exact concentration of silica HS-30. The diffusion coefficients of the microcapsule membrane,  $D_1$ , are much smaller, only about 17-20% as large as the  $D_m$

value. It is clear that of the variations in concentrations of AAm monomer, Bis-AAm cross-linker, initiator, and additive silica concentrations, the last exhibits the most influence on the pore size of the microcapsule membrane. While the AAm monomer, the Bis-AAm cross-linker and the initiator all alter the structure of the membrane, the additive silica physically blocks the membrane pores resulting in less target substrates diffusing into the microcapsule. The entrapment of aggregated silica can therefore be employed as an effective means to influence the mass transport properties of the membrane.

### 5.2.5 MWCO of pAAm-Alg microcapsules

The molecular weight cut-off (MWCO) of the membrane is one of the most crucial characteristics of the microcapsule [96]. It is defined as the lowest molecular weight substrate that is 90% retained by the membrane; in other words, it is the highest molecular weight substrate that can penetrate 10% of the way into the membrane [97].

To determine the cut-off properties of the standard pAAm-Alg microcapsule, an experiment similar to the diffusion experiments described above was carried out with compounds having different molecular weights (glucose 180 Da, maltose 360 Da, dextran T1 1.1 kDa, Insulin 5 kDa,  $\alpha$ -lactalbumin 15 kDa, and Trypsin 23 kDa). The probe molecules, which were smaller than the pore size of the pAAm-Alg membrane were allowed to diffuse from the medium surrounding the microcapsules into to the inner microcapsule core solution, while the molecules which were larger than the pore size remained excluded outside. The diffusion curves of the probe molecules are measured and plotted in Figure 5-11 and the calculated values of  $D_m$ ,  $S$ , and  $D_I$  for glucose and dextran T1 are listed in Table 5-13.

The results show that the concentrations of the bulk solutions decreased rapidly after the addition of microcapsules and then the decrease gradually slowed until it levelled off after 60 minutes. The combined diffusion coefficients of all the probe molecules,  $D_m$ , are around 30% of the values in pure water. The diffusion coefficients of the microcapsule membrane for the probe molecules are approximately 20% of the  $D_m$  values.

The higher the probe molecules molecular weight, the slower the probe molecules diffused into the microcapsule. The equilibrium concentrations of different probe molecules in the bulk solutions increased with an increase in the molecular weight. When the molecular weight was high enough so that the probe molecules could hardly penetrate through the membrane, the concentrations in the external medium remained unchanged.

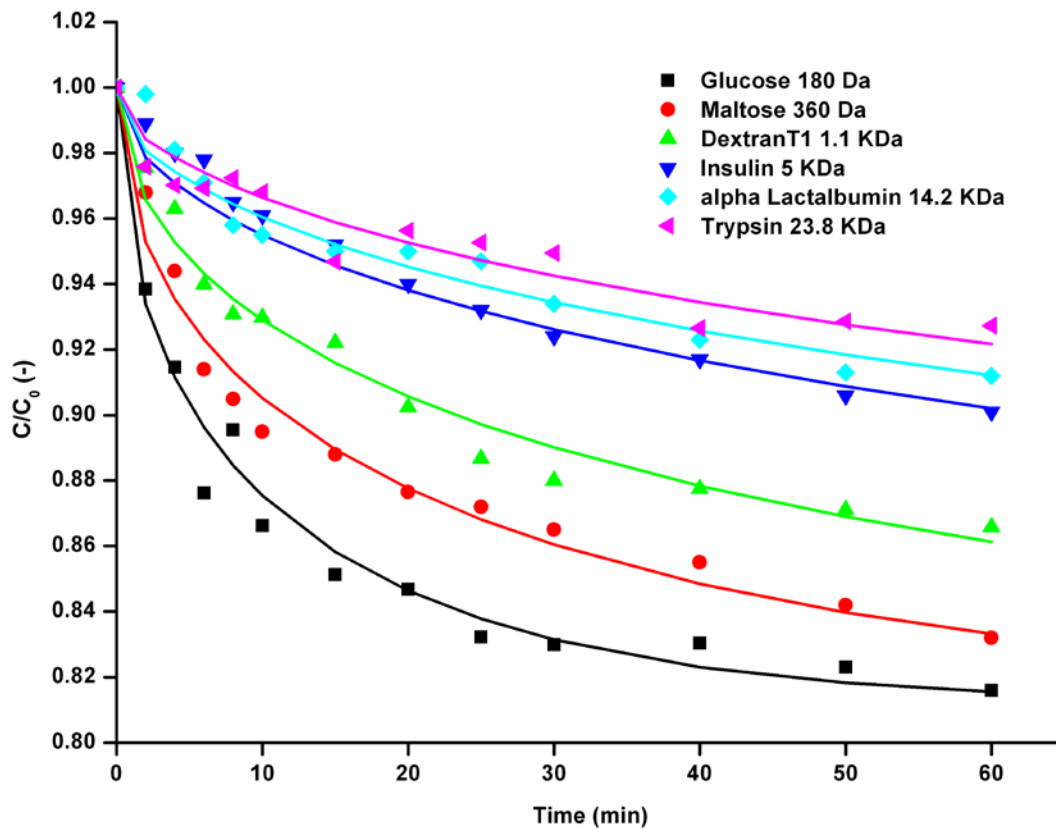


Figure 5-11: Diffusion curves of different probe molecules in pAAm-Alg microcapsules. The points are the experimental data and the solid curves represent the results calculated using Eq. 2-16.

Table 5-13: Diffusion coefficients ( $D_m$ ,  $D_1$ ,  $D_2$ , and  $S$ ) for different probe molecules in pAAm-Alg microcapsules

Probe molecules	$D_m$ (m <sup>2</sup> /s)	$S$ (%)	$D_1$ (m <sup>2</sup> /s)	$D_2$ (m <sup>2</sup> /s)
<b>Glucose (180 Da)</b>	$1.94 \times 10^{-10}$	0.079	$4,137 \times 10^{-11}$	$6.80 \times 10^{-10}$
<b>Maltose (360 Da)</b>	$9.20 \times 10^{-11}$	0.065	$1,701 \times 10^{-11}$	$4.80 \times 10^{-10}$ <sup>a</sup>
<b>DextranT1 (1.1 kDa)</b>	$5.87 \times 10^{-11}$	0.132	$1,645 \times 10^{-11}$	$1.11 \times 10^{-10}$
<b>Insulin (5.7 kDa)</b>	$1.67 \times 10^{-11}$	0.049	$2,840 \times 10^{-12}$	$1.59 \times 10^{-10}$ <sup>b</sup>
<b><math>\alpha</math>-lactalbumin (14 kDa)</b>	$1.28 \times 10^{-11}$	0.052	$2,220 \times 10^{-12}$	$1.01 \times 10^{-11}$ <sup>c</sup>
<b>Trypsin (23 kDa)</b>	$1.02 \times 10^{-11}$	0.050	$2,078 \times 10^{-12}$	$3.60 \times 10^{-11}$ <sup>d</sup>

a [88], b [98-99], c[24],d[100]

The relative changes in the initial concentrations of glucose, maltose, dextran T1, insulin,  $\alpha$ -lactalbumin, and trypsin at the equilibrium concentrations were 19%, 17%, 14%, 10%, 8% and 7% respectively. Glucose, maltose, and dextran T1 are above the cut-off threshold of 10% permeation for the probe molecules while insulin,  $\alpha$ -lactalbumin, and trypsin are equal to or below it. This indicates that the MWCO of the microcapsule membrane is below the molecular weight of insulin: 5.7 kDa. The difference between the relative concentrations of dextran T1 and insulin at equilibrium was small. The graph of the diffusion coefficients against the molecular weights was plotted to find the MWCO (Figure 5-12)

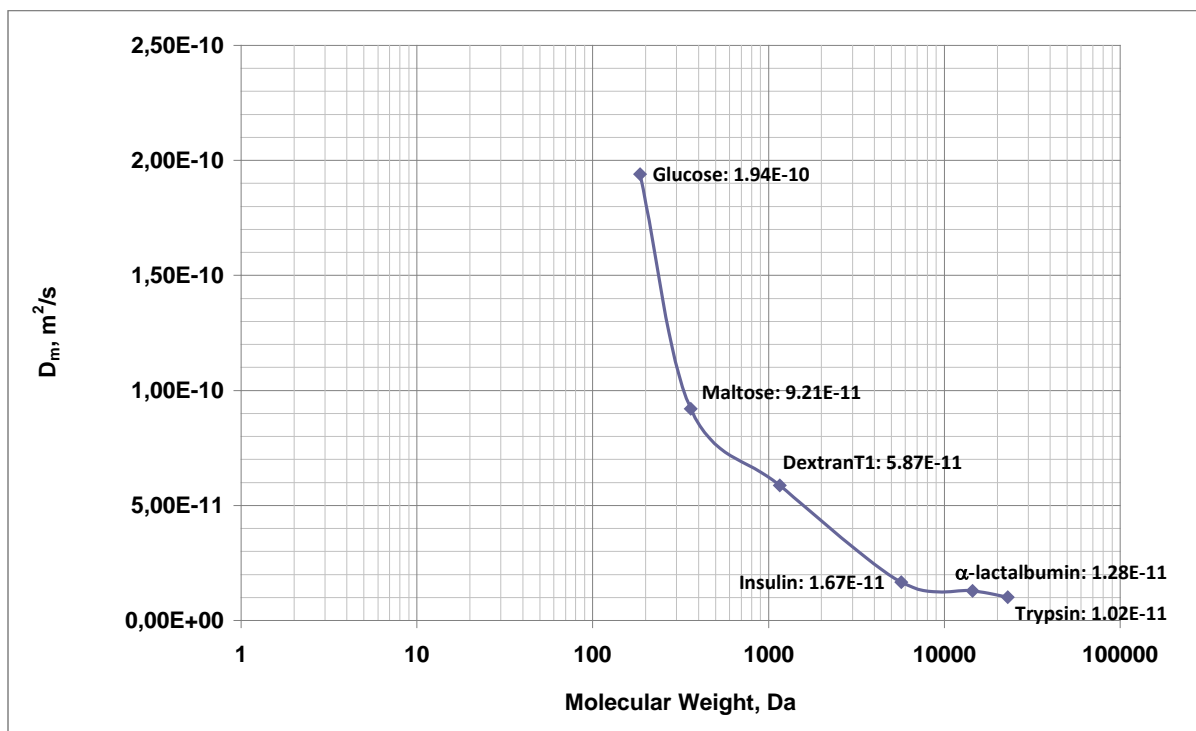


Figure 5-12: Diffusion coefficients versus molecular weights of glucose 180 Da, maltose 360 Da, dextran T1 1.1 kDa, Insulin 5 kDa,  $\alpha$ -lactalbumin 15 kDa and Trypsin 23 kDa

The results show a clear decrease in the diffusion coefficient with an increase in the molecular weight, with the diffusion coefficient levelling off to a minimum value in between the molecular weight of dextran T1 and insulin. Hence, the MWCO of a pAAm-Alg microcapsule is in the range of 1-5.7 kDa.

It should also be noted that the value of the diffusion coefficient of glucose in pAAm-Alg microcapsules determined in this work differs from that determined by Tanaka and Hannoun who determined the same value of diffusion coefficient in Ca-alginate as in water. However, our results are consistent with the conclusions of D.Yankov 2004 and Westrin and Axelsson

1991 [88,101], who suggested that the diffusion coefficients are strongly influenced by changes in the properties of the gel and the presence of additional substances, either in solution or in the gel. Due to the difference in structure between water and a pAAm-Alg membrane, there is no reason that the diffusion coefficient in water and in a pAAm-Alg membrane should exhibit the same value. In other words, the path length for the diffusing species, due to the stricture caused by gel structure, is increased, while the volume available for diffusion is decreased.

### **5.2.6 Summary**

To reveal the transport characteristics of a pAAm-Alg microcapsule, the diffusion coefficient and molecular weight cut-off were examined. Our study shows that the diffusion coefficient, which depends on the pore size of the pAAm-Alg microcapsule membranes, can be controlled by various physicochemical parameters, such as monomer, cross-linker, initiator, and additive silica concentrations. Since the diffusion coefficient of the microcapsule membrane accounts for 20% of the combined diffusion coefficient, it is apparent that the microcapsule membrane plays a decisive role in mass transport resistance.

Size selective transport may occur if the pore sizes of the microcapsule are smaller than the size of some of the permeating molecules. The MWCO experiment showed that, the pAAm-Alg microcapsule allowed glucose, maltose, and dextran T1 to diffuse through microcapsule membrane while excluding insulin,  $\alpha$ -lactalbumin, and trypsin outside the microcapsule membrane. Therefore, the pAAm-Alg microcapsules can act as a size-selective medium for substrate molecular weights between 1.1-5 kDa.

By adjusting the permeability and MWCO of the pAAm-Alg microcapsules, the mass transfer of substances through the microcapsule can be modified and the microcapsule can be effectively exploited as a micro-membrane reactor in the sense that the membrane shell mediates the transport of substrate and product. Other selective properties of this microcapsule such as hydrophobic and hydrophilic properties were also investigated in the next section, in order to obtain a more complete understanding of the permselective behaviour of pAAm-Alg microcapsules.

### **5.3 Multiple substrate competitive reactions: the determination of the specificity of lipase encapsulated in permselective microcapsules**

In the previous section, the mass transfer properties of pAAm-Alg microcapsules were studied and the MWCO, which dictates the size of the encapsulated active component retained within the microcapsule membrane, was ascertained. This section considers the study of other permselective properties of the microcapsule membrane towards mixed substrates. The ‘multiple substrate competitive reaction catalysed by non-specific enzymes’ is a suitable object for such reactive investigation. The lipase MML, which has a molecular weight of 35 kDa, was selected as the active component to be encapsulated in pAAm-Alg microcapsules and the reaction employed was the transesterification of fatty acid ethyl esters with alcohols.

The encapsulation of the lipase MML in pAAm-Alg microcapsules was performed according to section 4.1. The loading efficiency of the enzymes retained in the microcapsules before and after the reaction was determined. The selectivity behaviour of the enzyme encapsulated in the microcapsules in multiple substrate competitive reactions was tested and compared with that of the free enzymes. The transesterification reactions of fatty acid ethyl ester with alcohols were divided into 3 classes namely: the transesterification of fatty acid ethyl esters of different chain lengths with propanol, the transesterification of ethyl caprylate (C<sub>8</sub>) with different alcohols, and the transesterification of the highest selectivity systems for free and encapsulated enzymes toward fatty acid ethyl esters and alcohols.

#### **5.3.1 Loading efficiency of lipase MML in pAAm-Alg microcapsules**

The loading efficiency experiment was conducted following the method of Ma et al. 2009 and Wang et al. 2009 [84,85]. The values given are the average of triplicated experiments. The percentage loading efficiency of the encapsulated lipase MML in pAAm-Alg before and after reaction was found to be  $75.81 \pm 0.38$  and  $74.22 \pm 0.73$ , respectively. It is apparent that the pAAm-Alg microcapsule membrane can retain almost all enzymes after a reaction time of 48 hours.

### 5.3.2 Competitive reaction of fatty acid ethyl esters toward free and encapsulated lipase MML in pAAm-Alg microcapsules

In the first step, the fatty acid chain length specificity of free lipase MML and the encapsulated lipase in pAAm-Alg were compared. Equal molarities of seven fatty acid ethyl esters from C<sub>2</sub> to C<sub>14</sub> containing an even number of carbon atoms were mixed in n-pentane in the presence of n-propanol as a nucleophile. Samples were withdrawn from the reaction at given time intervals for gas-liquid chromatographic analysis. The concentrations of propyl ester of different chain lengths are shown in Figure 5-13 and the specificity constants of each substrate are given in Table 5-14.

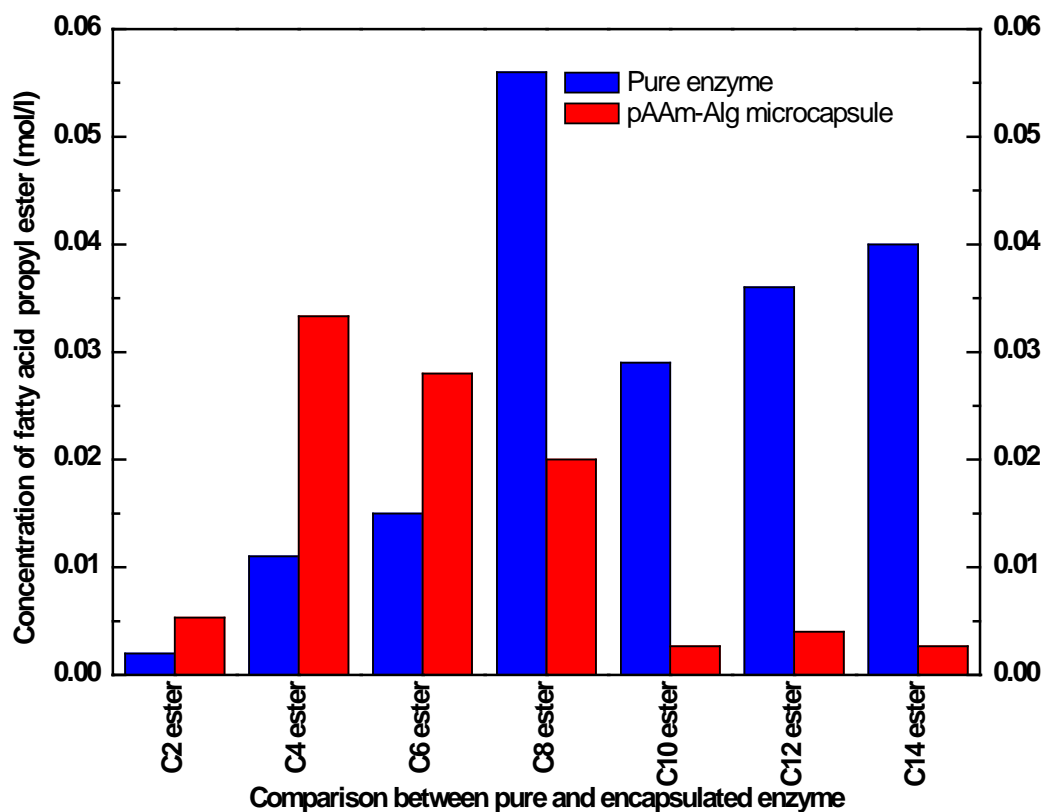


Figure 5-13: Concentrations of propyl esters of different chain lengths from free enzyme and encapsulated enzyme in pAAm-Alg microcapsules

The results show that while the free enzyme lipase MML showed the highest preference toward ethyl caproate C<sub>8</sub>-ethyl ester (as also observed by M. Rangheard 1989), the encapsulated lipase in the pAAm-Alg microcapsules showed the greatest specificity toward ethyl butyrate or the C<sub>4</sub>-ethyl ester. Comparing the encapsulated and free enzymes, more than twice times the amount of C<sub>2</sub>-ethyl ester and C<sub>4</sub>-ethyl ester was converted by the encapsulated

lipase in the pAAm-Alg microcapsules. This is attributed to the hydrophilic properties of the pAAm-Alg membrane. Most of the long chain fatty acid C<sub>8</sub>-C<sub>14</sub> ethyl esters, which are hydrophobic substrates, were preferentially excluded by the hydrophilic pAAm-Alg membrane. The hydrophilic pAAm-Alg membrane is more selective toward short chain fatty acid C<sub>4</sub> and C<sub>6</sub>, resulting in more short chain fatty acid esters reacting with the encapsulated enzymes.

Table 5-14: Specificity constant values for transesterification of different acyl donors C<sub>2</sub> to C<sub>14</sub> ethyl ester with n-propanol toward free and encapsulated lipase MML in pAAm-Alg microcapsules

Type of enzyme	specificity constant ( $1/\alpha$ )						
	C <sub>2</sub>	C <sub>4</sub>	C <sub>6</sub>	C <sub>8</sub>	C <sub>10</sub>	C <sub>12</sub>	C <sub>14</sub>
<b>Free enzymes</b>	0.025	0.137	0.199	<b>1.000</b>	0.420	0.535	0.628
<b>pAAm-Alg microcapsule</b>	0.153	<b>1.000</b>	0.794	0.417	0.087	0.091	0.084

Table 5-14 clearly shows that the encapsulation of enzymes has a major effect on the specificity of the lipase MML toward fatty acids ethyl esters. While the free enzyme exhibited the best substrate specificity towards C<sub>8</sub>-ethyl ester, the encapsulated lipase showed the highest preference on C<sub>4</sub>-ethyl ester, both of which were taken as the benchmark system ( $1/\alpha = 1$ ). The next best substrate for the free enzyme was the long chain fatty acid, C<sub>14</sub>-ethyl ester ( $1/\alpha = 0.628$ ), while that for the encapsulated enzymes was the short chain fatty acid, C<sub>6</sub>-ethyl ester ( $1/\alpha = 0.794$ ). For free enzymes, C<sub>2</sub>-C<sub>6</sub> have some of the lowest specificities, with specificity constants below 0.2, while for encapsulated enzymes, C<sub>10</sub>-C<sub>14</sub> ethyl esters exhibit the least specificity, with the specificity constants below 0.1. This again supports the observation that the free enzyme lipase MML prefers long chain fatty acid ethyl esters, while the encapsulated enzyme shows high selectivity toward short chain fatty acid ethyl esters.

### 5.3.3 Competitive reaction of alcohols toward free and encapsulated lipase MML in pAAm-Alg microcapsules

In the second step, the competitive reaction between different alcohols for the free enzyme and encapsulated enzymes in pAAm-Alg microcapsules was tested using the transesterification of C<sub>8</sub> ethyl ester with different alcohol acceptors: methanol, n-propanol, n-butanol, and n-pentanol. Samples were withdrawn from the reaction at given time intervals



for gas-liquid chromatographic analysis. The concentrations of C<sub>8</sub> ester with different alkyl groups are shown in Figure 5-14 and the specificity constants of each alcohol are given in Table 5-15.

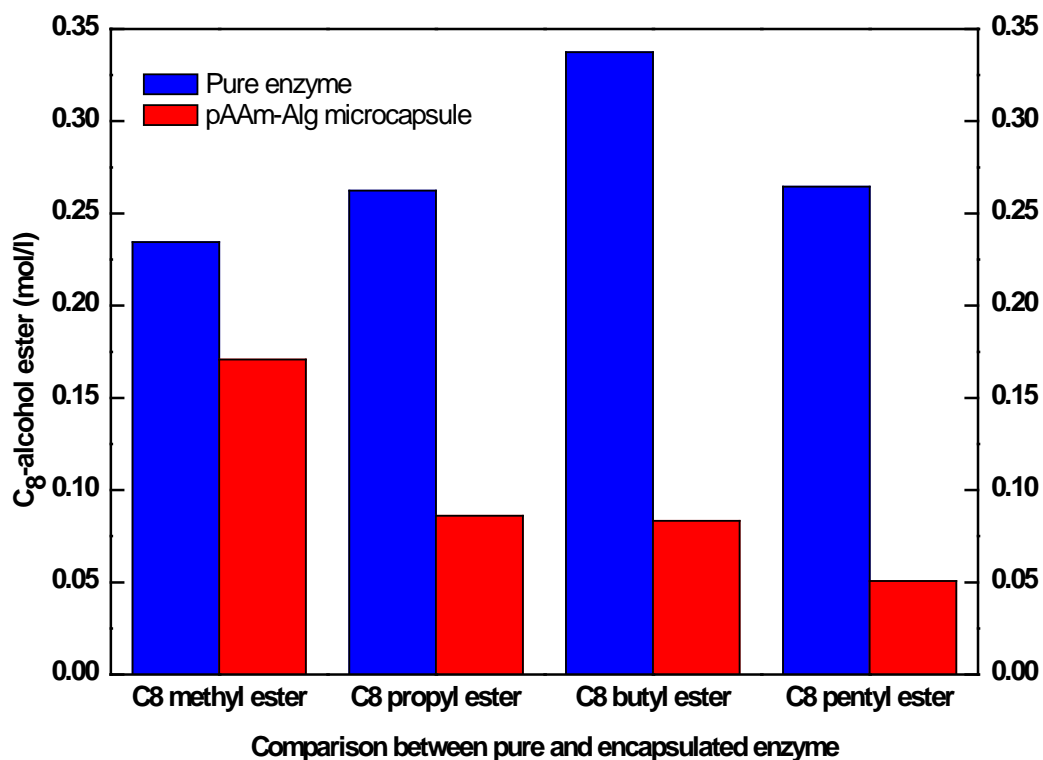


Figure 5-14: Concentrations of C<sub>8</sub> ester with different alkyl groups from free enzyme and encapsulated enzyme in pAAm-Alg microcapsules

Table 5-15: Specificity constant values for transesterification of C<sub>8</sub> ethyl octanoate with different alcohol acceptors: methanol, n-propanol, n-butanol, n-pentanol in pAAm-Alg microcapsules

Type of enzyme	specificity constant ( $1/\alpha$ )			
	Methanol	n-propanol	n-butanol	n-pentanol
Free enzyme	0.620	0.714	<b>1.000</b>	0.721
Encapsulated enzyme	<b>1.000</b>	0.479	0.462	0.276

The results show that the free and encapsulated enzymes in the microcapsule exhibited different preferences toward alcohol acceptors. While the free enzyme was highly specific for n-butanol, the encapsulated enzymes in the pAAm-Alg microcapsules are highly specific towards methanol. The pAAm-Alg microcapsule membrane exhibited higher selectivity

toward smaller alcohols than to larger alcohols, which can be attributed to the molecular weight and high viscosity of the large alcohols that inhibited their transportation through the microcapsule membrane. The molecular weight and viscosity of methanol, n-propanol, n-butanol and n-pentanol are 32, 60, 74, 88 g/mol and 0.59, 1.94, 3 and 4 mP respectively. The alcohols with smaller size and lower viscosities can pass through the microcapsule membrane more easily than those with a larger molecular weight and higher viscosity.

Table 5-15 shows that while the free enzyme exhibited the best substrate specificity toward n-butanol, the encapsulated lipase showed high selectivity toward methanol, both of which were taken as the benchmark system ( $1/\alpha = 1$ ). The next best substrates for the free enzymes were n-pentanol and n-propanol ( $1/\alpha = 0.721$  and  $0.714$ , respectively) while those of encapsulated enzymes were n-propanol and n-butanol ( $1/\alpha = 0.479$  and  $0.462$ , respectively). The free enzyme showed the least specificity towards methanol, while the least specificity for the encapsulated enzymes was for n-pentanol. These results support the observation that the encapsulation of enzymes by the pAAm-Alg microcapsule plays an important role in the effective selectivity of the lipase MML toward alcohols.

#### **5.3.4 Competitive reaction among the most selective fatty acid ethyl esters and alcohols toward free and encapsulated lipase MML in pAAm-Alg microcapsules**

The third step was conducted in order to reveal the maximum selectivity difference between the free and encapsulated lipase MML. The fatty acid ethyl ester and alcohols having the highest specificity for free and encapsulated lipase from the foregoing experiments were used as substrates. The transesterification of mixed of  $C_4$  and  $C_8$  ethyl ester with methanol and n-butanol were conducted using the free and encapsulated enzyme. Samples were withdrawn from the reaction at given time intervals for gas-liquid chromatographic analysis. The concentrations for  $C_4$  methyl ester,  $C_4$  butyl ester,  $C_8$  methyl ester and  $C_8$  butyl ester are shown in Figure 5-15 and the specificity constants of each substrate are given in Table 5-16.

In the mixed system of fatty acid ethyl esters  $C_4$  and  $C_8$  with the alcohol acceptors, methanol and n-butanol, the free enzyme showed the highest preference for  $C_8$  ethyl ester and n-butanol while the encapsulated enzymes in pAAm-Alg microcapsules exhibited the best selectivity for  $C_4$  ethyl ester and n-butanol. The specificity of encapsulated enzyme in pAAm-Alg microcapsule toward  $C_4$ -n-butanol and  $C_4$ -methanol is more than twice that of the free

enzyme. This is the result of the hydrophilic properties of pAAm-Alg microcapsule membrane, which is more selective to hydrophilic substrates, short chain fatty acid- C<sub>4</sub> ethyl ester. However, the reason why encapsulated enzyme favours n-butanol over methanol remains unclear.

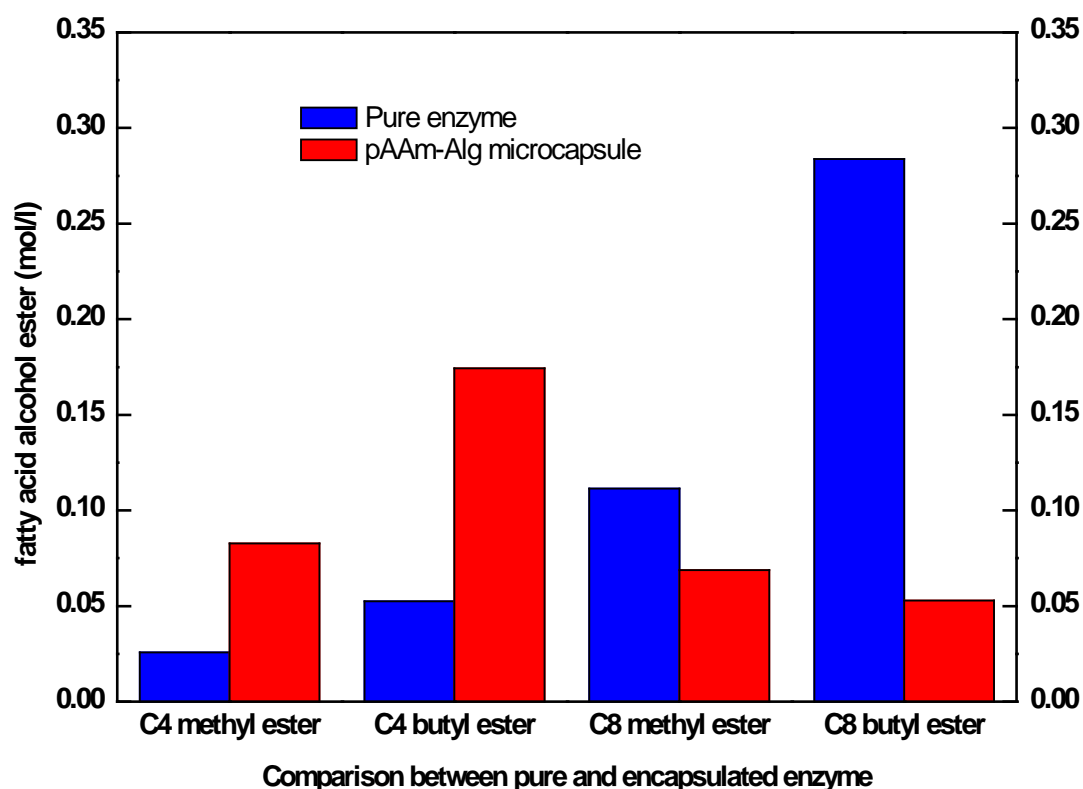


Figure 5-15: Concentrations of C<sub>4</sub> methyl ester, C<sub>4</sub> butyl ester, C<sub>8</sub> methyl ester and C<sub>8</sub> butyl ester from free enzyme and encapsulated enzyme in pAAm-Alg microcapsules

Table 5-16: Specificity constant values for transesterification of C<sub>4</sub>, C<sub>8</sub> ethyl ester with methanol, n-butanol in pAAm-Alg microcapsules

Type of microcapsule	Specificity constant ( $1/\alpha$ )			
	C <sub>4</sub> -methanol	C <sub>4</sub> -n-butanol	C <sub>8</sub> -methanol	C <sub>8</sub> -n-butanol
Free enzyme	0.072	0.150	0.334	<b>1.000</b>
Encapsulated enzyme	0.449	<b>1.000</b>	0.371	0.282

Table 5-16 shows that the best substrate specificity towards the most selective fatty acid ethyl esters and alcohols for the free and encapsulated lipase MML in pAAm-Alg microcapsule are C<sub>8</sub>-butanol and C<sub>4</sub>-butanol respectively which were thus taken as the benchmarks ( $1/\alpha = 1$ ). The next best substrate for the encapsulated enzyme is C<sub>4</sub>-methanol ( $1/\alpha = 0.449$ ) while that for

the free enzyme is, C<sub>8</sub>-methanol ( $1/\alpha = 0.334$ ), indicating that the chain length of fatty acid dominates the selectivity of the free and encapsulated enzyme.

### 5.3.5 Summary

From the above results, it can be concluded that for mixed substrates of fatty acid ethyl esters and alcohols, free enzymes showed high specificity toward long chain fatty acid ethyl esters (C<sub>8</sub> upward) and a longer chain alcohol, n-butanol, while encapsulated enzymes in pAAm-Alg microcapsules exhibited high selectivity toward short chain fatty acid ethyl esters (C<sub>4</sub> and C<sub>6</sub>) and the short chain alcohol, methanol which is the consequence of the hydrophilic property of pAAm-Alg microcapsule membrane. These results suggest that pAAm-Alg microcapsules can be used as a powerful tool to manipulate the overall enzyme selectivity toward permeable substrates.

## 5.4 Modification of pAAm-Alg microcapsules with hydrophobic IPPAAm monomer

From the preceding section, it can be appreciated that short chain fatty acids and lower alcohols were selected by encapsulated lipase MML in pAAm-Alg microcapsules as result of hydrophilic membrane showing a greater preference for hydrophilic or more water-soluble substrates. In order to regulate and fine tune the selectivity of the pAAm-Alg microcapsule membrane further, IPPAAm, a hydrophobic monomer, was added to the polymer solution.

In biotechnology, Isopropyl acrylamide (IPPAAm) is well-known as thermo-responsive monomer [102-104]. However, another distinct property of IPPAAm is the combination of both hydrophobic and hydrophilic properties, as the result of the hydrophilic amide group and the hydrophobic isopropyl groups in its side chains. The specificity of encapsulated enzyme in hydrophilic/hydrophobic pAAm-IPPAAm-Alg membrane towards fatty acid ethyl ester and alcohols was studied by repeating the multiple competitive reaction experiments described earlier.

### 5.4.1 Characterisation of modified pAAm-IPPAAm-Alg microcapsules

The lipase MML encapsulated in pAAm-Alg and pAAm-IPPAAm-Alg microcapsules were successfully prepared by using both ionic gelation and the co-polymerisation method. pAAm-IPPAAm-Alg microcapsules at different concentrations of IPPAAm were prepared by

maintaining the composition of 3.5 % w/w Alg, 19% AAm, 1% Bis-AAm and 0.2 % initiator while varying the IPPAAm concentrations from 1 to 10% w/w. The size and membrane thicknesses of the microcapsules were determined by photographing them with a stereo-microscope. The effects of modification of pAAm-Alg microcapsules with IPPAAm monomer in different concentrations on the diameter and membrane thickness of the microcapsules is shown in the Table 5-17. The values reported are the average values from five replicate experiments.

Table 5-17: Diameter and membrane thickness of pAAm-Alg and pAAm-IPPAAm-Alg microcapsules at different IPPAAm concentrations

<b>Microcapsule</b>	<b>Diameter (mm)</b>	<b>Membrane thickness (mm)</b>	<b>No. of Capsules (min<sup>-1</sup>)</b>
<b>pAAm-Alg</b>	3.020	0.234	28
<b>pAAm-0.5% IPPAAm-Alg</b>	3.031	0.239	28
<b>pAAm-1% IPPAAm-Alg</b>	3.039	0.244	27
<b>pAAm-2.5% IPPAAm-Alg</b>	3.122	0.253	26-27
<b>pAAm-3.75% IPPAAm-Alg</b>	3.109	0.279	24-25
<b>pAAm-5% IPPAAm-Alg</b>	3.147	0.288	20-22
<b>pAAm-10% IPPAAm-Alg</b>	3.172	0.332	17-18

The results show that the average microcapsule diameter and membrane thickness was only slightly affected by the modification of pAAm-Alg microcapsules with the hydrophobic monomer IPPAAm. The average diameter and membrane thickness slightly increased with increasing IPPAAm monomer levels, which could be attributed to the greater co-polymerisation of AAm and IPPAAm monomer, forming thicker membranes. However, the production rate of pAAm-IPPAAm-Alg microcapsules at higher contents of IPPAAm is decreased, which could be the result of higher viscosity and larger flow resistance.

#### 5.4.2 Loading efficiency of encapsulated lipase MML in pAAm-IPPAAm-Alg at different concentrations

The loading efficiency experiment was conducted according to the method of Lijuan et al. 2009 and Zhongun et al. 2009 [84,85]. The values obtained represent the average of triplicate experiments. The percentage loading efficiency of the encapsulated lipase MML in pAAm-IPPAAm-Alg microcapsules at different IPPAAm concentrations before and after reaction was estimated from the activity and the results are presented in Table 5-18.

Table 5-18: Loading efficiency of encapsulated lipase MML in pAAm-IPPAAm-Alg microcapsules at different IPPAAm concentrations

Microcapsule	Loading Efficiency	Loading Efficiency
	Before reaction	After reaction (48hr)
<b>pAAm-co-0.5% IPPAAm-Alg</b>	76.06 ± 0.35	75.36 ± 0.97
<b>pAAm-co-1% IPPAAm-Alg</b>	78.97 ± 0.14	76.79 ± 0.24
<b>pAAm-co-2.5% IPPAAm-Alg</b>	79.95 ± 0.71	78.05 ± 0.31
<b>pAAm-co-3.75% IPPAAm-Alg</b>	81.16 ± 0.67	79.19 ± 0.62
<b>pAAm-co-5% IPPAAm-Alg</b>	52.87 ± 0.13	44.86 ± 0.60
<b>pAAm-co-10% IPPAAm-Alg</b>	49.22 ± 0.63	42.75 ± 0.49

The results demonstrate that the addition of IPPAAm in pAAm-Alg microcapsule slightly affects the loading efficiency. It can be recognised that microcapsules prepared from pAAm-IPPAAm-Alg at concentrations of IPPAAm from 0.5-3.5% exhibited 97% retention after the reaction. However, the loading efficiency and the retention of microcapsule membranes prepared with IPPAAm at concentrations 5 % and 10 % decreased to around 50 % and 85 % respectively, which could be the result of microcapsule breakage or enzyme leakage during the reaction.

### 5.4.3 Competitive reaction of fatty acid ethyl esters toward free and encapsulated enzyme lipase MML in pAAm-IPPAAm-Alg microcapsules

In the first step, the chain length specificity of free lipase MML and encapsulated lipase in pAAm-IPPAAm-Alg at different concentrations were tested. Equal molarities of seven ethyl esters of fatty acid from C<sub>2</sub> to C<sub>14</sub> containing an even number of carbon atoms were mixed in n-pentane in the presence of n-propanol as a nucleophile. Samples were withdrawn from the reaction at given time intervals for gas-liquid chromatographic analysis. The concentrations of propyl ester at different chain lengths are shown Figure 5-16 and the specificity constants of each substrate are given in Table 5-19.

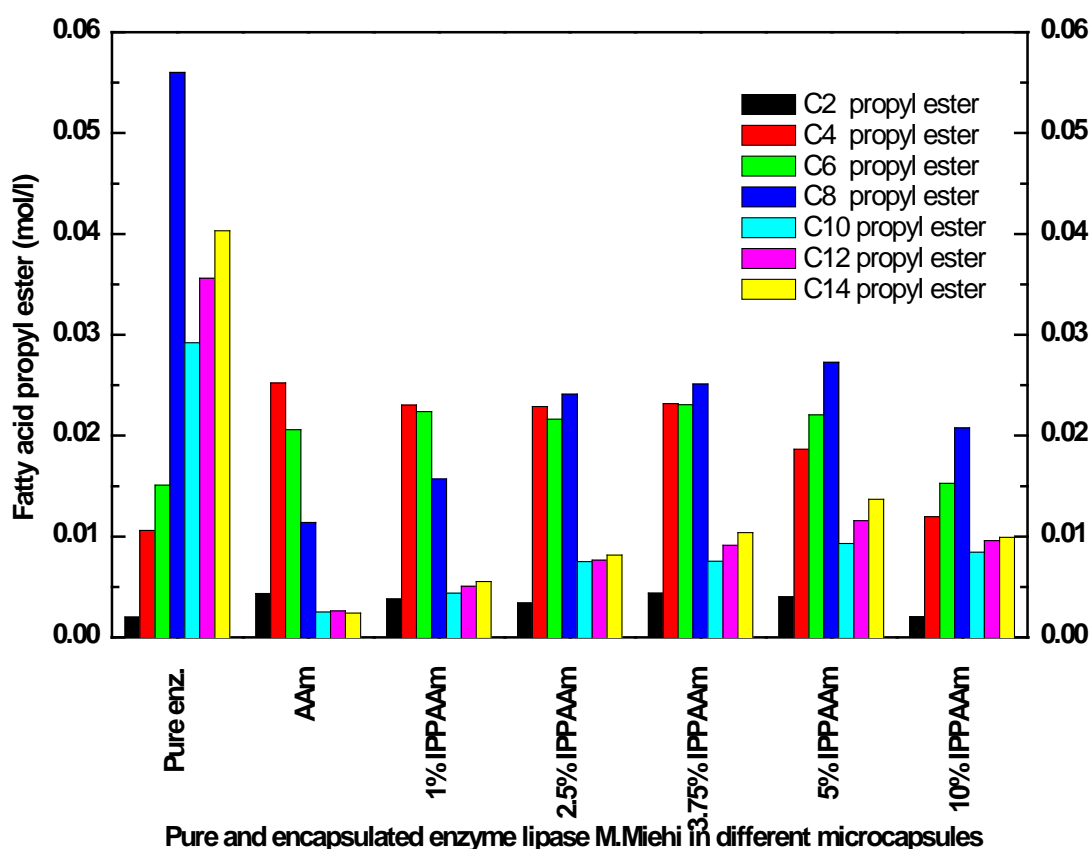


Figure 5-16: Concentrations of propyl ester for different chain lengths with free and encapsulated enzyme in pAAm-Alg and pAAm-IPPAAm-Alg microcapsules.

The results indicate that the modification of the pAAm-Alg microcapsule membrane with IPPAAm shifted the specificity of the encapsulated lipase MML toward hydrophobic substrates. At 1% IPPAAm, the specificity of encapsulated enzyme remained the same as in

the pAAm-Alg microcapsules, which favoured C<sub>4</sub> ethyl ester. However, for 2.5% IPPAAm concentration, the specificity of encapsulated enzyme shifted to C<sub>8</sub> ethyl ester, which is attributed to the fact that the higher the IPPAAm level, the higher the specificity of the encapsulated enzyme toward long chain fatty acids (increase in specificity constant value in C<sub>10</sub> to C<sub>14</sub>)

By co-polymerisation of the hydrophilic pAAm-Alg microcapsule membrane with hydrophobic IPPAAm monomer, the activity of the encapsulated lipase can be shifted from short chain to long chain fatty acids. The specificity of the encapsulated enzymes toward long chain fatty acid was higher, which may be caused by allowing of the permeation of hydrophobic substrate into the microcapsules, while hydrophilic substrates are partitioned away from the active site of the enzyme. Consequently, long chain fatty acid propyl esters were produced.

Table 5-19: Specificity constant values for transesterification of different acyl donors C<sub>2</sub> to C<sub>14</sub> ethyl ester with n-propanol in various media/microcapsules

Microcapsule	Specificity constant (1/α)						
	C <sub>2</sub>	C <sub>4</sub>	C <sub>6</sub>	C <sub>8</sub>	C <sub>10</sub>	C <sub>12</sub>	C <sub>14</sub>
<b>Free enzyme</b>	0.025	0.137	0.199	<b>1.000</b>	0.420	0.535	0.628
<b>pAAm-Alg</b>	0.153	<b>1.000</b>	0.794	0.417	0.087	0.091	0.084
<b>pAAm-1%IPPAAm-Alg</b>	0.148	<b>1.000</b>	0.968	0.652	0.171	0.199	0.217
<b>pAAm-2.5%IPPAAm-Alg</b>	0.126	0.943	0.884	<b>1.000</b>	0.283	0.289	0.309
<b>pAAm-3.75%IPPAAm-Alg</b>	0.154	0.912	0.907	<b>1.000</b>	0.272	0.332	0.380
<b>pAAm-5%IPPAAm-Alg</b>	0.142	0.674	0.801	<b>1.000</b>	0.332	0.413	0.490
<b>pAAm-10%IPPAAm-Alg</b>	0.089	0.548	0.712	<b>1.000</b>	0.380	0.434	0.449

Table 5-19 clearly demonstrates that both the free enzyme and the encapsulated enzyme in pAAm-IPPAAm-Alg microcapsules at IPPAAm concentrations of 2.5-10% exhibited the greatest substrate specificity towards C<sub>8</sub>-ethyl ester, while the encapsulated lipase in pAAm-Alg and in pAAm-IPPAAm-Alg microcapsules at a IPPAAm concentration of 1% showed the highest preference for C<sub>4</sub>-ethyl ester. These were then taken as the benchmark systems (1/α =1). However, while the next best substrate for the free enzyme is the long chain fatty acid,



C<sub>14</sub> ethyl ester ( $1/\alpha = 0.628$ ), that of encapsulated enzyme in both in pAAm-Alg and in pAAm-IPPAAm-Alg microcapsule is a shorter chain fatty acid, either C<sub>4</sub> ethyl ester or C<sub>6</sub>-ethyl ester ( $1/\alpha = 0.794-0.968$ ). These results indicate that the selectivity can be regulated precisely by the encapsulation of enzymes in microcapsules, depending on the exact properties of the microcapsule membrane.

#### 5.4.4 Competitive reaction of alcohols toward free and encapsulated enzyme lipase MML in pAAm-IPPAAm-Alg microcapsules

In the second step, the competitive reaction between different alcohols for the free and encapsulated enzyme was tested by the transesterification of C<sub>8</sub> ethyl ester with different alcohol acceptors, methanol, n-propanol, n-butanol and n-pentanol. Samples were withdrawn from the reaction at given time intervals for gas-liquid chromatographic analysis. The concentrations of C<sub>8</sub> ester with different alkyl groups are shown in Figure 5-17 and the specificity constant of each alcohol are given in Table 5-20.

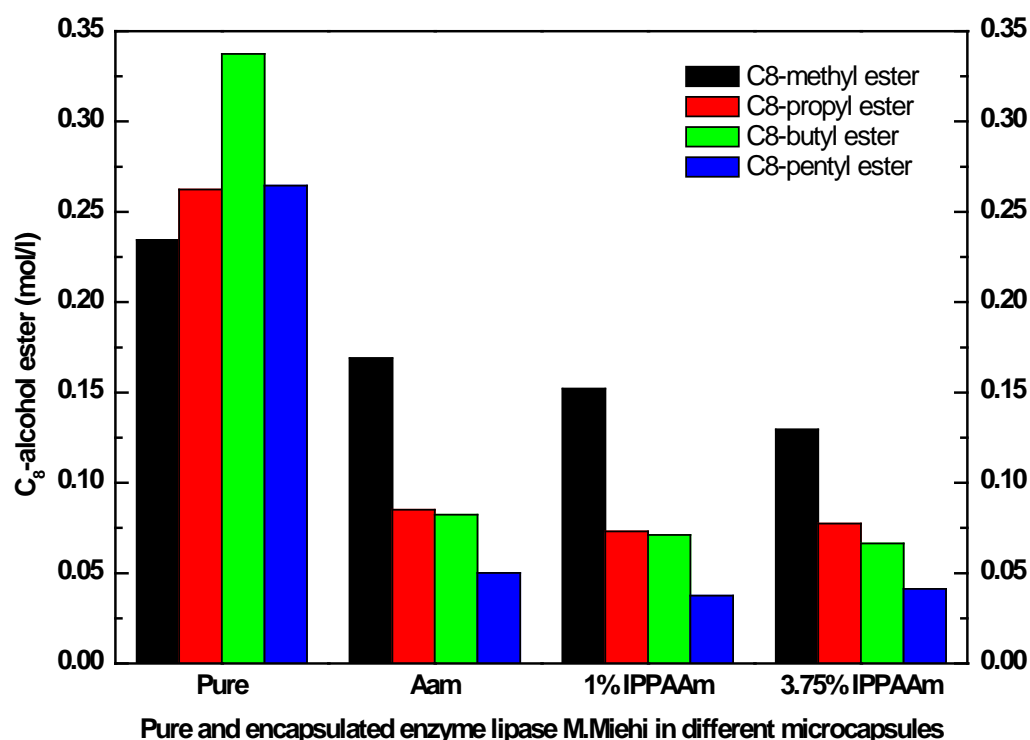


Figure 5-17: Concentration of C<sub>8</sub> ester with different alkyl groups for free and encapsulated enzyme in pAAm-Alg and pAAm-IPPAAm-Alg microcapsules

The results show that the free and encapsulated enzymes in the microcapsule exhibited different preferences towards alcohol acceptors. While the free enzyme was more specific

toward n-butanol, the encapsulated enzymes were more selective for methanol. Modification of pAAm-Alg microcapsule with IPPAAm showed no significant influence on specificity of lipase to the alcohol. pAAm-Alg and pAAm-IPPAAm-Alg microcapsule membranes both exhibited selectivity to smaller rather than to larger alcohols, which can be attributed to the size and high viscosity of the larger alcohol molecules that impedes their transportation through the microcapsule membrane. The alcohols with the smaller molecular weight and lower viscosity can pass through the microcapsule membrane more easily than those of a larger size and higher viscosity.

Table 5-20: Specificity constant values for transesterification of C<sub>8</sub> ethyl octanoate with different alcohol acceptors; methanol, n-propanol, n-butanol, n-pentanol in various media

Microcapsule	Specificity constant ( $1/\alpha$ )			
	Methanol	n-propanol	n-Butanol	n-pentanol
<b>Free Enzyme</b>	0.620	0.714	<b>1.000</b>	0.721
<b>pAAm-Alg</b>	<b>1.000</b>	0.479	0.462	0.276
<b>pAAm-1%IPPAAm-Alg</b>	<b>1.000</b>	0.457	0.444	0.230
<b>pAAm-2.5%IPPAAm-Alg</b>	<b>1.000</b>	0.577	0.492	0.301

Table 5-20 shows that while the free enzymes exhibited the best substrate specificity toward n-butanol, the encapsulated lipase showed the highest selectivity toward methanol. These were then taken as the benchmark systems ( $1/\alpha = 1$ ). The next best substrate for the free enzymes was n-pentanol ( $1/\alpha = 0.721$ ) while that for the encapsulated enzymes in both pAAm-Alg and pAAm-IPPAAm-Alg microcapsules was n-propanol ( $1/\alpha = 0.457-577$ ). The free enzyme showed the lowest specificity with methanol, while the worst specificity for the encapsulated enzyme was with n-pentanol. These results support the observation that the encapsulation of enzymes by either pAAm-Alg or pAAm-IPPAAm-Alg microcapsules plays an important role in the selectivity of lipase MML toward different alcohols.

### 5.4.5 Competitive reaction of the most selective fatty acid ethyl esters and alcohols toward free enzyme and encapsulated enzyme lipase MML in pAAm-IPPAAm-Alg microcapsules

The third step was conducted in order to reveal the highest selectivity behaviour of free and encapsulated enzyme. The fatty acid ethyl ester and alcohols which exhibited the highest specificity for free and encapsulated lipase in the previous experiments were used as substrates. The transesterification with free and encapsulated enzyme were conducted in mixed C<sub>4</sub> and C<sub>8</sub> ethyl ester with methanol and n-butanol. Samples were withdrawn from the reaction at given time intervals for gas-liquid chromatographic analysis. The concentrations for C<sub>4</sub> methyl ester, C<sub>4</sub> butyl ester, C<sub>8</sub> methyl ester and C<sub>8</sub> butyl ester are depicted in Figure 5-18 and the specificity constants of each substrate are given in Table 5-21.

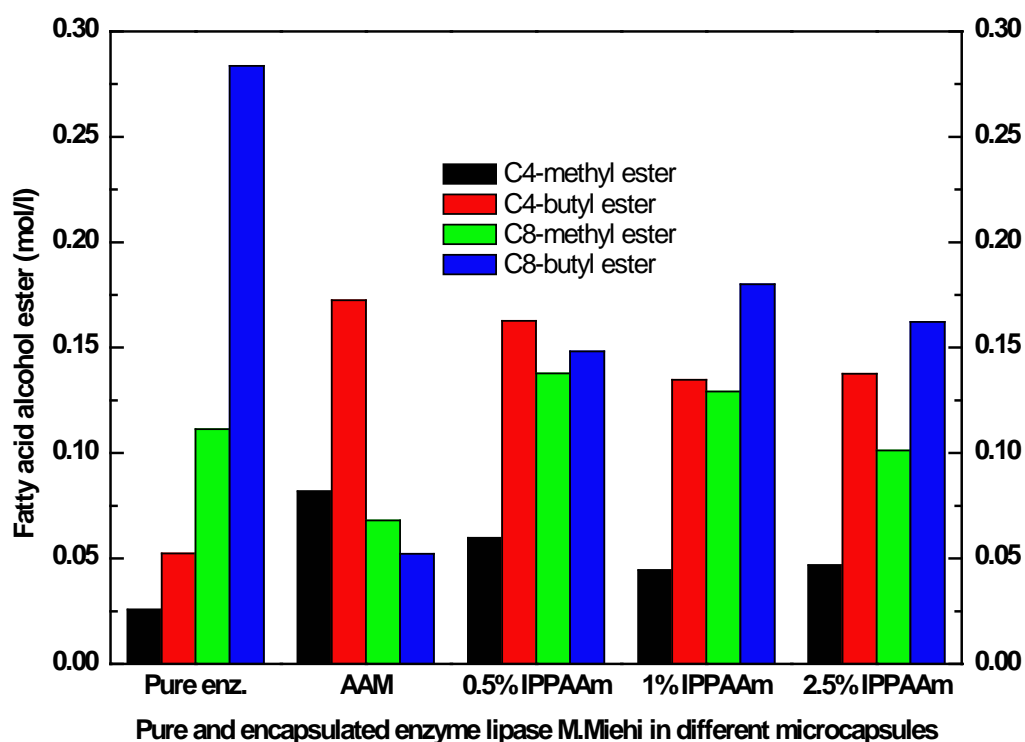


Figure 5-18: Concentrations of C<sub>4</sub> methyl ester, C<sub>4</sub> butyl ester, C<sub>8</sub> methyl ester and C<sub>8</sub> butyl ester for free enzyme and encapsulated enzyme in pAAm-Alg and pAAm-IPPAAm-Alg microcapsules

In a mixed system of fatty acid ethyl esters C<sub>4</sub> and C<sub>8</sub> ethyl ester with the alcohol acceptors, methanol and n-butanol, the free enzyme and the pAAm-IPPAAm-Alg microcapsules with IPPAAm 1% and 2.5 % w/w showed a high preference for C<sub>8</sub> and n-butanol while the pAAm-

Alg and the pAAm-IPPAAm-Alg microcapsules with IPPAAm 0.5% w/w exhibited high selectivity for C<sub>4</sub> and n-butanol.

Comparing the free and the encapsulated enzymes in both pAAm-Alg and pAAm-IPPAAm-Alg microcapsules, it can be clearly seen that more than twice the amount of C<sub>4</sub>-ethyl ester was converted by the encapsulated lipase in both microcapsules than by the free enzyme, as a result of the permselective microcapsule membrane properties.

Comparing the pAAm-Alg and the pAAm-IPPAAm-Alg microcapsules with IPPAAm 0.5% w/w, the amount of reacted C<sub>4</sub>-n-butanol and C<sub>4</sub>-methanol were nearly the same in both cases while the amount of reacted C<sub>8</sub>-methanol and C<sub>8</sub>-butanol increased significantly in the latter instance. This is attributed to the content of hydrophobic monomer IPPAAm in the microcapsule membrane, resulting in better permselectivity to hydrophobic substrates.

By modifying pAAm-Alg microcapsules with hydrophobic IPPAAm monomer, the amount of C<sub>8</sub>-methanol and C<sub>8</sub>-n-butanol which reacted increased as a consequence of the microcapsule membrane becoming more hydrophobic and hence more selective to the hydrophobic substrate C<sub>8</sub> ethyl ester.

Table 5-21: Specificity constant values for transesterification of C<sub>4</sub>, C<sub>8</sub> ethyl ester and methanol, n-butanol

Microcapsule	Specificity constant (1/α)			
	C <sub>4</sub> -methanol	C <sub>4</sub> -n-butanol	C <sub>8</sub> -methanol	C <sub>8</sub> -n-butanol
<b>Free Enzyme</b>	0.072	0.150	0.334	<b>1.000</b>
<b>pAAm-Alg</b>	0.449	<b>1.000</b>	0.371	0.282
<b>pAAm-0.5%IPPAAm-Alg</b>	0.346	<b>1.000</b>	0.833	0.903
<b>pAAm-1%IPPAAm-Alg</b>	0.226	0.726	0.694	<b>1.000</b>
<b>pAAm-2.5%IPPAAm-Alg</b>	0.268	0.835	0.600	<b>1.000</b>

Table 5-21 shows that the greatest substrate specificity towards the fatty acid ethyl esters and alcohols for the free lipase MML was with C<sub>8</sub>-butanol, while the best specificity towards the encapsulated enzymes was different according to the encapsulating membrane composition. The best substrate specificity for the encapsulated enzyme in pAAm-Alg and pAAm-IPPAAm-Alg microcapsules at IPPAAm 0.5% content was with C<sub>4</sub>-butanol while that for the

encapsulated enzyme in pAAm-IPPAAm-Alg microcapsules at IPPAAm 1 and 2.5% content is with C<sub>8</sub>-butanol, both of which were taken as the benchmark system ( $1/\alpha = 1$ ).

Comparing the encapsulated enzyme in pAAm-Alg and pAAm-IPPAAm-Alg microcapsules at IPPAAm 0.5% content, the next best substrate for the encapsulated enzyme in pAAm-Alg microcapsules was C<sub>4</sub>-methanol ( $1/\alpha = 0.449$ ) while that of encapsulated enzymes in pAAm-IPPAAm-Alg microcapsules at IPPAAm 0.5% content was C<sub>8</sub>-butanol ( $1/\alpha = 0.903$ ). This is attributed to the effect of the hydrophobic monomer, IPPAAm, resulting in the more hydrophobic substrate being selected by the microcapsule membrane.

When higher contents of IPPAAm are added to modify the pAAm-Alg microcapsules, at the level of 1 and 2.5% IPPAAm, the resulting pAAm-IPPAAm-Alg microcapsules shifted their greatest selectivity toward C<sub>8</sub>-butanol ( $1/\alpha = 1$ ), as with the free enzyme. However, the characteristics of the encapsulated enzyme in microcapsules is still maintained in that the C<sub>4</sub>-butanol was the next best substrate at specificity constant values 0.726 and 0.835 in the pAAm-IPPAAm-Alg microcapsule at 1 and 2.5% IPPAAm contents respectively.

In order to evaluate the difference in activity of the free and the encapsulated enzymes, the relative activities of the encapsulated enzymes in pAAm-Alg and pAAm-IPPAAm-Alg microcapsules have been presented in Figure 5-19.

The activity of free enzyme is taken to be 100 % for every reaction system. Comparing the free enzyme and the encapsulated enzyme in pAAm-Alg microcapsules, the latter exhibited a high activity for C<sub>4</sub>-n-butanol and C<sub>4</sub>-methanol of more than twice the value for the free enzyme. This is the result of the hydrophilic property of the pAAm-Alg microcapsule membrane, which is more selective toward the short chain fatty acid, C<sub>4</sub> ethyl ester. When the pAAm-Alg microcapsules were modified with hydrophobic IPPAAm monomer, the resultant microcapsules still exhibited high specificity toward C<sub>4</sub>-n-butanol, but less preference for C<sub>4</sub>-methanol. This may be attributed to the hydrophobic monomer, which may impede the transport of methanol which is less hydrophobic than n-butanol. On the other hand, it may be that methanol is being reacted with C<sub>8</sub> and depleted. It can also be recognised that the higher the content of IPPAAm in microcapsules, the lower the specificity of the encapsulated enzyme toward C<sub>4</sub>-methanol. In contrast, the activity for long chain C<sub>8</sub>-methanol and C<sub>8</sub>-butanol increased with higher amounts of IPPAAm.

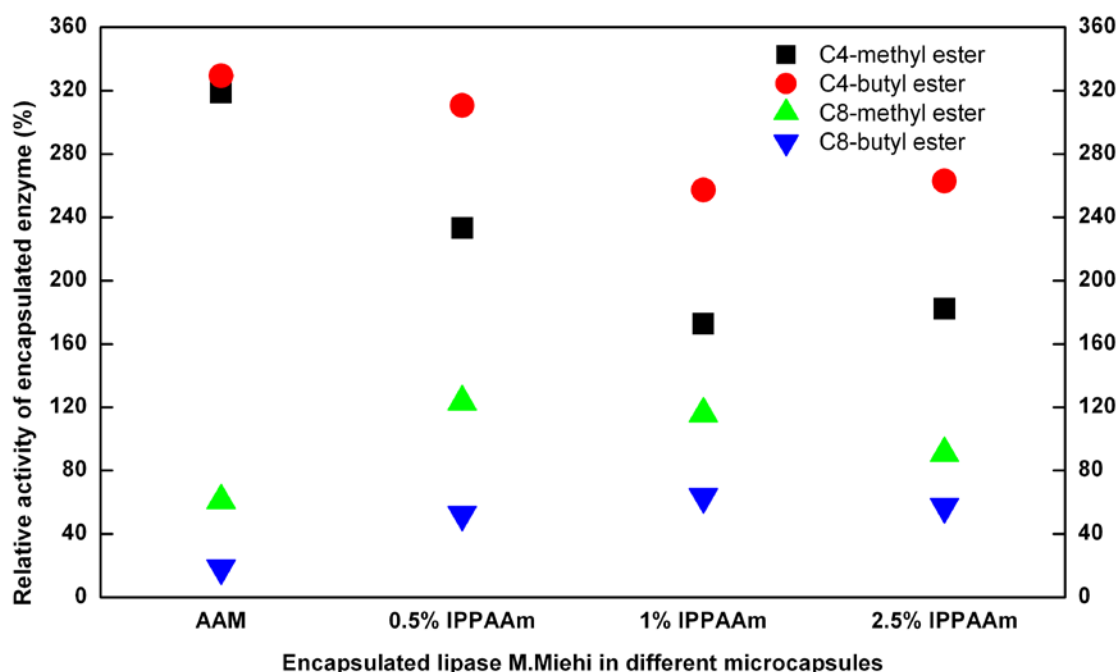


Figure 5-19: Relative activity of the encapsulated enzymes in pAAm-Alg and pAAm-IPPAAm-Alg microcapsules with respect to the free enzymes

The relative activity of C<sub>8</sub>-methanol and C<sub>8</sub>-butanol was improved from 50% to more than 80% and from 20% to more than 50% respectively, which can be attributed to the more hydrophobic monomer allowing greater amount of long chain fatty acid to react with the encapsulated enzyme in the microcapsules.

#### 5.4.6 Competitive reaction of fatty acid ethyl esters (C<sub>6</sub> and C<sub>8</sub>) and two alcohols toward free enzyme and encapsulated enzyme lipase MML in pAAm-IPPAAm-Alg microcapsules

From the results of fatty acid chain length selectivity investigation, the pAAm-IPPAAm-Alg microcapsules at 1% IPPAAm exhibited high specificity to not only to C<sub>4</sub> but also to C<sub>6</sub> ethyl ester (1.0 and 0.968). Highly selective conversion of C<sub>6</sub> and C<sub>8</sub> ethyl ester with methanol and n-butanol was conducted to confirm the permselective properties of the microcapsule membrane. The transesterification with free and encapsulated enzyme were conducted in a mixture of C<sub>6</sub> and C<sub>8</sub> ethyl ester with methanol and n-butanol. Samples were withdrawn from the reaction at given time intervals for gas-liquid chromatographic analysis. The concentrations of C<sub>6</sub> methyl ester, C<sub>6</sub> butyl ester, C<sub>8</sub> methyl ester and C<sub>8</sub> butyl ester are illustrated in Figure 5-20 and the specificity constants of each substrate are presented in Table 5-22.

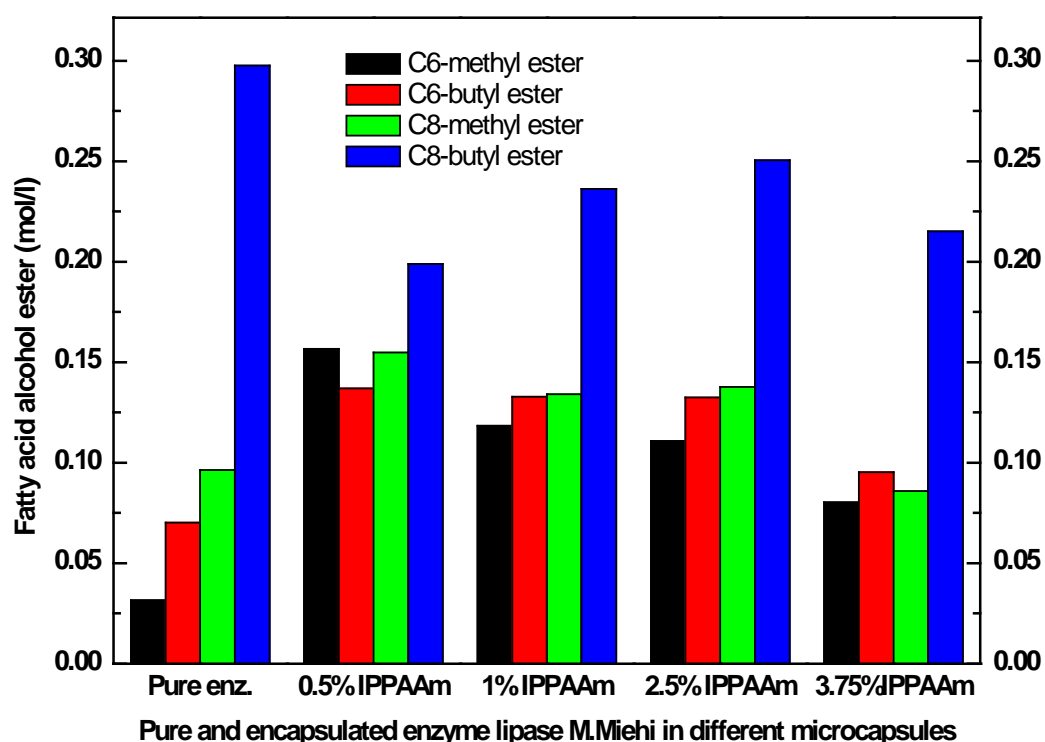


Figure 5-20: Concentrations of C<sub>6</sub> methyl ester, C<sub>6</sub> butyl ester, C<sub>8</sub> methyl ester and C<sub>8</sub> butyl ester for free enzyme and encapsulated enzymes in pAAM-Alg and pAAM-IPPAAM-Alg microcapsules

Table 5-22: Specificity constant values for transesterification of C<sub>6</sub> and C<sub>8</sub> ethyl ester with methanol and n-Butanol

Microcapsule	specificity constant (1/α)			
	C <sub>6</sub> -methanol	C <sub>6</sub> -n-butanol	C <sub>8</sub> -methanol	C <sub>8</sub> -n-butanol
<b>Free Enzyme</b>	0.083	0.191	0.267	<b>1.000</b>
<b>pAAM-0.5%IPPAAM-Alg</b>	0.766	0.661	0.756	<b>1.000</b>
<b>pAAM-1%IPPAAM-Alg</b>	0.463	0.524	0.529	<b>1.000</b>
<b>pAAM-2.5%IPPAAM-Alg</b>	0.402	0.487	0.508	<b>1.000</b>
<b>pAAM-3.75%IPPAAM-Alg</b>	0.341	0.366	0.408	<b>1.000</b>

In the mixed system of fatty acid ethyl esters, C<sub>6</sub> and C<sub>8</sub> ethyl ester, with the alcohol acceptors methanol and n-butanol, both of the free enzyme and the encapsulated enzyme in pAAM-IPPAAM-Alg microcapsules exhibited the highest preference for C<sub>8</sub> ethyl ester and n-butanol resulting in C<sub>8</sub>-butyl ester (1/α=1). The higher the amount of IPPAAM in microcapsule

membrane the greater the selectivity of the membrane to C<sub>8</sub>-butanol as opposed to the remaining substrates, as indicated by the decreasing value of specificity constant for the other substrates (C<sub>6</sub>-methanol, C<sub>6</sub>-butanol and C<sub>8</sub>-methanol). Moreover, the results can be interpreted in such a way, that the hydrophobic microcapsule membrane showed similar preference to both C<sub>6</sub> ethyl ester and C<sub>8</sub> ethyl ester, allowing both of them to pass through the membrane at the same rates.

However, the encapsulated enzymes in pAAm-IPPAAm-Alg microcapsule at 0.5% IPPAAm content demonstrated a significant improvement in selectivity toward C<sub>6</sub>-methanol in comparison to the free enzyme. The amount of C<sub>6</sub> methyl ester converted, which was the next best substrate for pAAm-IPPAAm-Alg microcapsules at 0.5% IPPAAm content, was almost five times higher than the values for the free enzyme. For the encapsulated enzyme, increasing the amount of hydrophobic IPPAAm monomer (1 and 2.5% IPPAAm content) resulted in a shift in the next best substrate from C<sub>6</sub>-methanol to C<sub>8</sub>-methanol. This can be attributed to the larger amount of hydrophobic IPPAAm monomer and the resulting more hydrophobic microcapsule membrane, resulting in more selective permeation of the hydrophobic substrate C<sub>8</sub> ethyl ester.

At 3.75% content of IPPAAm, the amount of substrate reacted and product generated decreased which may be due to a denser microcapsule membrane retarding the substrate transport through the microcapsule membrane.

It can also be recognized by comparing the amount of C<sub>6</sub> methyl ester with C<sub>4</sub>-methyl ester, that the conversion of C<sub>6</sub>-methyl ester was higher than that of C<sub>4</sub>-methyl ester in pAAm-IPPAAm-Alg microcapsules with 0.5, 1 and 2.5 % w/w IPPAAm content. This reflects the nature of the enzyme lipase MML, which prefers longer chain fatty acids to shorter ones. This result again confirmed that the encapsulation process did not modify the underlying catalytic property of the enzyme.

## 5.5 Reusability

In order to be applied industrially, the encapsulated enzyme lipase should be stable and reusable in multiple batches or continuous operation. An operational stability study was therefore performed with encapsulated lipase in pAAm-Alg microcapsules. The competitive reaction with high selectivity between C<sub>4</sub> and C<sub>8</sub> ethyl ester with the alcohol acceptors, methanol and n-butanol, was selected as a test system. The results are shown in Figure 5-21



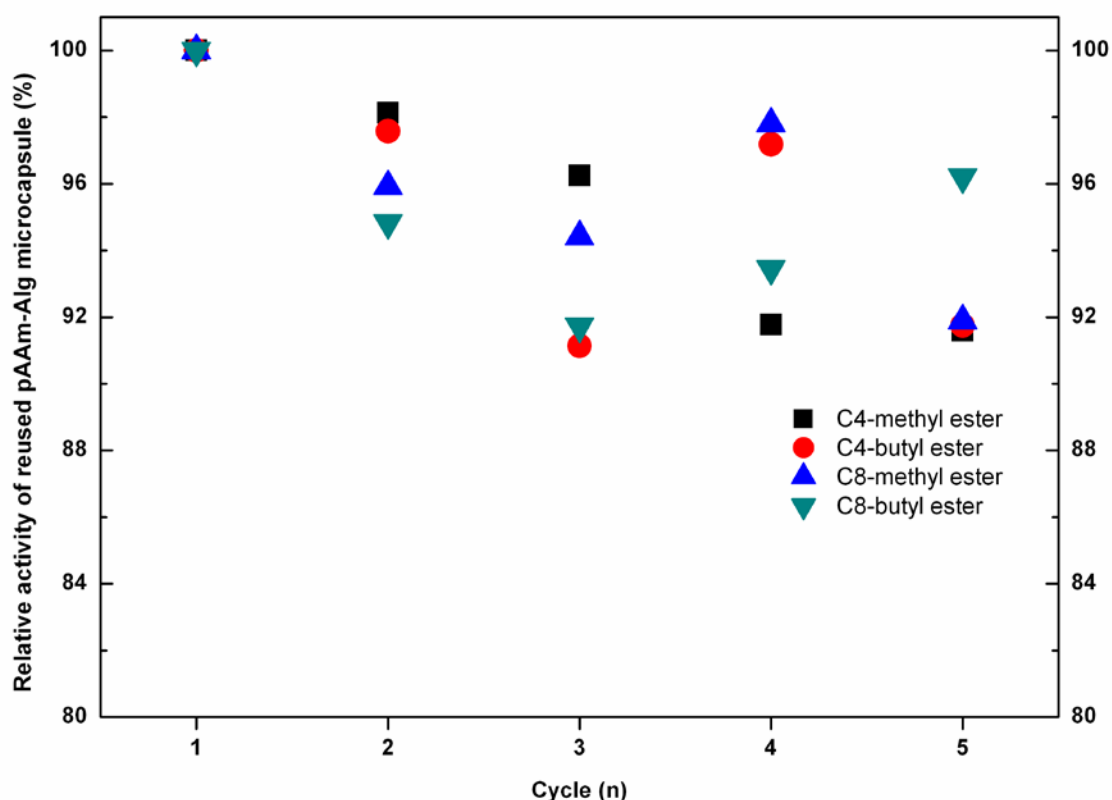


Figure 5-21: Relative activity of reused enzyme lipase encapsulated in pAAm-Alg microcapsules

The stability was monitored over the course of six successive cycles. 90% of the activity was maintained over five consecutive cycles of 48 hours each. The results showed that during the first five cycles, the encapsulated lipases in pAAm-Alg microcapsules were not inactivated by the transesterification reactions. The reaction activity was around 90% of the original activity for five cycles and then dropped to 75% for the sixth cycle, which may be the result of enzyme leakage or exhaustion.

In summary, the encapsulation of the enzyme lipase in either pAAm-Alg or pAAm-IPPAAm-Alg microcapsules seems to be a useful tool to regulate the specificity of lipases toward hydrophilic and hydrophobic substrates by their permselective membrane properties. pAAm-Alg microcapsules can be used to select hydrophilic substrates from a mixed system of hydrophobic and hydrophilic substrates due to their hydrophilic membrane characteristics. By modifying the pAAm-Alg microcapsule membrane with hydrophobic IPPAAm monomer, the selectivity of the pAAm-IPPAAm-Alg microcapsule membrane shifts to hydrophobic substrates, depending on the exact monomer content. The result of the reusability test showed that the reaction activity of encapsulated enzymes in pAAm-Alg microcapsules was

maintained at 90% of the original activity over five practical cycles of 48 hours each. This strategy may be useful for the production of esters where certain selective substrate properties, such as size and hydrophilic or hydrophobic nature, catalysed by the lipases may be desired.

We can thus conclude that the encapsulation of the lipase, MML, in pAAm-Alg microcapsules, in which the membrane is hydrophilic, enable us to greatly increase the specificity of lipases toward hydrophilic substrates. By modifying the pAAm-Alg microcapsules with a hydrophobic monomer, IPPAAm, the specificity of the encapsulated lipase can be shifted to hydrophobic substrates, depending on the concentration of IPPAAm used.

## **6 Mass transfer enhancement by encapsulated magnetic nanoparticles in the liquid core of microcapsules**

Published in: Enzyme immobilisation in permselective microcapsule, *Journal of Microencapsulation*, Aug 2011, Vol.28. No.5, p. 370-383

### **6.1 Background**

In order to generate convection within the microcapsule, and thus intensify mass transfer still further, one can incorporate fine particles with different properties to those of the core liquid and induce their motion by application of an external force [105]. Magnetic nanoparticles are especially suitable for this purpose, since they can be used not only to generate circulation within the liquid core of the microcapsule, but also to give rise to relative motion and thus enhanced mass transfer between the microcapsules and the surrounding bulk liquid and to facilitate the subsequent recovery of the microcapsules from the reaction medium. Several publications have previously reported the use of magnetic particles to enhance the mass transfer by controlling the movement of the magnetic particles via an alternating, external magnetic field. For example, Reichert found that mass transfer coefficients could be increased by up to 200% in this manner [106]. Observed enzyme activity was enhanced by 10-60% over that in the absence of a magnetic field and the rate of hydrolysis of starch to glucose was observed to increase in the presence of an alternating magnetic field [107].

This study reports the result of encapsulating magnetic nanoparticles in the liquid core solution of calcium alginate (Ca-Alg) microcapsules. The influence of a magnetic field on magnetic microcapsules and the effect of different concentrations of magnetic nanoparticles encapsulated inside the liquid core on the diffusion coefficient of substrates were investigated. Lastly, the reaction activities of the encapsulated enzyme dextranase in microcapsules with and without magnetic nanoparticles were compared.

### **6.2 Materials and Methods**

Medium viscosity 400 cp alginic acid sodium salt from brown algae (A2033), for which no M/G ratio was specified by the supplier; dextranase from *Penicillium* Sp. crude 05884-5 KU (41 kDa) from Sigma-Aldrich GmbH, Germany; D+-maltose monohydrate and bis-tris-buffer

from Fluka, Germany; anhydrous calcium chloride and ferrous chloride from Merck KGaA, Germany; ferric chloride from Merck Schuchardt OHG, Germany); 25% (w/w) aqueous ammonia solution from VWR International, France; Dextran T1 clinical grade MW 1.1KDa from Pharmacosmos, Denmark.

### 6.2.1 Preparation of Ca-Alg microcapsules

For full Ca-Alg microcapsules, in which the active component is bound to the microcapsule matrix material, 2 % (w/w) of the sodium alginate solution is mixed with dextranase. The concentration of enzyme in the resultant alginate solution is 3.87units/ml. This solution is then delivered through the peristaltic pump to the nozzle with a regulated air-jet flow of 1500 l/hr and subsequently dropped into the calcium chloride solution.

The hollow Ca-Alg microcapsules, those in which the core solution containing the active component is not gelled or incorporated into the shell membrane of the microcapsule, were prepared from separate 2 % (w/w) sodium alginate and 3.87 units/ml dextranase solutions. The ratio of the alginate solution flow rate to that of the dextranase was 9:1. The alginate solution was delivered through the peristaltic pump and the dextranase solution fed through the micro-gear pump to the nozzle. Uniform droplets were formed with the aid of a regulated air-jet flow of 1500 l/hr before dropping into the calcium chloride solution below. The loading of the enzyme dextranase in full and hollow microcapsules was determined according to the method of Lijuan et al. 2009 and Zhongun et al. 2009 which is explained in section 4.3.

### 6.2.2 Preparation of magnetic nanoparticles and magnetic microcapsules

The co-precipitation method was used to synthesise magnetic iron oxide nanoparticles [108]. A solution of 0.5 M ferric and ferrous chloride hydrate ( $FeCl_3 \cdot 6H_2O$  and  $FeCl_2 \cdot 4H_2O$ ) was mixed in a molar ratio of 2:1. 15ml of 25 % (w/w) ammonium hydroxide solution was then introduced into 40 ml of the solution forming a black precipitate. The magnetic magnetite form of iron oxide was produced according to the reaction equation:



After vigorous stirring for 30 minutes, the black precipitate obtained was washed with deionised water several times until a pH of 6.5 was attained. Roughly 7% (v/v) of the magnetic nanoparticles were suspended in water and examined by transmission electron microscopy (FEI CM200. TEM USA) operated at 160 kV.

The magnetic microcapsules were prepared in the same manner as the hollow microcapsules, except that a magnetic nanoparticles suspension at different concentrations was employed together with the enzyme dextranase as the core solution and delivered through a micro-peristaltic pump rather than the micro-gear pump to prevent plugging. The ratio of the alginate solution flow rate to that of the magnetic nanoparticles suspension flow rate was 24:1.

### **6.2.3 Influence of magnetic field on magnetic microcapsules**

The effect of a magnetic field on the magnetic microcapsules was studied by simply rotating a permanent magnet at various speeds adjacent to a beaker containing the magnetic microcapsules in a dilute suspension. The concentration of the magnetic nanoparticles suspension was 2mg/ml. The displacement of the magnetic microcapsules was measured as a function of the frequency of the alternating magnetic field.

### **6.2.4 Diffusion of dextran T1 from bulk liquid into microcapsules**

In order to study the influence of encapsulated magnetic nanoparticles in the liquid core of a microcapsule on the mass transfer behaviour inside the microcapsule, the diffusion characteristic of the microcapsules was examined. The diffusion studies were performed at room temperature in a 200 ml vessel with a Teflon stirrer. Predefined amounts (30 g) of microcapsules (~1600 microcapsules) were added to 70 ml of well-stirred dextranT1 solution at 5 g/l concentration and samples were withdrawn at regular intervals. Adequate stirring of the substrate solution was ensured to negate the liquid film resistance around the microcapsule. A normal magnetic stirrer and a stirrer bar were utilised with the full and hollow microcapsules, while a non-magnetic mechanical stirrer was applied with the magnetic microcapsules.

The concentration of the dextran T1 was determined using the DNS method [80] to ascertain the sugar concentration as explained in section 4.2. Samples were withdrawn at the end of 2, 4, 6, 8 and 10 minutes and then at the end of every 5 minutes up to 60 minutes. The change in substrate concentration with time was plotted and the diffusion coefficient was determined, following Crank's model (section 2.4.1).

To prepare the microcapsules for the diffusion experiment, an enzyme solution was not necessary for the full microcapsules and bi-distilled water was used as the core solution in the

hollow microcapsules. For the magnetic microcapsules, suspensions of magnetic nanoparticles at 1, 2, and 3 mg/ml in distilled water were used as the core solution.

### 6.2.5 Dextranase reaction activity

5mM of Bis-Tris-HCl buffer solution was prepared at pH 6.5 and used to control the pH of the solution in the enzyme activity test. First of all, the free enzymatic activity of dextranase was assayed as a benchmark for later work. 31 mg of dextranase in 70 ml buffer solution was mixed with 0.1 g dextran T1 in 30 ml buffer solution. Samples were then taken at different times and the reaction was terminated after 200 minutes. The enzyme activity was determined using the DNS method to ascertain the isomaltose concentration in the same manner as the determination of sugar concentration explained in section 4.2. The dextranase activity for the enzyme encapsulated in the microcapsules was determined in the same manner as for the free enzyme. A buffer solution was added to 42 ml of the microcapsule suspension to make the volume up to 80 ml. 0.1 g of dextran in 20 ml buffer solution was added to start the reaction. Samples were taken every 15 minutes and analysed in the same manner as for the free enzyme assay. The reaction activity test was conducted at room temperature  $25 \pm 2^\circ\text{C}$

## 6.3 Results and Discussion

### 6.3.1 Characterisation of Ca-Alg and magnetic microcapsules

Microscopic images of the full and hollow Ca-Alg microcapsules are presented in Figure 6-1. Both microcapsules display a uniform spherical appearance with a diameter of 1.7-2 mm. The surface of the microcapsule wall is smooth and the enzyme dextranase was trapped in the gel matrix of the full microcapsules or contained in the liquid core of the hollow microcapsules.

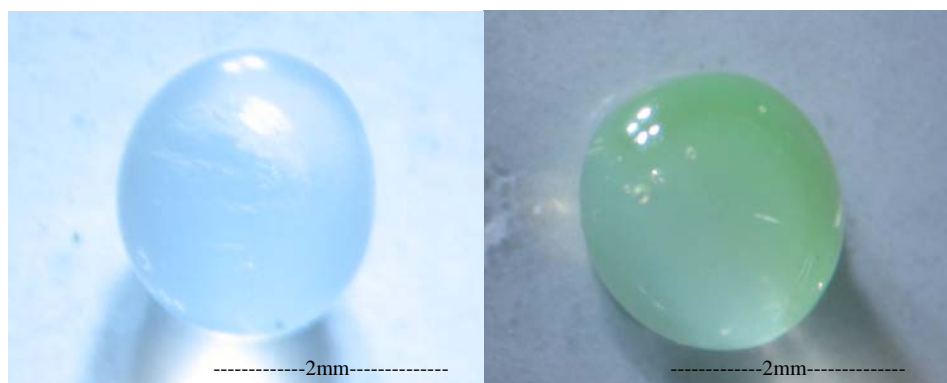


Figure 6-1: Images of a full (left) and a hollow (right) microcapsule

The wall thickness of the hollow microcapsules was estimated to be 0.17 mm ( $\pm$  0.03 mm). A suspension of black, Fe<sub>3</sub>O<sub>4</sub> nanoparticles was prepared by the co-precipitation method and subsequent encapsulation procedure carried out according to the details provided in the experimental method section. Photographic images of magnetic nanoparticles and a magnetic microcapsule are presented in Figure 6-2.

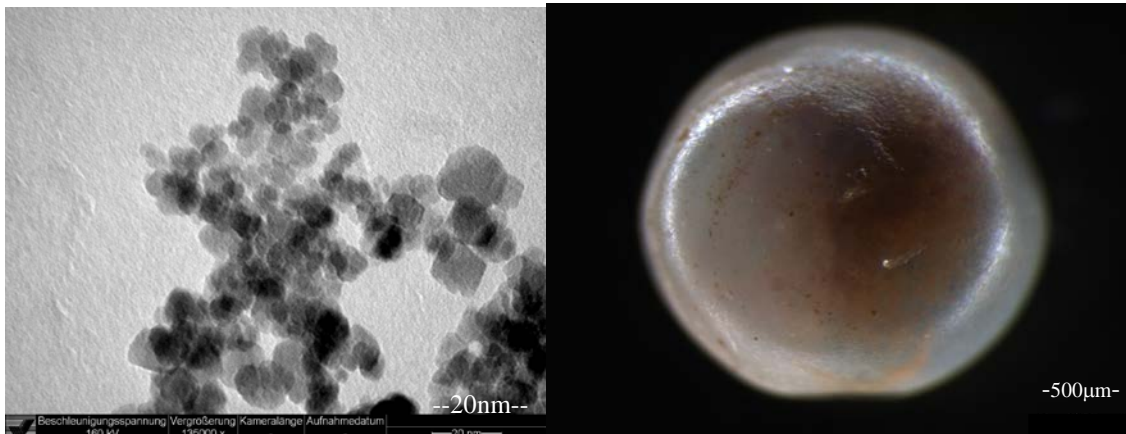


Figure 6-2: Images of magnetic nanoparticles (15-20 nm) and a magnetic microcapsule

TEM (Transmission electron microscope) observations indicated that the magnetic nanoparticles were not exactly spherical and lay in the size range of 15-20 nm. In the right image of Figure 6-2, the white area shows the alginate matrix while the dark area indicates the presence of the magnetic nanoparticle suspension. It can be clearly seen that the magnetic suspension is located at the periphery of the microcapsule instead of the desired location within the central core. This is probably due to the higher viscosity of the alginate solution compared to that of the iron-oxide magnetic nanoparticle suspension, which leads to the magnetic nanoparticles tending to accumulate at the bottom of the microcapsule. Moreover, there was considerable gelation of the magnetic nanoparticles within the alginate membrane instead of within the free suspension in the liquid core as sought.

### 6.3.2 Influence of a magnetic field on magnetic microcapsules

The magnetic microcapsules exhibited a good response to an external magnetic field, even at low concentrations of magnetic nanoparticles (0.2 % w/v). An alternating magnetic field was applied to the magnetic microcapsules at varying frequencies and the mean displacement of the microcapsules within an aqueous suspension was measured (Figure 6-3)

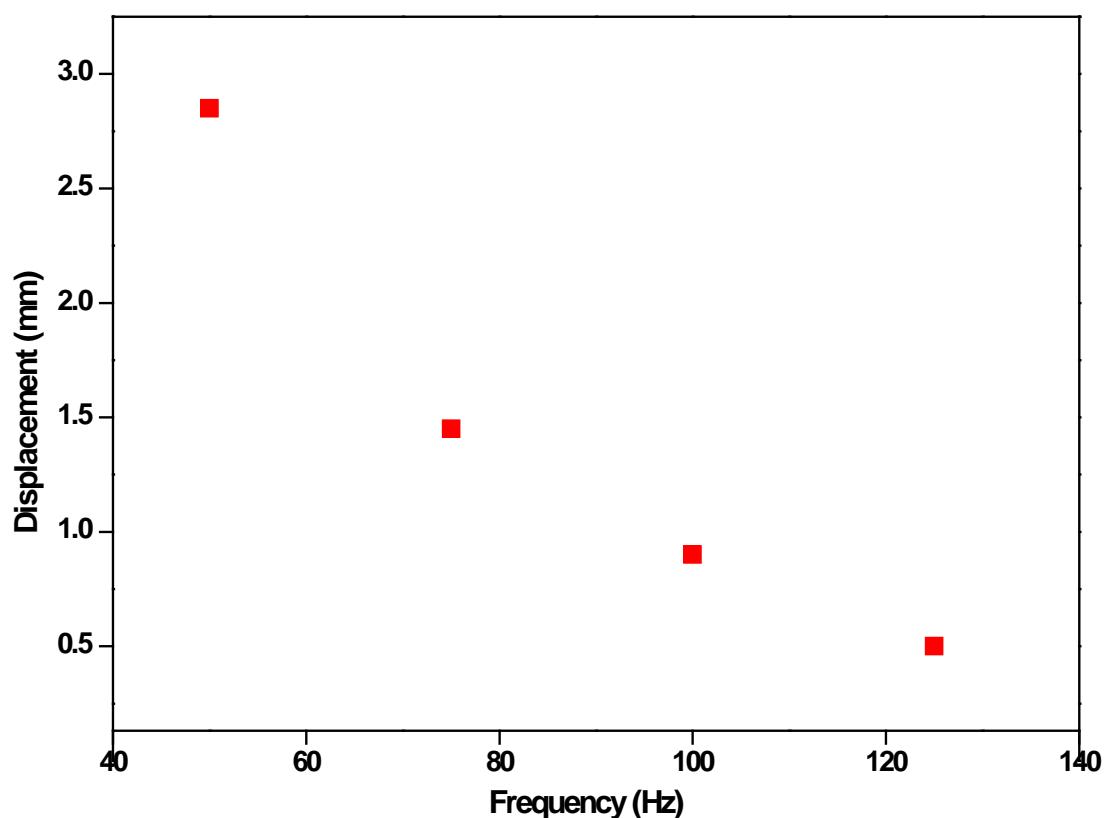


Figure 6-3: Displacement of magnetic microcapsules at various magnetic field frequencies

It is evident that the higher the frequency of the alternating magnetic field, the lesser the displacement and the faster the oscillations of the magnetic microcapsules. It was hoped that this effect would enhance the mass transfer of substrate from the bulk liquid to the microcapsule without the danger of a microcapsule rupture that could arise through more intensive stirring. In order to achieve the desired internal mixing of the liquid core, a sodium citrate treatment to partially solubilise the core-gel matrix was employed. However, it became apparent that the calcium alginate structure is too susceptible to dissolution in sodium citrate [109,110], so this approach was discarded. Nevertheless, control experiments were conducted to identify the possible influence of the magnetic nanoparticles on the mass transfer of substrate and enzyme activity.

### **6.3.3 Diffusion coefficient of dextran T1 into Ca-Alg and magnetic microcapsules**

In order to determine the influence of the encapsulated magnetic nanoparticles and their concentration on the diffusion coefficient, different types of microcapsules: full



microcapsules, hollow microcapsules, and magnetic microcapsules which encapsulated magnetic nanoparticles at 1, 2, and 3 mg/ml, were prepared and the diffusion experiments were carried out. Dextran T1 at an initial concentration of 5 g/l was used as a substrate solution and the microcapsules were dispersed in this substrate solution. The movements of magnetic nanoparticles inside the core solutions were controlled by the alternating magnetic field for which the frequency of rotation was set at 50 Hz. The substrate was allowed to diffuse from the medium surrounding the microcapsules into the inner core medium of the microcapsules. The substrate diffusion curve was obtained by measuring the concentration of the substrate in the external medium. The combined diffusion coefficient value,  $D_m$ , was calculated according to Crank's model. The results obtained are shown in Figure 6-4 and the values of the diffusion coefficients are given in Table 6-1.

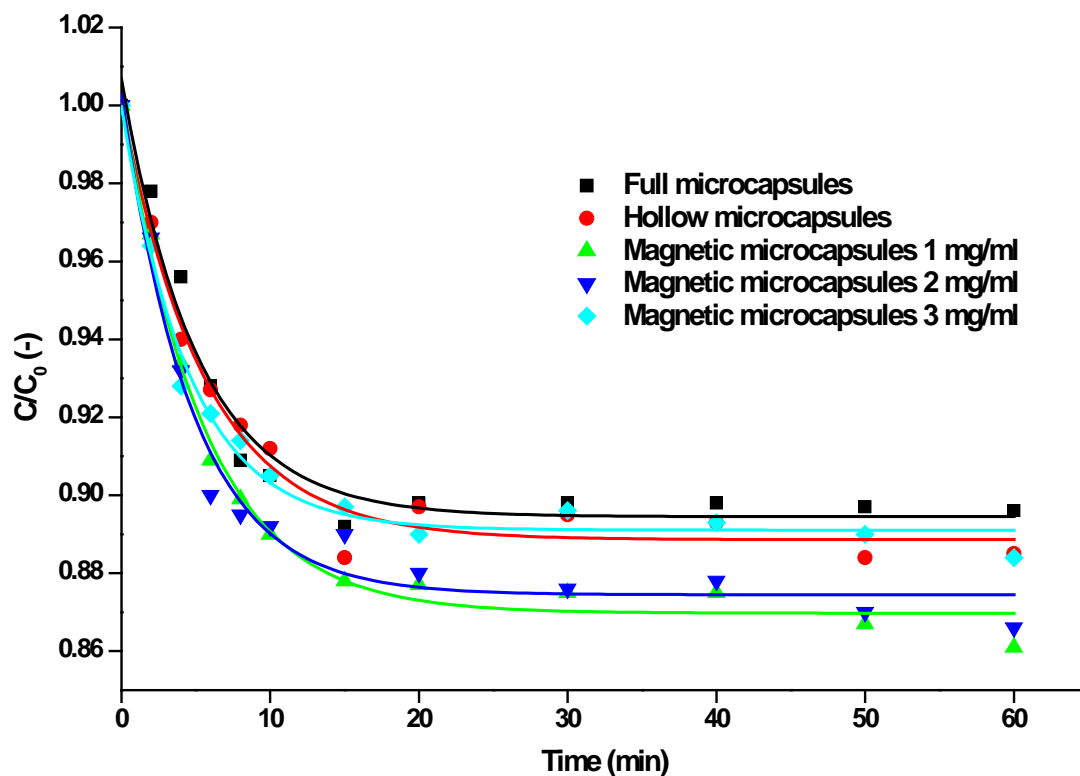


Figure 6-4: Concentration profiles of dextranT1 diffusing into full, hollow, and magnetic microcapsules with encapsulated magnetic nanoparticles at concentrations of 1, 2, and 3 mg/ml. The points are the experimental data and the curves represent the results calculated using the “Analysis data fitting (ExpDec1)” function from the “Origin” programme.

Table 6-1:  $D_m$  and  $S$  of dextran T1 diffusing into full, hollow, and magnetic microcapsules with encapsulated magnetic nanoparticles at concentrations of 1, 2, and 3 mg/ml

<b>Microcapsule</b>	<b><math>D_m</math> (m<sup>2</sup>/s)</b>	<b>S (%)</b>
<b>Full microcapsules</b>	$2.95 \times 10^{-11}$	0.0046
<b>Hollow microcapsules</b>	$3.44 \times 10^{-11}$	0.0030
<b>Magnetic microcapsules (1mg/ml)</b>	$5.73 \times 10^{-11}$	0.0026
<b>Magnetic microcapsules (2mg/ml)</b>	$5.39 \times 10^{-11}$	0.0034
<b>Magnetic microcapsules (3mg/ml)</b>	$3.55 \times 10^{-11}$	0.0035

The results show that the diffusion coefficient increases in magnetic microcapsules compared to hollow microcapsules and full microcapsules ( $5.73$ ,  $3.44$ , and  $2.79 \times 10^{-11}$  m<sup>2</sup>/s respectively). This confirms that the encapsulated magnetic nanoparticles which were influenced by the external alternating magnetic field can enhance the convection inside the core solution of the microcapsule.

The diffusion coefficient for the magnetic microcapsules at concentrations of 1 and 2 mg/ml increases significantly compared to that of hollow microcapsules, while remaining nearly constant at a concentration of 3 mg/ml. This could be the result of high concentrations of magnetic nanoparticles forming an agglomeration, resulting in the inhibition of transportation inside the microcapsules, hence reducing the diffusion coefficient.

Moreover, it can be seen by comparing hollow and full microcapsules, that hollow microcapsules exhibit a higher effective diffusion coefficient than full microcapsules ( $3.44$  and  $2.95 \times 10^{-11}$  m<sup>2</sup>/s respectively). This can be attributed to the fact that the substrate can move more easily inside the core solution of hollow microcapsules, while the diffusion through the gel matrix of the full microcapsules is impeded.

In line with the above results, magnetic microcapsules with encapsulated magnetic nanoparticles at a concentration of 2 mg/ml have been selected as the benchmark case when referring to magnetic microcapsules.

### 6.3.4 Loading efficiency of dextranase in full and hollow Ca-Alg microcapsules

The loading efficiency of dextranase immobilised in fresh full microcapsules was found to be  $0.633 \pm 0.041$  but fell to  $0.525 \pm 0.133$  after 3 hours of experimentation. The loading efficiency of dextranase encapsulated in fresh hollow microcapsules, on the other hand, was  $0.872 \pm 0.069$  and fell to  $0.664 \pm 0.051$  after the experiment. It is evident that for full microcapsules, during the gelation process the enzyme dextranase, which is supposed to be bound to the calcium alginate matrix, has a greater possibility of being leached out than for hollow microcapsules, in which the dextranase is enclosed in a calcium alginate shell. However, when the capsule is fully formed, full microcapsules exhibited better retention of enzymes than hollow microcapsules with 83% as opposed to 76 % of the reaction activity.

### 6.3.5 Enzyme activity of full and hollow-magnetic Ca-Alg microcapsules

The activities of free and encapsulated dextranase in full, hollow, and magnetic microcapsules were assayed under otherwise similar reaction conditions. Solutions of dextran T 1 were mixed with microcapsules containing the enzyme dextranase. The activities measured are illustrated in Figure 6-5.

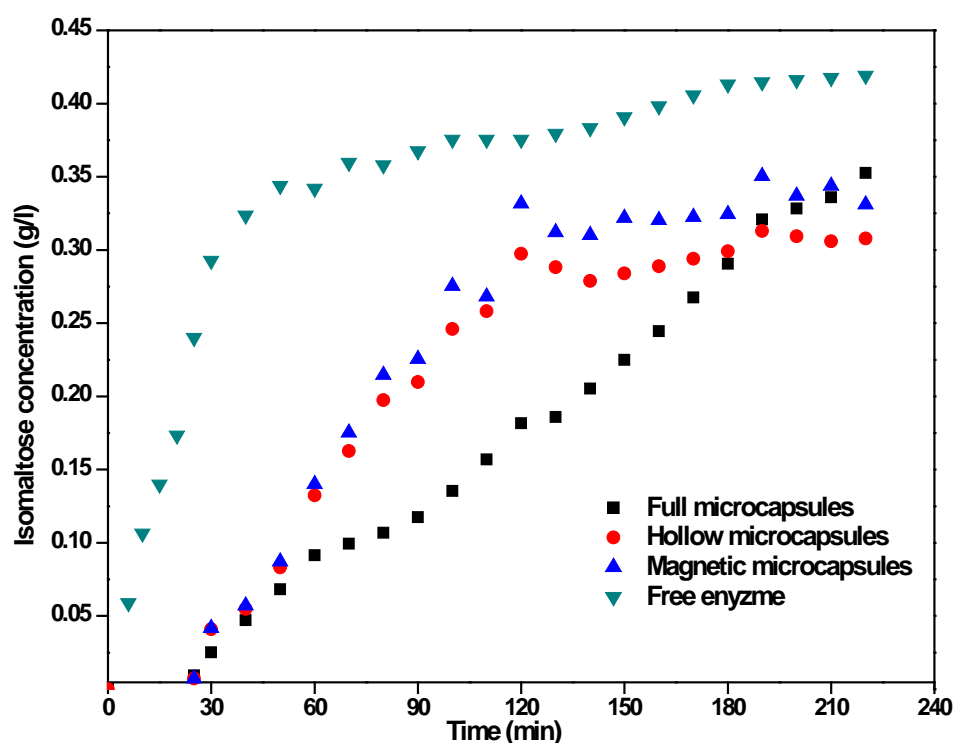


Figure 6-5: Isomaltose concentration generated by free and encapsulated dextranase

The results show that approximately 50% of the dextran was converted with free dextranase within the first 25 minutes, while virtually no production of isomaltose took place for the full and hollow microcapsules. This phenomenon can be explained by the concentration gradient of dextran between the bulk reaction medium and the microcapsules and by the resultant unsteady-state mass transfer process taking place in full and hollow microcapsules. Due to the significant difference between the dextran concentration inside and outside the microcapsules, an apparent drop of isomaltose concentration to negative values for the encapsulated enzyme occurred. Since the liquid core of the hollow microcapsules provides less mass transfer resistance to both the substrate and the product diffusion than the matrix of the full microcapsules, the diffusive flow of the dextran T1 and isomaltose into and out of the hollow microcapsules was significantly faster than that for the full microcapsules. The experiments were repeated six times and the standard deviation of the results was determined to be 0.11.

As a consequence, the reaction rate for hollow microcapsules was greater than that for full microcapsules. Compared to the conversion of free enzymes after 80 minutes, the conversion of hollow microcapsules was 55%, while that of full microcapsules was 30%. After 120 minutes, the conversion of dextranase in hollow microcapsules reached its final value at roughly 80% of the free enzymes value, whereas the dextranase immobilised in full microcapsules exhibited a conversion of only 48%. This is attributed to the superior mass transfer and lower steric inhibition of the dextranase encapsulated inside the liquid core solution of hollow microcapsules as opposed to that bound in the alginate matrix of full microcapsules.

The addition of magnetic nanoparticles inside the liquid core showed a slightly higher conversion, approximately 10% larger than, that of hollow microcapsules, due to a further enhancement in the mass transfer of substrate and product.

## 6.4 Conclusions

An initial attempt to incorporate magnetic iron-oxide nanoparticles into the liquid core of hollow microcapsules was performed and a simple alternating magnetic field arrangement was developed. The results showed that the diffusion coefficient of dextran T1 transported into magnetic microcapsules at optimum concentrations (1 and 2 mg/ml) is 50% higher than for non-magnetic hollow and full microcapsules. Hollow microcapsules were shown to yield superior substrate mass transfers over full microcapsules, resulting in higher conversions of

around 80% of the free enzyme values. Magnetic microcapsules showed slightly better conversion compared to hollow microcapsules, but still managed to attain nearly 90% of the free enzyme conversion. Hence, magnetic nanoparticles can be used as a tool to enhance mass transfer in the liquid core solution.

## 7 Summary and Outlook

Permselective pAAm-Alg microcapsules containing a liquid core solution were successfully prepared using a concentric double nozzle air-jet technique. The combination of natural and synthetic polymer yields more uniform and reproducible microcapsule shell structures than natural polymer alone. To determine the characteristics and transport properties of pAAm-Alg microcapsules, the diameter, membrane thickness and diffusion coefficients for different concentrations of monomer, cross-linker, and initiator were investigated. The results showed that higher monomer (pAAm) or cross-linker (Bis-AAm) concentrations can lead to smaller diameters and membrane thicknesses of the microcapsules which in turn reduced the diffusion coefficients due to formation of a denser gel. On the other hand, higher initiator concentrations resulted in larger microcapsule diameters and membrane thicknesses, but had a negligible effect on the diffusion coefficients. The inclusion of silica additives in the microcapsule membranes resulted in partial closure of the membrane pores and hence reduced substrate permeability. Since the diffusion coefficient of the microcapsule membrane accounts for 20% of the overall diffusion resistance, it is apparent that the microcapsule membrane plays an important role in mass transport. pAAm-Alg microcapsules with optimal characteristics and transport properties were prepared with concentrations of 3.5% Alg, 19% AAm, 1% bis-AAm and using 0.2% initiator.

Size-selective transport may occur if the pore sizes of the microcapsules are smaller than or comparable with the size of the permeating molecules. The MWCO experiment showed that pAAm-Alg microcapsules allowed glucose, maltose, and dextran T1 to diffuse through the microcapsule membrane relatively unhindered, while the diffusion of insulin,  $\alpha$ -lactalbumin and trypsin were more or less strongly inhibited. The pAAm-Alg microcapsules can therefore act as a size-selective medium for discriminating between substrates above and below the molecular weight range of 1.1-5 kDa.

Other permselective properties of this microcapsule, such as the hydrophobic and hydrophilic characteristics, were also investigated in depth. A multi-competitive, enzymatic reaction, catalysed by lipase from *M. Miehei*, was chosen to test the selectivity of free enzyme and enzyme encapsulated in pAAm-Alg microcapsules. While the free enzyme showed a high selectivity towards the transesterification of long chain fatty acid ethyl ester, the encapsulated

enzyme showed greater preference towards short chain fatty acid ethyl ester. This can be ascribed to the hydrophilic properties of the microcapsule membrane. By modifying the pAAm-Alg microcapsule membrane with the hydrophobic IPPAAm co-monomer, the selectivity of the pAAm-IPPAAm-Alg microcapsule membranes shifted to long chain fatty acid ethyl ester at a co-monomer content higher than 2.5% w/w, due to the more hydrophobic nature of the modified membrane.

It can therefore be concluded that the encapsulation of the enzyme lipase, in either pAAm-Alg or pAAm-IPPAAm-Alg microcapsules, can be a useful tool in regulating the specificity of the lipase towards hydrophilic or hydrophobic substrates according to their permselective behaviour in the microcapsule membrane. Moreover, the encapsulated enzymes in pAAm-Alg microcapsules retain about 90% of their initial catalytic activity even after being used for 5 reaction cycles – a total of 240 hours - indicating the high stability of both immobilised enzyme and microcapsules.

Future work to develop the permselective properties of microcapsules can possibly be achieved by the addition of the microcapsule shells as multilayer membrane. The layer-by-layer self-assembly technique offers the advantages of accurate control over size, composition, and the thickness of the multilayer shell which may, ultimately resulting in polyelectrolyte multilayer microcapsules which can encapsulate fine catalyst and govern various selective properties through the multilayer membrane.

## 8 Literature

- 1 Barth, E E., Ufer, A., Agar, D W.: Selectivity enhancement of microencapsulated enzymes with permselective shells. *Proceedings of the European Congress of Chemical Engineering (ECCE-6)*, Copenhagen, Denmark, 16-20 September (2007)
- 2 Konsoula, Z., Liakopoulou-Kyriakides, M.: Starch hydrolysis by the action of an entrapped in alginate capsules  $\alpha$ -amylase from *Bacillus subtilis*. *Process Biochemistry*, **41** (2006), P. 343-349
- 3 Nagel, B., Dellweg, H., Gierasch, L.M.: Glossary for chemists of terms used in biotechnology (IUPAC Recommendations 1992). *Pure and Applied Chemistry*. **64** (1992), P.143-168.
- 4 Yao, S., Cho, M.G.: Diffusion characteristics in Microcapsule. *Chinese journal of chemical engineering*. **6** (1998), P.116-123
- 5 Chai, Y., Mei, L.H., Wu, G.L., Lin, D.Q., Yao, S.J.: Gelation conditions and transport properties of hollow calcium alginate capsules. *Journal of chemical & engineering data*. Published online 21 June 2004 in Wiley Interscience (www.interscience.wiley.com) DOI : 10.1002/bit.201444
- 6 Koyama, K., Seki, M.: Cultivation of yeasts and plant cells entrapped in the low-viscous liquid-core of an alginate membrane capsule prepared using polyethylene glycol. *Journal of bioscience and bioengineering*. **97** (2004), P.111-118
- 7 Taqieddin, E., Amiji, M.: Enzyme immobilisation in novel alginate-chitosan core-shell microcapsules. *Biomaterials*, **25** (2004), P.1937-1945
- 8 Akiyama, R., Kobayashi, S.: Renaissance of immobilized catalyst. New types of polymer-supported catalysts, 'microencapsulated catalysts', which enable environmentally benign and powerful high-throughput organic synthesis. *Chemical Communications*. **4** (2003), P.449-460
- 9 Fuhrmann, H., Dwars, T., Michalik, D., Holzhüter, G., Grüttner, C., Kragl, U., Oehme, G.: Catalyst Encapsulation and Substrate Solubilization in Polymer-Surfactant Complexes and Their Use in a Membrane Reactor. *Advanced Synthesis & Catalysis*. **345** (2003), P.202-210
- 10 Milo, A., Meumann, R.: An chiral manganese salen catalyst encapsulated in a peptidic phosphonate homochiral solid for the enantioselective formation of diols by consecutive epoxidation and hydration reactions. *Chemical Communication*. **47** (2011), P. 2535-2537



- 
- 11 Yang, J., Ding, S., Radosz, M., Shen, Y.: Reversible Catalyst Supporting via Hydrogen-Bonding-Mediated Self-Assembly for Atom Transfer Radical Polymerisation of MMA. *Macromolecules*. **37** (2004), P.1728-1734
- 12 Kunna, K.:Catalyst Immobilisation via Electrostatic Interactions: Polystyrene-based Supports. Dissertation, Catalyst and Organic chemistry department, Eindhoven University of Technology, 2008 (ISBN: 978-90-386-1509-7)
- 13 Fraile, J.M., García, J.I., Lafuente, G., Mayoral J.A., Salvatella, L.:Bis(oxazoline)-copper complexes, immobilized by electrostatic interactions, as catalysts for enantioselective aziridination. *ARKIVOC*. **4** (2004), P.67-73
- 14 Shaikhutdinov, Sh.K., Naschitzki, R.M.M., Baumer, M., Freund, H.J.: Size and support effects for CO adsorption on gold model catalysts. *Catalysis Letters*. **86** (2003), P.211-219
- 15 Bartholomew, C.H., Pannell, R.B., Butler, J.L., Mustard, D.G.: Nickel-support interactions: their effects on particle morphology, adsorption, and activity selectivity properties. *Industrial and engineering chemistry product research and development*. **20** (1981), P.296-300
- 16 Zeng, J., Lee, J.Y., Chen, J., Shen, P.K., Song, S.: Increased metal utilization in carbon supported Pt catalyst by adsorption of preformed Pt nanoparticles on colloidal silica. *Fuel Cell*. **7** (2007), P.285-290
- 17 Hutchings, G.J., McMorn, P.: Heterogeneous enantioselective catalyst: strategies for the immobilisation of homogenous catalysts. *Chemical Society.Reviews*. **33** (2004), P.108-122
- 18 Zhao, X.S., Bao, X.Y., Guo, W., Lee, F.Y.: Immobilizing catalyst on porous materials. *Mater Today*. **9** (2006), P.32-39
- 19 Ghosh, S.K.: Functional coatings and microencapsulation : A general perspective. In *Functional Coatings*. WILEY-VCH Verlag GmbH & Co. KGaA, Weinheim, (2006).
- 20 Schneider, S., Feilen, P.J., Slotty, V. Kampfner, D., Preuss, S., Berger, S., Beyer, J., Pommersheim, R.: Multilayer capsules: a promising microencapsulation system for transplantation of pancreatic islets. *Biomaterials*. **22** (2001), P.1961-1970
- 21 Wang, W., Liu, X., Xie, Y., Zhang, H., Yu, W., Xiong, Y., Xie, W., Ma, X.: Microencapsulation using natural polysaccharides for drug delivery and cell implantation. *Journal of materials chemistry*. **16** (2006), P.3252-3267

- 22 Venkata, N.V.N., Prasanna, P.M., Sakarkar, S.N., Prabha S.K., Ramaiah, S.P., Srawan, G.Y.: Microencapsulation techniques, factors influencing encapsulation efficiency. Review in *Journal of microencapsulation*. **27** (2010), P.187-197
- 23 Vankelecom, I.F.J.: Polymeric membranes in catalytic reactors. *Chemical Reviews*. **102** (2002), P.3779-3810
- 24 Wang, F., Feng, J., Gao, C.: Manipulating the properties of coacervated polyelectrolyte microcapsules by chemical cross-linking. *Colloid polymer science*. DOI10.1007/s00396-008-1853-7
- 25 Zhang, P., Qian, J., Yang, Y., An, Q., Liu, X., Gui, Z.: Polyelectrolyte layer by layer self assembly enhanced by electric field and their multilayer membranes for separating isopropanol-water mixtures. *Journal of membrane sciences*. **320** (2008), P.73-77
- 26 Jeong, B., Gutowska, A.: Lessons from nature: stimuli responsive polymers and their biomedical applications. *Review in Trends in Biotechnology*. **20** (2002), P.305-310
- 27 Eposito, E., Cortesi, R., Bortolotti, F., Menegatti, E., Nastruzzi, C.: Production and characterisation of biodegradable microparticles for the controlled delivery of proteinase inhibitors. *International journal of pharmaceutics*. **129** (1996), P. 263-273
- 28 Tanaka, H., Matsumura, M., Veliky I.: Diffusion Characteristic of substrates in Ca-Alginate gel beads. *Biotechnology and bioengineering*. **26** (1984), P.53-58
- 29 Chai, Y., Mei, L.H., Wu, G.L., Lin, D.Q., Yao, S.J.: Diffusion coefficient in intrahollow calcium alginate microcapsule. *Journal of chemical & engineering data*. **49** (2004), P.475-478
- 30 Jin, W., Toutianoush, A., Tieke, B.: Size and charge selective transport of aromatic compounds across polyelectrolyte multilayer membranes. *Applied surface science*. **246** (2005), P.444-450
- 31 Striemer, C.C., Gaborski, R.T., McGrath, L.J., Fauchet, M.P.: Charge and size-based separation of macromolecules using ultrathin silicon membranes. *Letters Nature*. **445** (2007), P.749-753
- 32 Park, J.S., Ruckenstein, E., Selective permeation through hydrophobic-hydrophilic membranes. *Journal of applied polymer science*. **38** (1989), P.453-461

- 33 Dautzenberg, H., Schuldt, U., Lerche, D., Woehlecke, H., Ehwald, R.: Size exclusion properties of polyelectrolyte complex microcapsules prepared from sodium cellulose sulphate and poly[diallyldimethylammonium chloride]. *Journal of membrane science*. **162** (1999), P. 165-171
- 34 Buonomenna, M.G., Choi, S.H., Drioli, E.: Catalysis in polymeric membrane reactors: the membrane role. *Asia-Pacific Journal of Chemical Engineering*. **5** (2009), P.26-34
- 35 Bansode, S.S., Banarjee, S.K., Gaikwad, D.D., Jadhav, S.L., Thorat, R.M.: Microencapsulation : A review. *International journal of pharmaceutical sciences review and research*. **1** (2010), P.38-43
- 36 Antipoy, A.A., Sukhorukov, G.B.: Polyelectrolyte multilayer capsules as vehicles with tunable permeability. *Advances in colloid and interface science*. **111** (2004), P.49-61
- 37 Haag, R., Roller, S.: Polymeric supports for the immobilisation of catalyst. *Topics in current chemistry*. **242** (2004), P.1-42
- 38 McHugh, J D.: A guide to seaweed industry. *FAO Fisheries Technical Paper*. No.441, 2003.
- 39 Martinsen, A., Storro, I., Skjark-Braek, G.: Alginate as immobilisation material: III Diffusional properties. *Biotechnology and Bioengineering*. **39** (1992), P.186-194
- 40 Wijffels, R.H., Buitelaar, R.M., Bucke, C., Tramper, J.: Immobilized Cells: Basic and Applications. *Progress in Biotechnology*. **11** (1996), P.19-29
- 41 Yamagiwa K., Korazawa T., Ohkawa A.: Effects of alginate compositions and gelling conditions on diffusional and mechanical properties of calcium alginate gel beads. *Journal of chemical engineering of Japan*. **28** (1995), P.463-467
- 42 Oyaas, J., Storro, I., Svendsen, H., Levine, D.W.: The effective diffusion coefficient and distribution constant for small molecules in calcium-alginate gel beads. *Biotechnology and Bioengineering*. **47** (1995), P.492-500
- 43 Roger, S., Talbot, D., Bee, A.: Preparation and effect of  $\text{Ca}^{2+}$  on water solubility, particle release and swelling properties of magnetic alginate films. *Journal of Magnetism and Magnetic Materials*. **305** (2006), P.221-227

- 44 Setty, C.M., Sahoo, S.S., Sa, B.: Alginate-coated alginate-polyethyleneimine beads for prolonged release of furosemide in simulated intestinal fluid. *Drug development and industrial pharmacy*. **35** (2005), P.435-436
- 45 Vieira, E.F.S., Costa, L.P., Cestari, A.R.: Preparation and characterisation of polyalginate–glutaraldehyde membranes–Swelling analysis by microcalorimetry and adsorption kinetics of cationic dye. *Journal of applied polymer science*. **118** (2010), P.857-865
- 46 Nunes, M.A., Vila-Real, H., Fernandes, P.C., Ribeiro, M.H.: Immobilisation of naringinase in PVA-alginate matrix using an innovative technique. *Applied Biochemistry and Biotechnology*. **160** (2010), P.2129-2147
- 47 Wyss, A., Stockar, U., Marison, I.W.: Production and Characterisation of liquid core capsules made from cross linked acrylamide co-polymers for biotechnological application. *Biotechnology and Bioengineering*. **86** (2004), P.563-572
- 48 Menter, Paul. www.Bio-rad.com. 2000. (06 January 2012).www.bio-rad.com/webroot/web/pdf/lsr/literature/Bulletin\_1156.pdf
- 49 Kroschwitz, J I. Concise encyclopedia of polymer science and engineering.: John Wiley, New York, 1990
- 50 Kurk, E.A., Orakdogan, N., Okay, O.: Preparation of homogeneous polyacrylamide hydrogels by free-radical cross-linking co-polymerisation. *European polymer journal*. **43** (2007), P.2913-2921
- 51 Kele, H., Celk, M., Sacak, M., Aksu, L.: Graft co-polymerisation of methyl methacrylate upon gelatin initiated by benzoyl peroxide in aqueous medium. *Journal of Applied Polymer Science*. **74** (1999), P.1547-1556
- 52 Xiao, C., Lu, Y., Liu, H., Zhang, L.: Preparation and physical properties of blend films from sodium alginate and polyacrylamide solutions. *Journal of Macromolecular Science, Part A*. **37** (2000), P.1663-1675
- 53 Tridib, T., Singh, R.P.: Characterisation of polyacrylamide-grafted sodium alginate: A novel polymeric flocculant. *Journal of Applied polymer science*. **81** (2001), P.3296-3308
- 54 Kulkarni, R.V., Mallikarjun Setty, C., Sa, B.: Polyacrylamide-g-alginate based electrically responsive hydrogel for drug delivery applicatrion: Synthesis, characterisation, and formulation development. *Journal of applied polymer science*. **115** (2010), P.1180-1188

- 55 Ufer, A.: Aufbau und Inbetriebnahme einer lufunterstützten konzentrischen Doppeldüse zur Herstellung alginabasierter Mikrokapseln und Untersuchungen zu ihren prozessintensivierenden Eigenschaften. Diplomarbeit, Bio-Chemie-ingenieurwesen, TU Dortmund, Dortmund, 2006.
- 56 Sinnott, R.K., Coulson, J.M., Richardson, J.F.: Chemical engineering design. Elsevier Butterworth. Heinemann. 4<sup>th</sup> edition. P.201, 2005
- 57 Yi, W., Ma, J., Liu, Y., Liu, X., Xiong, Y., Xie, Y., Ma, X.: Insight into permeability of protein through microcapsule membranes. *Journal of membrane science*. **269** (2006), P.126-132
- 58 Kondo, T.. Preparation and permeability characteristics of microcapsule membranes. *Journal of controlled release*. **11** (1990), P.231-224
- 59 Kondo, T.. Microcapsules: their science and technology. *Journal of Oleo science*. **50** (2001), P.81-95
- 60 Amsden, B., Turner, N.: Diffusion characteristics of calcium alginate gels. *Biotechnology and bioengineering*. **65** (2000), P.605-610
- 61 Geankoplis, C. J.: Transport processes. Allyn and Bacon, Inc, Boston Massachusetts: 1983.
- 62 Crank, J. The mathematics of diffusion. Oxford: Clarendon Press, 1975
- 63 Zhu, X.X., Masaro, L.: Physical models of diffusion for polymer solutions, gels and solids. *Progress in Polymer Science*. **24** (1999), P.731-775
- 64 Amsden, B.: Solute diffusion in hydrogels. An examination of the retardation effect. *Polymer Gels and Networks*. **6** (1998), P.13-43
- 65 Nguyen, A.L., Luong, J.H.T.: Diffusion in  $\kappa$ -carrageenan gel beads. *Biotechnology and Bioengineering*. **28** (1986), P.1261-1267
- 66 Deleuze, H., Langrand. G., Millet. H., Baratti. J., Buono G., Triantaphylides C.: Lipase-catalysed reactions in organic media: competition. *Biochimica et Biophysica Acta*. **911** (1987), P.117-120
- 67 Balcao, V.M., Paiva, A.L., Malcata, F.X.: Bioreactors with immobilized lipases: State of the art. *Enzyme and Microbial Technolgy*. **18** (1996), P.392-416

- 68 Pavia, A.L., Balcao, V.M., Malcata, F.X.: Kinetics and mechanism of reactions catalysed by immobilized lipases. *Enzyme and microbial technology*. **27** (2000), P.187-204
- 69 Furutani, T, Su, R, Ooshima, H, Kato, J.: Simple screening method for lipase for transesterification in organic solvent. *Enzyme and Microbial Technology*. **17** (1995), P.1067–1072
- 70 Hwang, S., Ahn, J., Lee, S., Lee, T.G., Haam, S., Lee, K., AHN, Ik-Sung A., Jung, J.K.: Evaluation of cellulose-binding domain fused to a lipase for the lipase immobilisation. *Biotechnology Letters*. **26** (2004), P.603-605
- 71 Liu, C.H., Lin Y.H., Chen C.Y., Chang J.S.: Characterisation of Burkholderia lipase immobilized on celite carriers. *Journal of the Taiwan Institute of Chemical Engineering*. **40** (2009), P.359-363
- 72 Rodrigues, D.S., Mendes, A., Adriano, W. S., Gonçalves, L.R.B., Giordano, L.C.: Multipoint covalent immobilisation of microbial lipase on chitosan and agarose activated by different methods. *Journal of Molecular Catalysis B: Enzymatic*. **51** (2007), P.100-109
- 73 Rangheard, M.S., Langrand, G., Triantaphylides, C., Baratti, J.: Multi-competitive enzymatic reactions in organic media: a simple test for the determination of lipase fatty acid specificity. *Biochimical et Biophysical Acta*. **1004** (1989), P.20-28
- 74 Zaks, A., Klibanov, A.M.: Enzyme-catalysed processes in organic solvents. *Proceedings of the national academy of sciences of the United states of America (PNAS)*. **82** (1985), P.3192-3196
- 75 Langrand, G., Baratti, J., Buono, G., Triantaphylides, C.: Enzymatic separation and resolution of nucleophiles: A predictive kinetic model. *Biocatalysis*. **1** (1988), P.231-248
- 76 Derewenda, Z.S., Sharp, A.M.: News from the interface: the molecular structures of triacylglyceride lipases. *Trends in Biochemical Sciences*. **18** (1993), P.20–25
- 77 Ahmed, S.N., Kazlauskas, R.J., Morinville, A.H, Grochulski, P., Schrag, J.D., Cygler, M.: Enantioselectivity of *Candida rugosa* lipase toward carboxylic acids: A predictive rule from substrate mapping and X-ray crystallography. *Biocatalysis and Biotransformation*. **9** (1994), P.209–225

- 78 Dodson G, W.: A Catalytic triads and their relatives. *Trends in biochemical sciences*. **9** (1998), P.347-352
- 79 Fersht, A.: Enzyme structure and mechanism (Second Edition) W H Freeman, New York. P.111 (1984)
- 80 Miller, G.L.: Use of dinitrosalicylic acid reagent for determination of reducing sugar. *Analytical Chemistry*. **31** (1959), P.426-428
- 81 Bradford, M.M.: A rapid and sensitive method for the quantitation of microgram quantities of protein utilizing the principle of protein-dye binding. *Analytical Biochemistry*. **72** (1976), P.248-254
- 82 Coradin, T., Nassif, N., Liage, J.: Silica-alginate composites for microencapsulation. *Apply Microbiol Biotechnology*. **61** (2003), P.429-434
- 83 Sakai, S., Ono, T., Ijima, H., Kawakami, K.: Permeability of alginate/sol-gel synthesized aminopropyl-silicate/alginate membrane templated by calcium-alginate gel. *Journal of Membrane Science*. **205** (2002), P.183-189
- 84 Ma, L., Lu, W., Wen, J.: Encapsulation of lactate dehydrogenase in carbon nanotube doped alginate-chitosan capsules. *Journal of Molecular Catalysis B: Enzymatic*. **56** (2009), P.102-107
- 85 Wang, Z., Qian, L., Wang, X., Zhu, H., Yang, F., Yang, X.: Hollow DNA/PLL microcapsules with tuneable degradation property as efficient dual drug delivery vehicles by chymotrypsin degradation. *Colloids and Surfaces A: Physicochemical and Engineering Aspects*. **332** (2009), P.164-171
- 86 Schwinger, C.: Vergleich verschiedener Verkapselungsmethoden zur Immobilisierung von Zellen. Dissertation, Ingenieurwissenschaftlicher Bereich, Physikalische Chemie der Polymere. Martin Luther Universität Halle-Wittenberg (2004)
- 87 Brandenberger, HR., Widmer, F.: Immobilisation of highly concentrated cell suspensions using the laminar jet breakup technique. *Biotechnology Progress*. **15** (1999), P.366-372
- 88 Yankov, D.: Diffusion of glucose and maltose in polyacrylamide gel. *Enzyme and Microbial Technology*. **34** (2004), P.603-610

- 89 Shigeri, Y., Koishi, M., Kondo, T.: Studies on microcapsules: VI. Effect of variations in polymerisation condition on microcapsule size. *Canadian Journal of Chemistry*. **48** (1970) P.2047-2051
- 90 Somasundaran, P.: Encyclopedia of Surface and Colloid Science. CRC Press, P.634, 2004
- 91 Thomas, WM., Wang, WD.: Encyclopedia of polymer science and engineering. John Wiley& Sons. New York. P.169-211. 1985
- 92 Wolters, G.H., Fritschy W.M., Gerrits, D., Van Schilfagaarde, R.: A versatile alginate droplet generator applicable for microencapsulation of pancreatic-islets. *Journal of Applied Biomaterials*. **3** (1992), P.281-286
- 93 McMurry, J.: Organic Chemistry. Thomson-Brooks/Cole, section 13.9, 2004
- 94 Lebrun, L., Junter, G.A: Diffusion of sucrose and dextran through agar gel membranes. *Enzyme Microbial Technology*. **15** (1993), P.1057-1062
- 95 Sayil, C., Okay, O.: Macroporous poly(N-Isopropyl)acrylamide networks: formation conditions. *Polymer*. **42** (2001), P.7639-7652
- 96 Wang, K.Y., Matsuura, T., Chung, T.S., Fen Guo, W.: The effects of flow angle and shear rate within the spinneret on the separation performance of poly(ethersulfone) (PES) ultrafiltration hollow fiber membranes. *Journal of Membrane Science*. **240** (2004), P.67-79
- 97 Ramos-Olmosa, R., Roggel-Hernandez, E., Flores-Lopez, L., Wai Lin, S., Espinoza-Gomez, H.: Synthesis and Characterisation of asymmetric ultrafiltration membranes made with recycled polystyrene foam and different additives. *Journal of the Chilean Chemical Society*. **53** (2008), P.1705-1708
- 98 Nauman, J.V., Campbell, P.G., Lanni, F., Anderson, J.L.: Diffusion of Insulin-Like Growth Factor-I and Ribonuclease through Fibrin Gels. *Biophysical Journal*. **92** (2007), P.4444-4450
- 99 [http://en.wikipedia.org/wiki/Insulin-like\\_growth\\_factor\\_1](http://en.wikipedia.org/wiki/Insulin-like_growth_factor_1) (13.01.2011) MW of IGF 7.6 KDa
- 100 Plomp, M., McPherson, A., Larson, S.B., Malki, A.J.: Growth Mechanism and kinetics of trypsin crystallization. *Journal of physical chemistry B*. **105** (2001), P.542-551
- 101 Westrin, B.A., Axelsson, A.: Diffusion in gels containing immobilized cells: a critical review. *Biotechnology and Bioengineering*. **38** (1991), P.439-446



- 
- 102 Okahata, Y., Noguchi, H., Seki, T.: Thermoselective permeation from a polymer-grafted capsule membrane. *Macromolecules*. **19** (1986), P.493-494
- 103 Kono, K., Okabe, H., Morimoto, K., Takagishi, T.: Temperature-dependent permeability of polyelectrolyte complex capsule membranes having N-isopropylacrylamide domains. *Journal of Applied polymer science*. **77** (2000), P.2703-2710
- 104 Chu, L.Y., Park, S.H., Yamaguchi, T., Nakao, S.: Preparation of micron-sized monodispersed thermoresponsive core-shell microcapsules. *Langmuir*. **18** (2002), P.1856-1864
- 105 Goubergrits, L., Affeld, K., Debaene, P., Kertzsch, U.: Investigation of transport phenomena inside a microcapsule. *Annals of the New York Academie of Sciences*. **972** (2002), P.200-205
- 106 Reichert, C., Hoell, W.H., Franzreb, M.: Mass transfer enhancement in stirred suspensions of magnetic particles by the use of alternating magnetic fields. *Powder Technology*. **145** (2004) P.131-138
- 107 Sakai, Y., Osada, K., Takahashi, F., Takada, S.: Preparation and properties of immobilized glucoamylase on a magnetically anisotropic carrier comprising a ferromagnetic powder coated by albumin. *The chemical society of Japan*. **65** (1992), P.3430-3433
- 108 Gahsemi, E., Mirhabib, A., Edrissi, M.: Synthesis and rheological properties of an iron oxide ferrofluid. *Journal of Magnetism and Magnetic Materials*. **320** (2008), P.2635-2639
- 109 Boninsegna, S., Roberto, D.T., Renzo, D.M.: Alginate Microspheres Loaded with Animal Cells and Coated by a Siliceous Layer. *Journal of Sol-Gel Science and Technology*. **26** (2003), P.1151-1157
- 110 Lee, G.M., Gray, J.J., Palsson, B.O.: Effect of trisodium citrate treatment on hybridoma cell viability. *Biotechnology Techniques*. **5** (1991), P.295-298

## 9 Appendix A

### 9.1 Analytical Equipment

#### 9.1.1 Light microscopy and Stereo-microscopy

Light microscope and stereo microscope were used to characterize the microcapsule in this study. A light microscope utilizes visible light and magnifying lenses in order to produce better resolution than the eye. Resolution is the ability to differentiate two objects as separate embodiments, rather than seeing them blurred together. A light microscope can achieve magnifications up to 1500x and resolutions down to about 0.2  $\mu\text{m}$ . It can also view images in colour, an essential advantage in comparison to electron microscopes.

The two types of light microscopes (Figure 9-1) can be distinguished from the position of the source of light into transmitted-light microscope and reflected-light microscope [1].

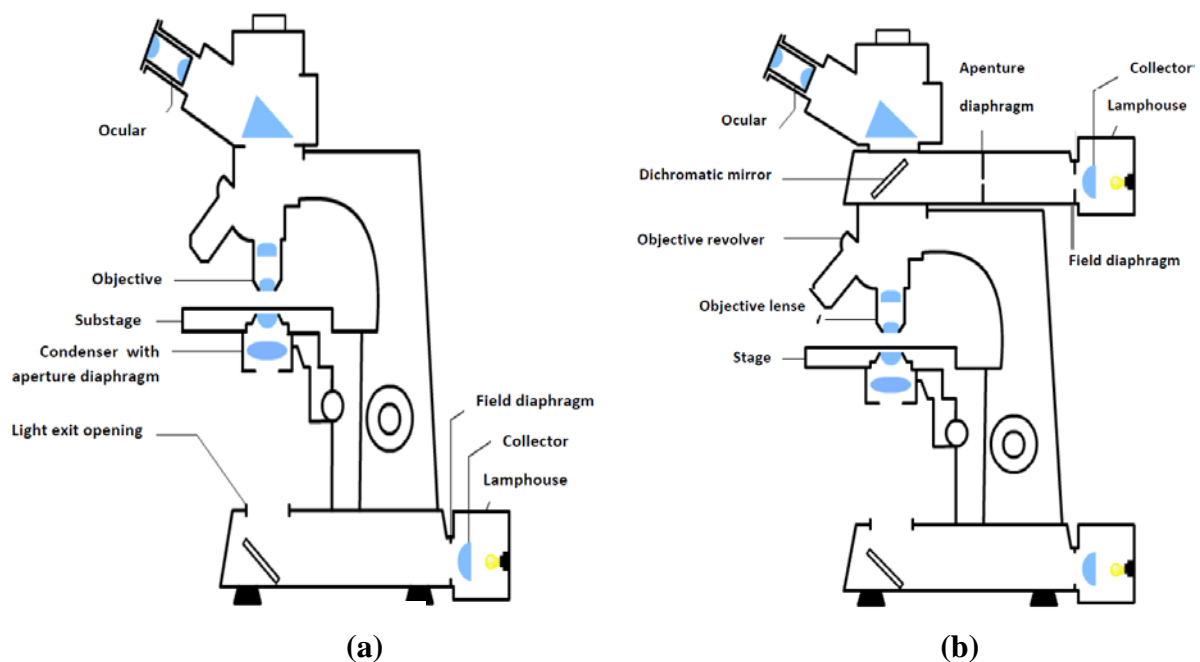


Figure 9-1: (a) Transmitted light microscope (b) Reflected light microscope

In transmitted-light microscopes, the light comes from below and passes through the specimen before it is absorbed by the objective lens. With this kind of microscope, transparent or thinly-sliced samples are essential in achieving good results. Unlike the transmitted-light

microscopes, the reflected-light microscopes utilize light either from above through the lens onto the specimen or radiated from the side of the microscope. The light that is reflected from the sample is again absorbed by the objective lens. Therefore it can be used for very thick and opaque specimens. This microscope is commonly used in fluorescence microscopy or in the material science (mineralogy) [2].

A stereo microscope (Figure 9-2) or dissecting microscope is an optical microscope which uses two separate optical paths to provide slightly different viewing angles in order to produce a three-dimensional visualization of a specimen. The total magnification achieved in a stereo microscope is the product of the objective and eyepiece magnifications as well as the contribution of any intermediate or external auxiliary magnifying lens systems. This microscope is generally applied for microsurgery, watch-making and small circuit board manufacturing and inspection.



Figure 9-2: A LEICA MZ-95 stereo microscope [3]

### 9.1.2 Rotational Viscometer

The rotational viscometer is used to measure dynamic viscosity  $\eta$  of polymer solution. The viscosity is calculated from the measured torque and rotational speed as well as the dimensions of the measuring geometry. The dynamic viscosity  $\eta$  is calculated from shear rate  $\dot{\gamma}$  and shear stress  $\tau$ , which are obtained from the number of rotation  $\dot{n}$ .

$$\eta = \frac{\tau}{\dot{\gamma}} \quad (\text{eq. 9-1})$$

In rheology, there are two types of fluids, namely Newtonian and non-Newtonian fluids. The viscosity of a Newtonian fluid is constant, i.e. independent of shear rate and shear stress, for a

given temperature and pressure. On the contrary, the viscosity of a non-Newtonian fluid is dependent on temperature, pressure, shear rate and shear stress. The viscosity of polymer solution exhibits non-Newtonian fluid behaviour as Schwinger [4] reported that the viscosity of polymer solution decreases with increasing of shear stress.

### 9.1.3 Tensiometer

A tensiometer is utilized to measure the surface tension ( $\sigma$ ) of a liquid. Its operational principle is based on the Du Noüy Ring Method where the liquid is raised until contact with a surface is registered. The sample is then lowered again so that the liquid film produced beneath the ring is stretched (Figure 9-3).

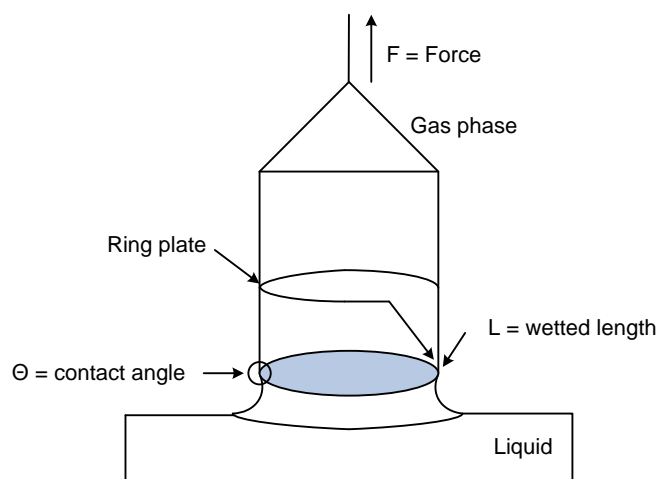


Figure 9-3: Schematic diagram of the ring method tensiometer [5]

As the film is stretched a maximum force is produced. At this maximum point the force vector is exactly parallel to the direction of motion and the contact angle ( $\theta$ ) is  $0^\circ$ . The surface tension can be calculated using the following equation:

$$\sigma = \frac{F_{\max} - F_V}{L \cdot \cos \theta} \quad (\text{eq. 9-2})$$

Where.  $\sigma$  is the surface tension.  $F_{\max}$  is the maximum force.  $F_V$  is the weight of volume of the liquid lifted.  $L$  is the wetted length and  $\theta$  is the contact angle.

## 9.2 Calibration of peristaltic pump and micro-gear pump

Both micro gear and peristaltic pumps were calibrated before further experiments. The calibration was done in order to determine the flow rates of the pumps. Pump flow rate verification is important to system accuracy. After the nozzle was set, the pump was fed with water with different flow rate. After 5 minutes, the mass of water coming out of the nozzle was weighed. The results were then converted to unit ml/min. This calibration was done for both peristaltic and micro gear pumps. The calibration curves are given in Figure 9-4 below.

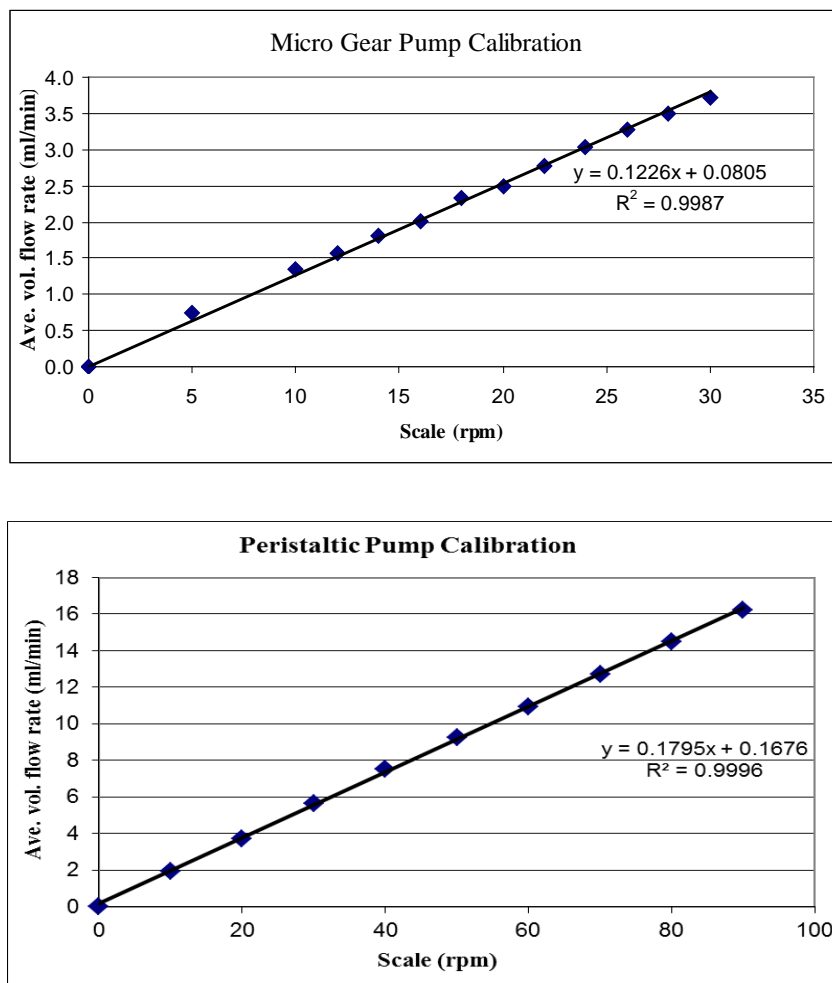


Figure 9-4: Calibration curves for micro-gear and peristaltic pumps with water

From the previous study, it was mentioned that the rotational flow rate of the pump used to pump the polymer-alginate solution should be  $<75$ .

## Reference

1 <http://www.biologyreference.com/La-Ma/Light-Microscopy.html>

2 [http://www.univie.ac.at/mikroskopie/1\\_grundlagen/mikroskop/bauarten/2\\_durchlicht.htm](http://www.univie.ac.at/mikroskopie/1_grundlagen/mikroskop/bauarten/2_durchlicht.htm)

3 <http://www.leica-microsystems.com/products/stereo-microscopes-microscopes>

4 Schwinger, C.: Vergleich verschiedener Verkapselungsmethoden zur Immobilisierung von Zellen. Dissertation, Ingenieurwissenschaftlicher Bereich, Physikalische Chemie der Polymere. Martin Luther Universität Halle-Wittenberg (2004)

5 <http://www.kruss.de/en/theory/measurements/surface-tension/ring-method.html>

# **Curriculum Vitae**

## **Personal Data**

Name: Pavadee Pachariyanon  
Date of birth: 29 September 1981  
Place of birth: Bangkok, Thailand  
Nationality: Thai  
Marital status: Married

## **School Education**

1997-2000 Triam Udom Suksa, Bangkok, Thailand

## **Academic Studies**

2000-2004 Bachelor of Engineering (Chemical)  
Chulalongkorn University, Bangkok, Thailand  
2005-2007 Master of Science in Chemical Engineering  
TU Dortmund, Dortmund, Germany

## **Internships**

2003 Rayong Olefins Co. Ltd., Rayong, Thailand

## **Occupations**

02-09. 2005 The Shell Company of Thailand Limited, Bangkok, Thailand  
Since April 2008 Research Associated at Institute of Reaction engineering B  
TU Dortmund, Dortmund, Germany